[Escriba aquí]

Universidad del País Vasco Euskal Herriko Unibertsitatea
NAZIOARTEKO BIKAINTASUN CAMPUSA
CAMPUS DE EXCELENCIA INTERNACIONAL

Departamento de Fisiología

Facultad de Medicina y Odontología

Role of SOX17 in the regulation of the biliary phenotype and in cholangiocarcinogenesis

Tesis presentada por

MAITE MERINO AZPITARTE

Donostia, 26 de Febrero de 2016

Role of SOX17 in the regulation of the biliary phenotype and in cholangiocarcinogenesis

Tesis presentada por

Maite Merino Azpitarte

Para la obtención del título de doctor en

***Investigación Biomédica* por la**

Universidad del País Vasco/Euskal Herriko Unibertsitatea

Tesis dirigida por

Dr. D. Jesús María Bañales Asurmendi

Dr. D. Luis Bujanda Fernández de Piérola

AKNOWLEDGEMENTS

AGRADECIMIENTOS

Acknowledgements

I want to thank my two PhD supervisors, Dr. Jesús María Bañales and Dr. Luis Bujanda, for allowing me to perform this Dissertation in the Department of Liver and Gastrointestinal Diseases of the Biodonostia Health Research Institute (Donostia University Hospital).

I acknowledge the University of the Basque Country (UPV/EHU) for enabling me to develop my PhD in the Department of Physiology and the “Zabalduz” program (UPV/EHU) for granting my PhD during these 3 years of Thesis (March 2013 – March 2016). Moreover, we thank the Spanish “Instituto de Salud Carlos III” for funding this project (FIS Project PI15/01132).

I thank my lab team at the “Liver Diseases Group” as well as all the components of the Biodonostia Institute for supporting me (personally and professionally) during this time.

I would also like to acknowledge the valuable help received from the external collaborators: Dr. Jose Juan García Marín (Univ. of Salamanca, Spain), Dr. Sergio Gradilone (Hormel Institute, Univ. of Minnesota, USA), Dr. Robert Huebert (Mayo Clinic, Rochester, MN, USA), Dr. Ana María Aransay (CIC Biogune, Bilbao), Dr. José Luis Lavín (CIC Biogune, Bilbao) and Dr. Maite García (CIMA of the Univ. of Navarra), who improved the results of this project.

Finally, to my dear family who are the best of my life.

Agradecimientos

Quiero empezar agradeciendo afectuosamente a mis directores de tesis, los Drs. Jesús M. Bañales y Luis Bujanda, por permitirme realizar la tesis doctoral en su Grupo y por la ayuda continuada que siempre me han brindado:

Al Dr. Jesús M. Bañales, por ayudarme a hacer que este importante proyecto de investigación multidisciplinar sea una realidad en tan solo tres años. Por enseñarme a pensar científicamente, y a diseñar y analizar los experimentos con gran rigor. Por enseñarme más de lo que cualquier otro me haya enseñado, a ser cauta, pensativa, determinante, elocuente y práctica.

Al Dr. Luis Bujanda, por su apoyo continuado durante estos tres años de tesis doctoral y permitir que este proyecto de investigación haya sido posible. Por su trato cercano y amable, y por ser siempre tan proactivo.

La culminación de este trabajo no habría sido posible sin el apoyo incondicional de los componentes del Departamento de Enfermedades Hepáticas y Gastrointestinales del Instituto de Investigación Sanitaria Biodonostia, por lo que quiero agradecérselo de forma individual:

A la Dra. María Jesús Perugorria, por estar siempre que la necesitamos. Sin su sabiduría, su guía, su cariño, su determinación, su persona en general, ninguno seríamos capaces de realizar la mitad de lo que conseguimos. Ella me ha enseñado muchísimo en estos años, por ello quiero agradecerle con todo mi corazón la tutela y el apoyo que he recibido de ella. Estoy segura de que conseguirás muchos y valiosos logros.

A la Dra. Patricia Muñoz, un referente del laboratorio. Por ayudarme siempre que lo he necesitado. Espero que todo te vaya bien en Dinamarca, y que logres todos los objetivos que te has marcado. Eres una gran luchadora, por lo que algo me dice que lo lograrás.

A Ander Arbelaiz, por tu calidez y sosiego. ¿Qué habría hecho sin ti? Eres la voz de la paciencia, la voz de la tranquilidad, la voz de la lógica... Sin tus palabras de apoyo, regaño, consuelo, amistad, conciliación,… jamás habría conseguido tener la capacidad de relajarme. Jamás habría sido capaz de tomarme las cosas negativas como algo que no puedes controlar, sino de lo que debes aprender y seguir adelante; o de tomarme las cosas positivas como instrumento de impulso y continuidad. Eres un hombre fantástico y no deseo que tu personalidad cambie un ápice.

A Oihane Erice, por tu gran ayuda en parte de los experimentos de esta tesis doctoral. Eres muy trabajadora y no te rindes jamás. Estoy segura de que conseguirás grandes logros.

A Álvaro Santos, por su alegría. Eres una de las personas más responsables que he conocido, y al mismo tiempo, una de las más cómicas. Tu diversión es como una gripe que se contagia por el laboratorio, y cuando faltas se nota. Tu impetuosidad forma parte de tu encanto y del cariño que te has ganado. No pierdas tu viveza nunca jamás.

A la Dra. Elisa Lozano, por tu gran ayuda durante este proyecto de investigación. Te agradezco enormemente tu ayuda desinteresada en la escritura de esta tesis doctoral.

A Aitor Esparza, por tu compañerismo, amabilidad y alegría. Espero que tu tesis llegué a muy buen puerto. Estoy segura de que aprovecharás a fondo estos años.

Al Dr. Raúl García y colaboradores de Anatomía Patológica, sin los cuales no hubiera sido posible realizar los estudios en biopsias de pacientes.

No quiero olvidarme de otras personas que han pasado por el laboratorio como son Delia, Ibone, Javi y Myrian. De cada uno de vosotros he aprendido algo positivo y os deseo lo mejor en vuestras etapas futuras.

Finalmente, no quisiera olvidarme de los que me han apoyado en el transcurso de toda mi vida, de mis buenas y malas decisiones, de mis alegrías y tristezas, de mis ilusiones perdidas y sueños alcanzados; en definitiva de mi familia. Aunque haya miembros de la misma que no se encuentran entre los vivos, ellos también, junto a los que sí lo están, siguen en mi entorno impulsándome a ser mejor y conseguirlo todo. Mis más sinceras gracias a mi aita, allá donde estés, y a mi ama, por traerme a este mundo en las circunstancias menos apropiadas. Gracias a mi ama sobretodo, por ser mi luz, mi molde, mi conciencia. Gracias a mi hermana, “mi pitus”, a la que quiero a más no poder. Una hermana que ha aprendido todo de mí, de la que me siento orgullosa y que ahora me educa con mis propios consejos, cuando ella es la peque y seguirá siendo la peque eternamente. Gracias a mi aitaorde, que por mucho que no sea mi aita de sangre, hemos aprendido a querernos, respetarnos, apoyarnos y protegernos como harían un padre y una hija. Y gracias al resto de mi familia, que por fin aprecian el esfuerzo que he hecho para lograr uno de mis objetivos, la realización de la Tesis Doctoral.

ABBREVIATIONS

AA	amino acid
AAV	adeno-associated virus
AE2	anion exchanger 2, chloride/bicarbonate exchanger
AFP	alpha-fetoprotein
AHCYL1	adenosylhomocysteinase like 1
ARID1A	AT rich interactive domain 1A
ATCC	American type culture collection
ATP1B1	Na^+/K^+-ATPase β1 subunit
BCA	bicinchoninic acid
BCL2	B-cell lymphoma 2
BICC1	bicC family RNA binding protein 1
BMP	bone morphogenetic protein
BMS1P5	BMS1 ribosome biogenesis factor pseudogene 5
BSA	bovine serum albumin
C9orf80	integrator complex cubunit 3
C14orf85	inositol-tetrakisphosphate 1-kinase antisense RNA 1
CA125	cancer antigen 125 (also known as Mucin 16)
CA19-9	carbohydrate antigen 19-9
CA242	tumor marker antibody
CAFs	cancer-associated fibroblasts
CAKUT	congenital anomalies of the kidney and the urinary tract
CCA	cholangiocarcinoma
CD133	prominim 1 (PROM1)
CD24	glycosyl phosphatidylinositol-anchored protein
CDCP1	CUB domain containing protein 1

Abbreviations

CDK4	cyclin-dependent kinase 4
CDKN2A	cyclin-dependent kinase inhibitor 2A
CDKN2AIPNL	CDKN2A interacting protein N-terminal like
CDKN2B	cyclin-dependent kinase inhibitor 2B
cDNA	complementary DNA
CEA	carcinoembryonic antigen
CF	cystic fibrosis
CFTR	cystic fibrosis transmembrane conductance regulator
cHCC-CCA	combined hepatocellular carcinoma-cholangiocarcinoma
CK	cytokeratin
CK1	casein kinase 1
cMYC	myc protooncogene protein
CO_2	carbon dioxide
CRC	colorectal cancer
CREB1	cAMP response element-binding protein
cRNA	complementary RNA
CSCs	cancer stem cells
CT	computed tomography
CTR1	cationic aminoacid transporter 1
CTRL	control
CYFRA21-1	CK19 soluble fragment detectable in serum
DAPI	40,6-diamidino-2-phenyindole
DCBLD2	discoidin, CUB and LCCL domain containing 2
dCCA	distal cholangiocarcinoma
DDX51	dead (Asp-Glu-Ala-Asp) box polypeptide 51

DE	definitive endoderm
dH_2O	distilled water
DKK	dickkopf WNT signaling pathway inhibitor
DMEM/F-12	dulbecco's modified eagle's medium/Ham's F-12 nutrient mixture
DMSO	dimethyl sulfoxide
DNA	deoxyribonucleic acid
DNAJA1	DNA J (Hsp40) homolog subfamily A member 1
DNMT	DNA methyltransferase
dNTPs	deoxynucleoside triphosphates
DPBS	dulbecco's phosphatase-buffered saline
DTT	dithiothreitol
DUSP19	dual specificity phosphatase 19
EC	endothelial cells
ECL	enhanced chemoluminiscence
ECM	extracellular matrix
EDTA	ethlylenediaminetetraacetic acid
eGFP	enhanced green fluorescent protein
EGFR	epidermal growth factor receptor
EHBDs	extrahepatic bile ducts
EID2B	EP300 interacting inhibitor of differentiation 2B
EMT	epithelial-to-mesenchymal transition
ENT1	equilibrative nucleoside transporter 1
EPCAM	epithelial cell adhesión molecule

Abbreviations

ERBB2/NEU	receptor tyrosine-kinase erbB2/proto-oncogene neu (also known as tyrosine kinase-type cell surface receptor HER2)
ERCC1	excision-repair cross-complementation group 1
ERCP	endoscopic retrograde cholangiopancreatography
EUS	endoscopic ultrasound
FBS	fetal bovine serum
FBW7	F-box and WD repeat domain-containing 7
FDA	food and drug administration
FGF	fibroblast growth factor
FGFR2	fibroblast growth factor receptor 2
5-FU	5-fluorouracil
FN	fibronectin
FOXA2	forkhead box A2
FOXF1	forkhead box F1
FZD	frizzled
GAPDH	glyceraldehyde-3-phosphate dehydrogenase
gDNA	genomic DNA
GSK3β	glycogen synthase kinase 3 beta
HCC	hepatocellular carcinoma
HDACs	histone deacetylases
HE	hepatic endoderm
HHEX	hematopoietically expressed homeobox
HIATL2	hippocampus abundant transcript-like 2
HMG	high mobility group
HNF1β	hepatocyte nuclear factor 1 beta

HNF6	hepatocyte nuclear factor 6
HP	hepatic progenitor
HPC	hepatic progenitor cell
HRP	horseradish peroxidase
HS	hepatic specification
HSPA1B	heat shock 70kDa protein 1B
iCCA	intrahepatic cholangiocarcinoma
iDCs	iPSC-derived cholangiocytes
IDH	isocitrate dehydrogenase
IF	immunofluorescence
IFI6	interferon-alpha inducible protein 6
IFI27	interferon-alpha inducible protein 27
IFIT1	interferon-induced protein with tetratricopeptide repeats 1
IFNGR1	interferon-gamma receptor 1
IG	intraductal growth
IGFBP3	insulin-like grwoth factor binding protein 3
IHBDs	intrahepatic bile ducts
IL6	interleukin 6
iPSCs	induced pluripotent stem cells
ITPRIPL2	inositol 1,4,5-triphosphate receptor interacting protein-like 2
JAG1	Jagged-1
JNK	c-Jun N-terminal protein kinase
KCNH6	K^+-channel voltage-gated eag-related subfamily H member 6

KCTD1	potassium channel tetramerization domain containing 1
KIF14	kinesin family member 14
KLF4	kruppel-like factor 4
KRAS	ki-ras2 Kirsten rat sarcoma viral oncogene homolog
LEF	lymphoid enhancer factor
LRRFIP1	leucine rich repeat (In FLII) interacting protein 1
M-MLV	moloney-murine leukemia virus
MCL	mantle cell lymphoma
MCL1	myeloid cell leukemia
MDR	multidrug resistance
MET	mesenchymal-to-epithelial transition
MF	mass forming
MGEA5	meningioma expressed antigen 5
MMPs	metalloproteinases
MMR	mismatch repair
MOC	mechanisms of chemoresistance
MOI	multiplicity of infection
MPRs	mannose 6-phosphate receptors
MPZL2	myelin protein zero-like protein 2
MRI	magnetic resonante imaging
miRNAs	microRNAs
mRNA	messenger RNA
mtRNA	mitochondrial RNA
MUC5AC	mucin 5AC, oligomeric mucus/gel-forming
NAC	N-acetylcysteine

NaCl	sodium chloride
NaF	sodium fluoride
NCAM	neural cell adhesion molecule
NHC	normal human cholangiocytes
NT	nucleotide
O/N	overnight
OATP1A2	organic anion-transporting polypeptide-1, A2
OC2	onecut factor 2
OCT1	organic cation transporter 1
OCT4	octamer-binding transcription factor 4
ORF	open reading frame
P/S	penicillin/streptomycin
PBC	primary biliary cirrhosis
PBGs	peribiliary glands
PBS	phosphatase buffered saline
PBRM1	polybromo 1
pCCA	perihilar cholangiocarcinoma
PCR	polymerase chain reaction
PCT	percutaneous transhepatic cholangiography
PDAC	pancreatic ductal adenocarcinoma
PDE4C	phosphodiesterase 4 C, cAMP-specific
PDT	photodynamic therapy
PDX1	pancreatic and duodenal homeobox 1
PEI	polyethylenimine
PET	positron emission tomography

Abbreviations

PI	periductal infiltrating
PIK3CA	phosphatidylinositol-4,5-biphosphate 3-kinase catalytic subunit alpha
PKD2	polycystic kidney disease 2
PLDs	policystic liver diseases
PNPT1	polynucleotide phosphorylase
POFUT1	protein O-fucosyltransferase 1
PP2A	protein phosphatase 2A
prEF1a	elongation factor 1α promoter
PSC	primary sclerosing cholangitis
qPCR	quantitative polymerase chain reaction
RARRES1	retinoic acid receptor responder (tazarotene induced) 1 [also known as tazarotene-induced gene 3 (TIG3)]
RCSB	research collaboratory for structural bioinfomratics
RIN	RNA integrity number
RIPA	radio-immunoprecipitation assay
RN7SL1	RNA 7SL cytoplasmic 1
RNA	ribonucleic acid
ROS	reactive oxygen species
RP	random primers
RPM	revolutions per minute
RPMI	roswell park memorial institute
RRP7B	ribosomal RNA processing 7 homolog B (*S. cerevisiae*)
RT	reverse transcription
RYBP	ring1A and YY1 binding protein

SALL4	spalt-like trasncription factor 4
SDS-PAGE	sodium dodecyl sulfate polyacrylamide gel electrophoresis
SER	serine
SERPINA1	serine-protease inhibitor A 1
SFRP	secreted frizzled-related protein
SHH	sonic hedgehog
shRNA	short hairpin RNA
siRNA	small interferente RNA
SMAD4	smad family member 4
SOCS3	suppressor of cytokine signaling 3
SOX	sry (sex-determining region y) box
ST	septum transversum
STAT3	signal transducer and activator of transcription 3
STX12	syntaxin 12
TAA	thioacetamide
TACC3	transforming, acidic coiled-coil containing protein 3
TβR	serine-threonine kinase receptor
TBS	tris-buffered saline
TCF	T-cell factor
TERT	telomerase reverse transcriptase
TGFβ	transforming growth factor beta
TGF1β	transforming growth factor 1 beta
THBP	ter-butyl hydroperoxide
THR	threonine
TM4SF4	transmembrane 4 L six family member 4

Abbreviations

TP53	tumor protein p53
TPs	thymidine phosphorylases
TSP1	thrombospondin-1
TXLNA	taxilin alpha
UNG1	uracil-DNA glycosylase-1
UV	ultraviolet
Wnt	wingless and integration site
WST-1	water soluble tetrazolium salt 1
XF/FF	xeno-free/feeder-free
XPNPEP3	x-prolyl aminopeptidase 3
ZMAT3	zinc finger matrin-type 3
ZO-1	zonula occludins

INDEX

A mi Familia

I. INTRODUCTION

I.1. The liver

The liver is the largest organ of the human body, and is located in the upper right corner of the abdomen (Figure I.1.A) [1]. It performs multiple metabolic and homeostatic functions such as: a) synthesis and storage of glycogen, fat and fat soluble vitamins, b) synthesis and release of different products such as glucose, plasma proteins, clotting factors, urea, c) bile production, as well as d) drugs detoxification, among others [2, 3]. The liver is composed by different cell types (Figure I.1.B): *i*) parenchymal cells or hepatocytes, *ii*) sinusoidal fenestrated endothelial cells, *iii*) perisinusoidal stellate cells, *iv*) intraluminal phagocytic kupffer cells, and *v*) biliary duct epithelial cells. These cells interact with each other executing specific functions. The main cell type in the liver is the hepatocyte, which represents ~80% of the total volume and performs most of the liver functions [3].

The liver has a unique vascular system and its blood supply is divided between the hepatic artery (~25-30%) and the portal vein (~70-75%). The hepatic artery provides oxygenized blood to the liver and the portal vein carries a nutrient-enriched blood from the small intestine [4]. Both types of blood, arterial and portal, end up mixing within the hepatic sinusoids before draining into the systemic circulation through the hepatic venous system, for example the central vein (Figure I.1.B) and the inferior cava vein [4]. Following the portal venous system trajectory it is distinguishable the intrahepatic biliary tree (Figure I.1.B) [4], composed by bile epithelial cells (termed cholangiocytes) that participate in the regulation of bile composition.

A) **B)**

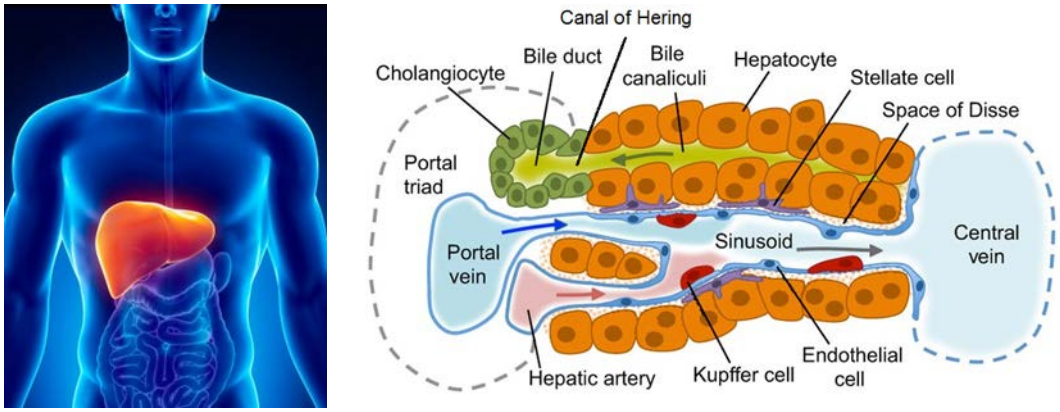

Figure I.1. A) Anatomical localization of the liver in a human body (http://es.123rf.com). B) Liver cell types, and blood and bile flow in the liver (modified from Gordillo M et al, 2015, Development) [5].

I.2. Biliary tract

I.2.1. Anatomy

The biliary tree is a network of interconnected ducts of increasing diameter from the liver to the intestine, which can be subdivided into intrahepatic bile ducts (IHBDs) and extrahepatic bile ducts (EHBDs) [6]. IHBDs start at the ductule-canalicular junction with the canals of Hering (Figure I.1.B), which are located at the periphery of the portal tracts facing the periportal hepatocytes [7]. IHBDs continue with the bile ductules and the interlobular septal area and segmental ducts [6]. EHBDs consist of right and left hepatic ducts, common hepatic duct, gallbladder with the cystic duct, common bile duct, and hepato-pancreatic ampulla. The resultant bile drains into the duodenum (Figure I.2) through the papilla of Vater [6]. The right and left hepatic ducts and the proximal portion of the EHBDs are collectively called “perihilar bile ducts” [8].

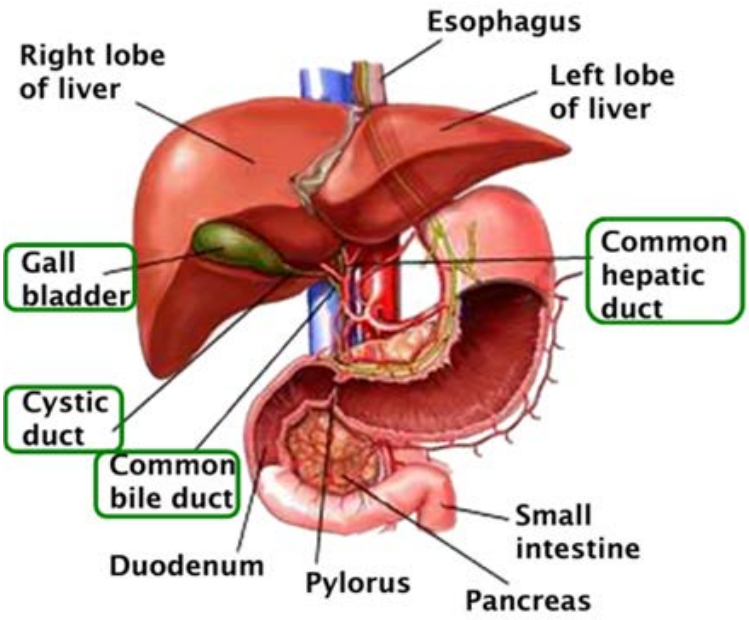

Figure I.2. Anatomy of the extrahepatic biliary system (modified from http://www.myschoollights.com/human-liver.html).

I.2.2. Bile duct epithelial cells: cholangiocytes

The bile ducts are lined by specialized epithelial cells called “cholangiocytes”. Cholangiocytes, which represent ~3-5% of total liver cells, play key roles in the regulation of bile flow and composition. They are involved in the fluidization and alkalinization of the primary bile generated in the canaliculus of hepatocytes [9], and may participate in the reabsorption of bile acids [10].

Cholangiocytes are characterized by the presence of a single primary cilium that extends from the apical membrane into the bile duct lumen (Figure I.3) [11]. This antenna-like bulge is a sensory organelle that functions as a mechano-[12], chemo- [13] and osmo-sensory organelle [13, 14], which detects changes in bile flow, composition and osmolarity and has an important role in cholangiocyte physiology and pathophysiology [11, 12]. It is formed by an axoneme and a

centriole-derived basal body [11]. The axoneme is composed by 9 duplets of acetylated alpha-tubulin located in the peripheria of the cilium, indicating its main sensory function and no duplets in the center, indicating the lack of capacity to move the fluids [11].

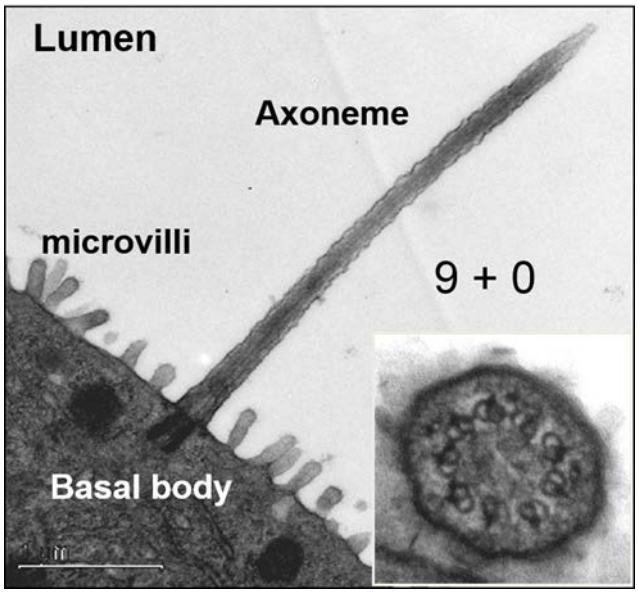

Figure I.3. The normal structure of a cholangiocyte primary cilium composed by a basal body and an axoneme, and cross- ciliary section of the primary cilium showing 9 duplets of acetylated alpha-tubulin in the peripheria (modified from Masyuk TV *et al*, The American Journal of Pathology, 2004) [15].

I.2.3. Embryogenesis and development

I.2.3.1. Gestational stages and biliary system embryogenesis

In mammalian embryos, the hepatobiliary system derives from the ventral foregut endoderm [16]. In humans, in particular, the first formation of bile ducts and liver is the hepatic diverticulum, which starts as a thickening of the endoblastic epithelium of the foregut endoderm at the 18-day of gestation [17]. In the 22-day of gestation the hepatic diverticulum is well formed (Figure I.4) [17]. In the development of the human biliary system, the EHBDs develop from

the embryonic hepatic diverticulum whereas the IHBDs originate within the liver from the ductal plate [18, 19].

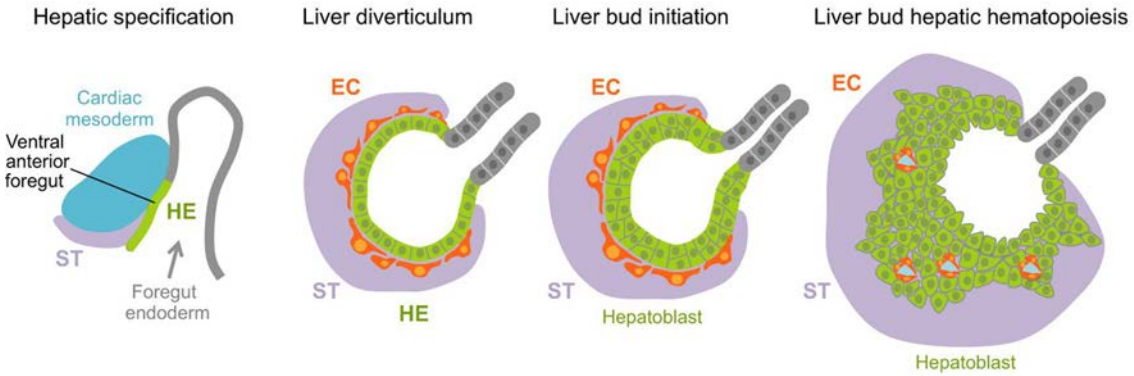

Figure I.4. Liver diverticulum and bud formation in mouse. HE: hepatic endoderm; ST: septum transversum; EC: endothelial cells [5].

During the 29-34 days of gestation, the embryo (~5 mm in length) shows in the hepatic diverticulum a protruding bud that represents the initial formation of the gallbladder, the cystic duct, and common bile duct [17]. For up to 8 weeks of gestation, the extrahepatic biliary tree further develops through lengthening of the caudal part of the hepatic diverticulum [20]. In the 34-day of the embryo, the common hepatic duct is a broad, funnel-like structure in direct contact with the developing liver, without a recognizable left or right hepatic duct [17]. The distal portions of the right and left hepatic ducts develop from the extrahepatic ducts and are clearly defined tubular structures by 12 weeks of gestation. On the other hand, the proximal portions of the main hilar ducts derive from the first intrahepatic ductal plates [21]. The EHBDs and the developing intrahepatic biliary tree maintain luminal continuity from the very start of organogenesis throughout the development [21].

During the first 7 weeks of human embryonic life, there is no IHBD system in the developing liver [17]. Around the eighth week of gestation, the primitive

hepatoblasts adjacent to the mesenchyme around the largest hilar portal vein branches increase the expression of cytokeratins (CK) 8, 18, and 19, and form cylindrical-sleeve cell-layer called “ductal plate” (Figura I.5) [22]. The ductal plate is a flat muralium of primitive biliary epithelium that develops in the mesenchyme along the branches of the portal vein. By 20 weeks of gestation, weak immunoreactivity for CK7 appears in the cells of the developing ducts [22]. The immunoreactivity for CK7 gradually increases and extends into more peripheral ducts [17], thus conforming the intrahepatic and hilar bile ducts.

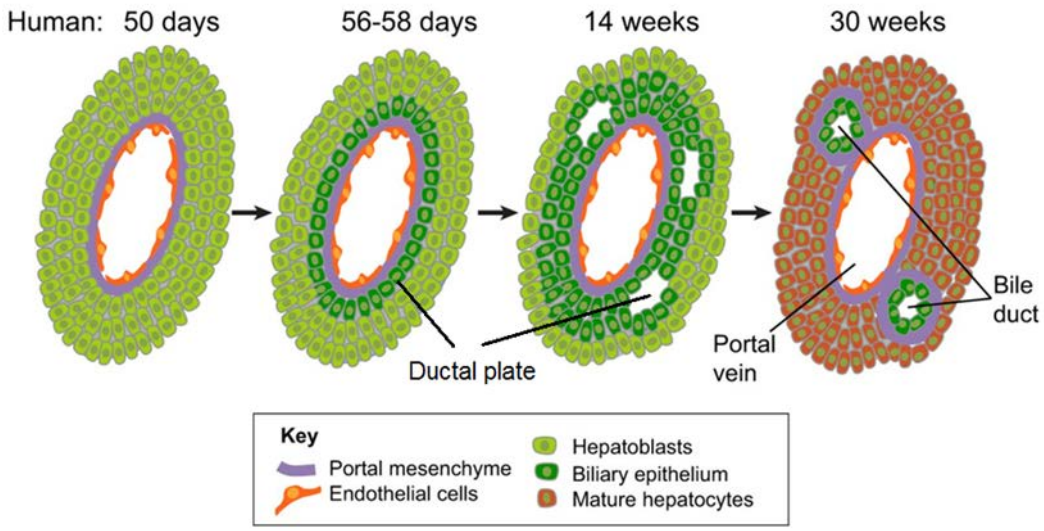

Figure I.5. Bile duct development through ductal plate formation (modified from Gordillo M *et al*, Development, 2015) [5].

I.2.3.2. Signaling pathways

Several molecular pathways and transcription factors are involved in the differentiation of the liver and biliary tract. Among the key transcription factors, hematopoietically expressed homeobox (Hhex), hepatocyte nuclear factor 6 (HNF6) and hepatocyte nuclear factor 1 beta (HNF1β) participate in the development of the liver and the biliary system [23-25]. Biliary cell differentiation

is induced in the fetal liver by a periportal gradient of activin/transforming growth factor-beta (activin/TGFβ) signaling, the extent of which is controlled by the inhibitory influence of HNF6 and the onecut factor 2 (OC2) [17, 26]. The Notch pathway may act in parallel or downstream of the activin/TGFβ signaling pathway to further support the biliary differentiation or to repress the hepatocytic differentiation program in these cells [17, 26].

The transcription factor sex-determining region y box (SOX) 17 seems to play also a key role in the differentiation of the biliary tree. Thus, in the week 8.5 of murine gestation, SOX17 and the pancreatic and duodenal homeobox 1 (PDX1) are essential for the differentiation of the biliary system and the ventral pancreas [16]. PDX1+ cells that begin to express SOX17 give rise to the development of the extrahepatic biliary system (i.e. gallbladder, common hepatic duct, cystic duct) and those that only express PDX1 result in the origin of the ventral pancreatic system [16]. Moreover, development of gallbladder further requires the expression of the forkhead box f1 (*Foxf1*) gene [17].

I.2.4. Cholangiocyte regeneration

In humans, the regenerative origin of the mature biliary epithelial cells is dependent of their localization along the biliary tract. Thus, mature cholangiocytes may originate from differentiation of inmature cholangiocytes present in the channels of Hering, as well as from progenitor cells present in intrahepatic and extrahepatic peribiliary glands (PBGs) [27]. The PBGs are niches of stem/progenitor multipotent cells inserted in the walls of the bile tree. They can be localized in the whole bile tree, except in the gallbladder [28].

However, similar cells −presumably committed progenitor cells− are found in the gallbladder, which express endoderm markers similar to those expressed by the peribiliary gland cells [6, 29]. The highest density of peribiliary glands is located at the cystic duct, the common hepato-pancreatic duct and the hilum common hepatic duct. These cells express classic endodermal transcription factors (i.e. SOX17, SOX9, FOXA2, HNF6, SALL4) and typical superficial markers of endodermal progenitors (i.e. EpCAM, NCAM, CD133) (Figure I.6) [27].

A **B**

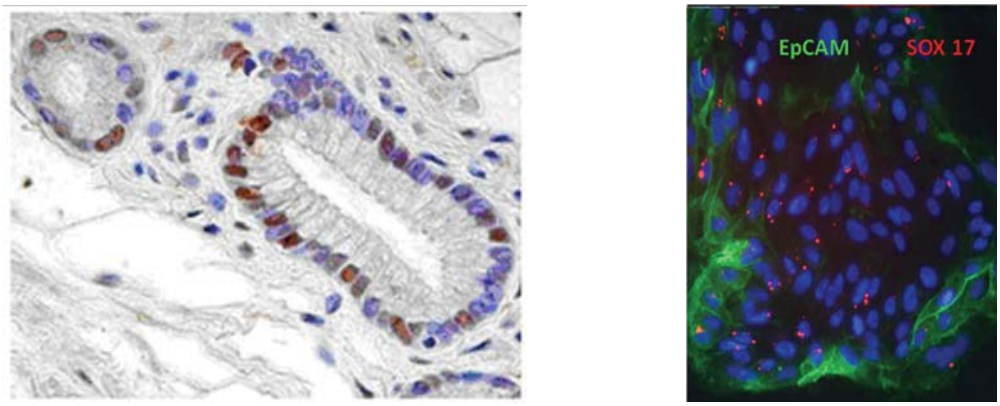

Figure I.6. A) Peribiliary gland cells expressing nuclear SOX17. B) Culture of isolated cells from peribiliary glands expressing perinuclear SOX17 (red) and citoplasmic EpCAM (green), endodermal transcription factor and superficial marker, respectively [27].

PBGs contain progenitor-like cells which normally proliferate and are responsible for the renewal of the surface epithelium-generating mature cells such as cholangiocytes, goblet cells (in the middle of the biliary tree), hepatocytes (near the liver) or islet cells (near the pancreas) [6]. The maturational process of the PBG cells shows a progress of decrease or loss of stem/progenitor cell markers and acquisition of mature cell markers [6].

I.2.5. Cholangiopathies

Cholangiocytes are also the central target of different diseases termed cholangiopathies, which in general show substantial morbidity and mortality. There are different types of cholangiopathies that can be subclassified according to their etiology in: a) immune-associated [i.e. primary biliary cirrhosis (PBC) [30] and primary sclerosing cholangitis (PSC) [31]], b) infectious (i.e. *Cryptosporidium parvum*) [32], c) genetic [i.e. polycystic liver diseases (PLDs) [33], cystic fibrosis (CF) [34] and Alagille´s syndrome [34]], d) vascular (i.e. postischemic cholangiopathies) [35, 36], e) idiopathic (i.e. biliary atresia [37] and sarcoidosis idiopathic childhood/adulthood ductopenia [38]), f) neoplastic (i.e. cholangiocarcinoma) [30], and g) drug-induced (i.e. fluorouracil-induced) [39, 40] (Figure I.7). Cholangiopathies share some common features such as inflammation, innate immune responses, cholangiocyte proliferation, as well as tissue repair processes.

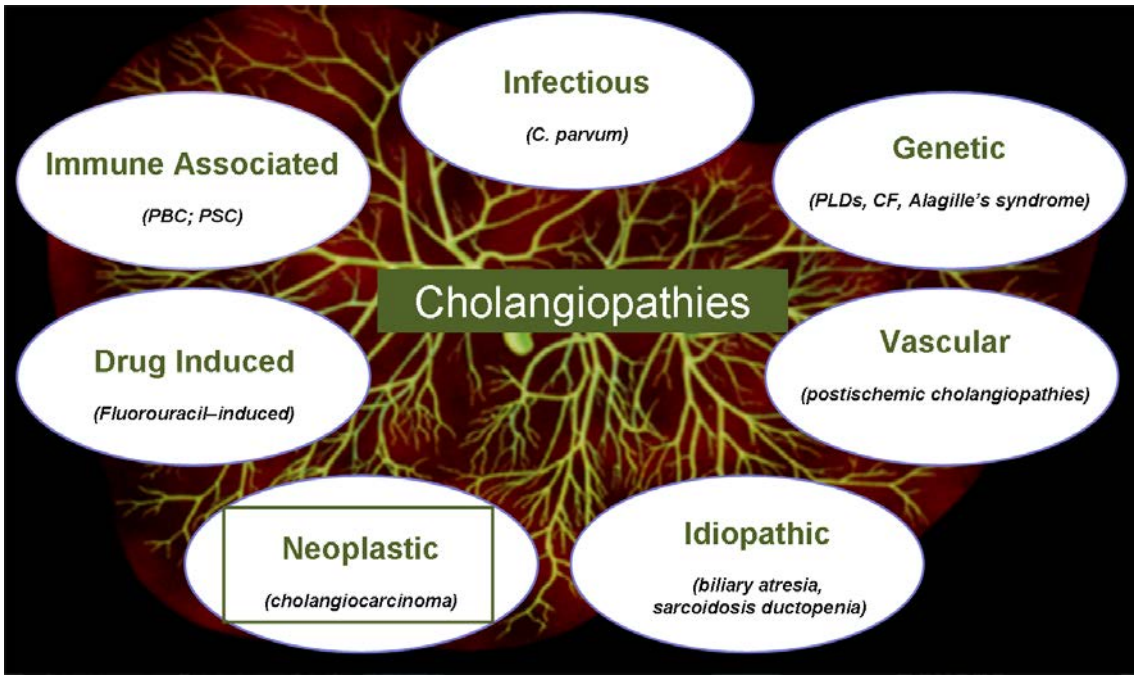

Figure I.7. Schematic representation of the main cholangiopathies.

I.3. Cholangiocarcinoma

Cholangiocarcinoma (CCA) is a heterogeneous group of malignancies with features of biliary tract differentiation. It is the second most frequent malignant liver tumor after hepatocellular carcinoma (HCC) and accounts for ~3% of all gastrointestinal cancers [41]. The incidence is increasing worldwide but differs between countries [42, 43]. Thus, Eastern countries such as Thailand, China and Korea show higher rates (>6/100.000) than Western countries (<4/100.000) [44]. CCA is generally diagnosed in elderly people (~60-70 years-old) and is more frequent in men than women [8].

I.3.1. Classification

I.3.1.1. Anatomical

CCA is usually classified according to the anatomical localization as intrahepatic (iCCA), perihilar (pCCA), and distal (dCCA) (Figure I.8) [41, 45]. iCCA involves both hepatic ducts and proximal bile ducts, pCCA the perihilar bile duct, and dCCA the common bile duct [8]. pCCA is the most common type (~50%) followed by dCCA (~40%) and iCCA (~10%) [41].

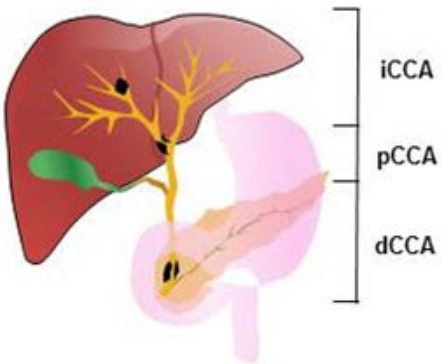

Figure I.8. Anatomical localization of CCAs. Schematic figure showing the types of CCA according to the anatomical classification [41].

I.3.1.2. Morphological

Based on the gross appearance, iCCAs may exhibit three basic growth morphological patterns: *i*) mass lesion formation or “mass forming (MF)” in the liver parenchyma, *ii*) flat or nodular sclerosing growth of the affected bile duct with thickening of the duct wall and surrounding tissue and luminal stenosis, also named as “periductal infiltrating” (PI), and *iii*) intraductal growth (IG) in the bile duct lumen (Table I.1) [46-48].

CCA Subtype	Dimensions	Location (Intra or Extra-hepatic)	Pathology	Method of Spread
Mass forming	Central mass; depends on location (IH up to 15 cm; EH 1–2 cm)	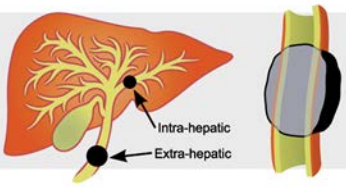	• Gray white mass • Poor cellular differentiation • Well defined, wavy, or lobulated borders • May have central fibrosis and necrosis	• Grows outward into lumen • Invades liver parenchyma through peribiliary venous plexus • Intrahepatic metastasis is common in advanced stages
Periductal-infiltrating	0.5–6 cm long (up to 1cm in the case of EH tumors)		• Concentric thickening of bile duct wall • Later stages appear branch-like • Usually highly differentiated	• Invades bile duct wall • Spreads along axis of bile ducts
Intraductal growing	Usually small and flat; later stages may fill bile duct lumen		• Tumors within lumen • Frond-like foldings	• Spreads superficially along mucosal surface • Sloughing of tumor cells can initiate secondary tumors • Invasive intraductal CCA can also occur

Table I.1. Classification of CCAs according to the tumor morphology [48].

Growth patterns similar to PI or IG can be observed in pCCA and dCCA. However, pCCA usually adopt a nodular/PI growth pattern that represents the most frequent form (>80%) [49-51]. MF-iCCA generally occurs in chronic non-biliary liver diseases and arises in peripheral small bile ducts, whereas PI and IG types exclusively involve large-hepatic bile ducts [52].

I.3.1.3. Histological

Histologically, the vast majority of pCCA and dCCA are mucinous adenocarcinomas. In contrast, iCCAs are highly heterogeneous tumors [52-55]. Thus, iCCAs show two main histological subtypes, reflecting their anatomical origin along the intrahepatic biliary tree: *bile ductular type (mixed)* arising from small intrahepatic bile ducts and *bile duct type (mucinous)* arising from large intrahepatic bile ducts [52-55]. Interestingly, this histological subclassification corresponds to different clinico-pathological features. The *bile ductular type (mixed)* iCCAs display an almost exclusively MF growth pattern [52-55], and are frequently associated with chronic liver diseases (i.e. viral hepatitis or cirrhosis) [56]. Notably, *bile ductular type (mixed)* iCCAs share clinico-pathological similarities with CK19-positive hepatocarcinoma (HCC) [54, 57].

I.3.1.4. Cells of origin

CCAs of different locations exhibit pronounced heterogeneity, suggesting a potential different cellular origin [54]. The cell of origin is denominated as the normal cell that suffers the first cancer-causing mutation [58]. Possible cells of origin are hepatic stem cells, immature NCAM positive (NCAM+) cholangiocytes, mature (NCAM-) interlobular cholangiocytes, and peribiliary gland cells [59]. Additionally, the relationship between iCCA and combined HCC-CCA (cHCC-CCA) with hepatic progenitor cell (HPC) features highlights the potential participation of HPC in the development and progression of iCCA (Figure I.9) [54, 60].

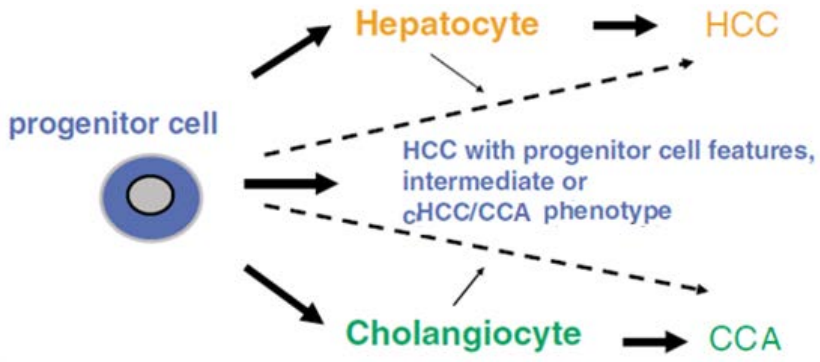

Figure I.9. Differentiation process of progenitor hepatic cells into hepatocyte, cholangiocyte or intermediate cells, which may pathologically become transformed into HCC, CCA or cHCC/CCA [60].

I.3.2. Risk factors

Several risk factors have been described for CCA, but however, most of the patients do not show any of them associated [41]. The most relevant are cirrhosis, viral hepatitis B and C, PSC, liver fluke infection, hepatolithiasis, biliary malformations and congenital diseases, such as choledocal cysts, Caroli's disease and congenital hepatic fibrosis. Moreover, general cancer risk factors such as elder-age, smoking, obesity or diabetes have also been described (Table I.2) [61-64]. Ethnic and environmental factors may also have important influence, particularly in the case of liver flukes. Hepatobiliary flukes such as *Opisthorchis viverrini* or *Clonorchis sinensis* are the main risk factors in Eastern regions and the leading cause of the high CCA incidence in these countries, due to their tradition of eating uncooked fish [44, 48, 65, 66]. Chronic exposure to toxins and/or chemicals may also be risk factors for CCA. Thus, the deposition in the liver of the radiographic agent *thorotrast* and the long-term exposure to high levels of chemicals such as *dichloromethane* and *1,2-*

dichloropropane have been shown to correlate with the development of CCA [67].

	iCCA	pCCA	dCCA
Risk factors	Primary sclerosing cholangitis (PSC), flukes, hepatolithiasis, genetic polymorphisms, Caroli's disease or choledochal cysts. Others: alcohol, smoking, fatty liver disease, diabetes, toxins, etc. Note: the majority of patients with CCA do not exhibit any of these risk factors.		
	Hepatitis C and B, cirrhosis and flukes	Mainly PSC	

Table I.2. Known risk factors for CCA [41].

I.3.3. Symptoms and diagnosis

CCAs are mostly asymptomatic in early stages of the disease. Thus, they are generally diagnosed in advanced stages, when the disease is widespread to other organs. Symptoms such as cholangitis, pruritus [68], jaundice, weight loss, abdominal pain, nausea/vomiting and fever may appear during the tumor progression [62]. Diagnosis is usually made by combining (Table I.3) [41]: *i*) imaging methods (Figure I.10) [i.e. computed tomography (CT), magnetic resonance imaging (MRI), endoscopic retrograde cholangiopancreatography (ERCP) or endoscopic ultrasound (EUS)], *ii*) analysis of non-specific serum tumor markers [i.e. carcinoembryonic antigen (CEA) and carbohydrate antigen 19-9 (CA19-9)], and *iii*) histological analysis of tumor biopsies.

<table>
<tr><th></th><th></th><th>iCCA</th><th>pCCA</th><th>dCCA</th></tr>
<tr><td rowspan="6">Diagnosis</td><td rowspan="2">Symptoms</td><td colspan="3">Non-specifics: cachexia, abdominal pain, weight loss, fatigue</td></tr>
<tr><td></td><td colspan="2">Usually diagnosed because of biliary obstruction.
Others: jaundice, pruritus and cholangitis</td></tr>
<tr><td>Markers</td><td colspan="3">Non-specific (combinations are suggested): CA19-9, CEA and AFP in serum, and CK7 in tissue. Other candidate markers: CA125, CK19, CYFRA21-1, MUC5AC, CA242, etc. in tissue.</td></tr>
<tr><td rowspan="3">Imaging</td><td colspan="3">CT and cross-sectional imaging studies</td></tr>
<tr><td rowspan="2">MRI and biopsy.
PET indicated to detect metastases.</td><td colspan="2">MRC</td></tr>
<tr><td>PCT → cytology is obtained</td><td>ERCP and EUS → cytology is obtained by both methods</td></tr>
</table>

Table I.3. Symptons and approaches employed for the diagnosis of iCCA, pCCA and dCCA [41].

Abbreviations: CA19-9: carbohydrate antigen 19-9; CEA: carcinoembryonic antigen; AFP: alpha-fetoprotein; CK7: cytokeratin 7; CA125: cancer antigen 125; CYFRA21-1: CK19 soluble fragments; MUC5AC: Mucin 5AC, oligomeric mucus/gel-forming; CA242: tumor marker antibody; CT: computed tomography; MRI: magnetic resonance imaging; PET: positron emission tomography; PCT: percutaneous transhepatic cholangiography; ERCP: endoscopic retrograde cholangiopancreatography; EUS: endoscopic ultrasound.

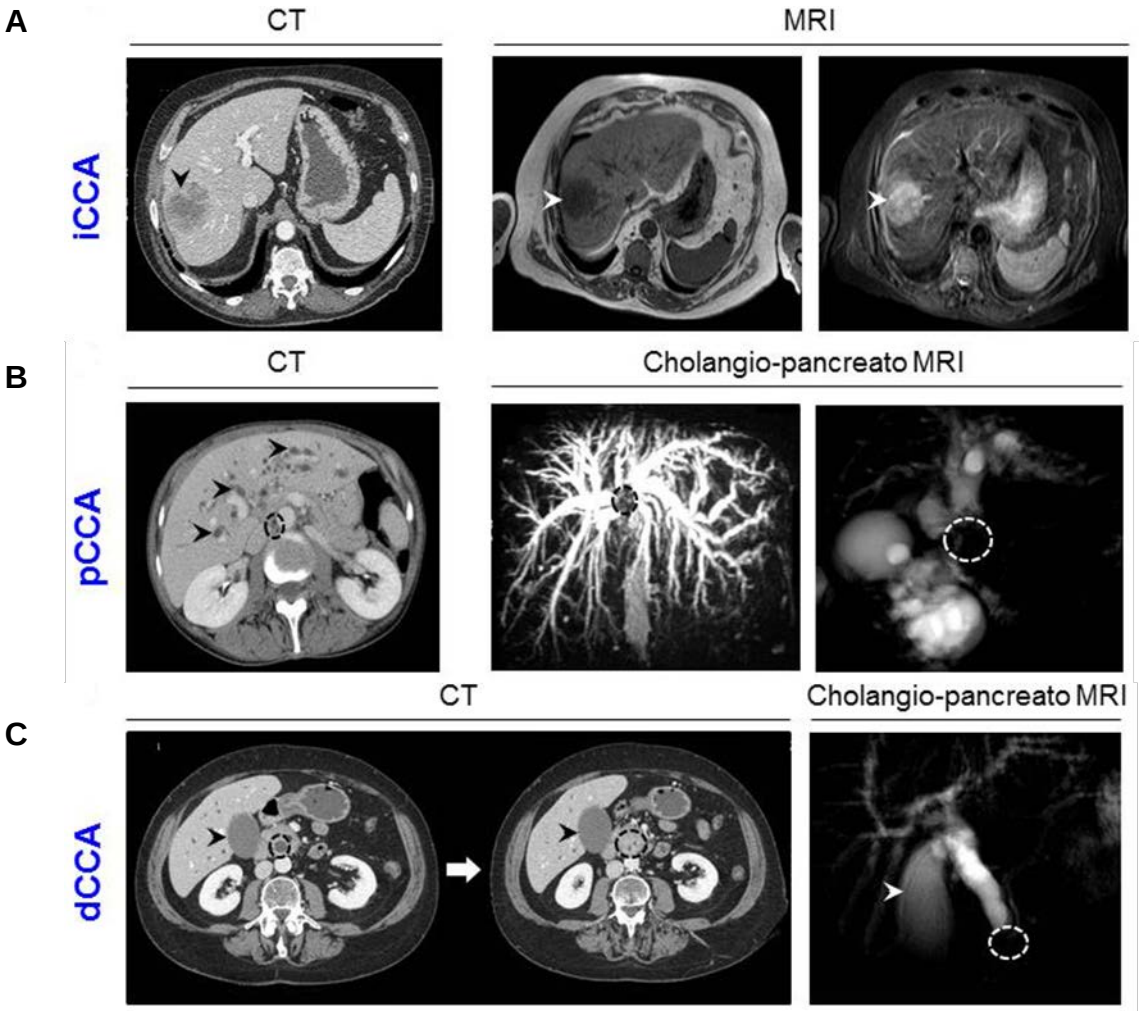

Figure I.10. Diagnostic imaging methods for CCA. (A) Images of intrahepatic CCA (arrow) by computerized tomography (CT) and magnetic resonance imaging (MRI). (B) Images of perihilar CCA (circle) by CT [dilatated bile ducts within the liver are shown (arrows)] and by cholangio-pancreato MRI. (C) Images of distal CCA (circle) with extended gallbladder (arrow) by CT (two sequential images) and cholangio-pancreato MRI [41].

I.3.4. Therapy

CCAs are usually asymptomatic. They are generally diagnosed when the tumor is at an advanced stage and no possibilities of resection are possible due to its size and/or dissemination status [8, 44, 69, 70].

I.3.4.1. Surgery

Currently, the only potential curative options for CCA are the complete surgical resection of the tumor or the liver transplantation, although chances of recurrence are high [41]. Surgical resection of the tumor is indicated for those patients that follow a strict criteria based on tumor size, vascular involvement, metastasis, presence of liver cirrhosis and/or dysfunction, portal hypertension and the general condition of the patient [71]. Thus, CCAs are resectable if the vascular and biliary ductal involvement is limited to one lobe of the liver and if there is no extrahepatic disease in patients who are suitable for surgery [72]. However, the 5- and 10-year survival rate after surgery is low.

I.3.4.2. Chemotherapy

Classical chemotherapies are mainly palliative due to the high chemoresistance of CCA tumors. CCA tumors have a multidrug resistance (MDR) phenotype based on the activation of different mechanisms of chemoresistance (MOC). In healthy cholangiocytes, MOCs are involved in the cell defense against toxic compounds [73]. However, in CCA these mechanisms enhance pharmacological chemoresistance. Briefly, they include impaired uptake of of sorafenib by inactivating mutations in organic cation transporter-1 (OCT-1) [74], as well as methotrexate, taxane and imatinib by organic anion-transporting polypeptide-1, A2 (OATP1A2) downregulation, implicated in lowering the intracellular amount of drug [75]. It has also been reported a poor response to gemcitabine and 5-fluorouracil (5-FU) associated with low expression of equilibrative nucleoside transporter 1 (ENT1) [76, 77] or inactivation of enzymes

such as thymidine phosphorylases (TPs) [78]. CCA chemoresistance has also been associated with reduced uptake of cisplatin due to modified expression of cationic aminoacid transporter 1 (CTR1)[79] and upregulation of B-cell lymphoma 2 (Bcl2) family members [80].

Furthermore, CCA chemoresistance is not only due to drug transport impairment, but also to strategies directed to repair or skip the damage produced by drugs, such as DNA lesions, mismatches, insertions and deletions. In CCA, DNA repair has been reported to be increased based on the upregulation of uracil-DNA glycosylase-1 (UNG1) [77]. On the other hand, DNA erroneous insertions or deletions in CCA are skipped because of a downregulation of proteins implicated in the mismatch repair (MMR) system, transforming CCA into a tumor with genetic instability, poorer prognosis and higher chemoresistance [81, 82].

I.3.4.3. Palliative

Palliative therapies such as biliary stent placement and/or photodynamic therapy (PDT) are commonly employed in patients with CCA [61, 83]. Endoscopic stent placement is employed to restore the biliary drainage and relief cholestasis [84]. PDT can also improve quality of life [85, 86]. On the other hand, since radiation is associated with significant morbidity in these patients (i.e. biliary strictures, hepatic decompensation, etc.) it is not generally recommended for CCA [87].

I.3.5. Genetics and epigenetics

I.3.5.1. Gene mutations

CCAs are characterized by genomic instability and gene mutations. However, general genomic studies are often limited to selected classical oncogenes and tumor suppressors [88]. Regarding chromosomal instability, iCCA has been associated to copy number losses on chromosomal arms 1p, 4q, 8p, 9p, 17p and 18q, and copy number gains on chromosomal arms 1q, 5p, 7p, 8q, 17q and 20q [88].

On the other hand, several genes downstream epidermal growth factor receptor (EGFR), including *EGFR*, are found mutated in CCA: *i*) activating mutations in *EGFR* (~15-20%) [89, 90], *ii*) hotspot activating missense mutations (9-32%) in phosphatidylinositol-4,5-bisphosphate 3-kinase catalytic subunit alpha (*PIK3CA*) [91, 92], and *iii*) gain of function mutations in Ki-ras2 Kirsten rat sarcoma viral oncogene homolog (*KRAS*, 8-54%) [93, 94].

Other frequent gene mutations are found in *TP53* (eCCA: 45%, iCCA: 35%), *KRAS* (eCCA: 40%, iCCA: 24%), *ERBB2* (eCCA: 25%), *SMAD4* (eCCA: 25%), *FBW7* (eCCA: 15%), *CDKN2A* (eCCA: 15%), *CDKN2B* (eCCA: 15%), *ARID1A* (iCCA: 20%), *IDH1* (iCCA: 18%), *MCL1* (iCCA: 16%) and *PBRM1* (iCCA: 11%) [95]. All the genetic alterations mentioned here, and many others identified also in CCA, have a deregulating effect in key networks, such as DNA repair, tyrosine kinase signaling, epigenetic remodelling factors, and so on. Among the altered key signaling pathways, a key pathway in cholangiocyte differentiation and biliary duct development, Notch, has been described to be deregulated in many cancers, including CCA, where it induces proliferation [96, 97]. Notch receptors (Notch 1-4) are usually overexpressed in CCA [96, 98]. Notch-4

overexpression has been correlated to poor survival in CCA patients[96] and the Notch inhibitor protein FBW7 is frequently inactivated by mutation in CCA [99].

Recurrent genetic variants have also been identified in the promoter of the human telomerase reverse transcriptase (*TERT*) in CCA [100]. Additionally, fibroblast growth factor receptor 2 (FGFR2) fusion gene products have also been reported, which are rare genetic alterations that have not been described in other liver cancers [101]. *FGFR2* may fusionate with other genes creating mixed genes such as *FGFR2-BICC1* [102, 103], *FGFR2-KIAA1598* [102], *FGFR2-TACC3* [103], *FGFR2-AHCYL1* [102], *FGFR2-MGEA5* [104], *FGFR2-KCTD1*[105] and *FGFR2-TXLNA* [105]. Those fusions facilitate oligomerization and FGFR2 kinase activation, which result in increased cell proliferation [101].

I.3.5.2. Epigenetic alterations

Epigenetic abnormalities associated to DNA methylation, histone modifications (i.e. acetylation/deacelylation) and microRNAs (miRNAs) dysregulation have been described in CCA and seem to play a key role in the etiopathogenesis of this cancer.

Patterns of aberrant DNA methylation have been reported in CCA, which affects complete chromosomes, such as a highly predominant hypermethylation on chromosome 2 or on the X-chromosome [106]. The expression of different genes has been described to be dysregulated in CCA due to promoter hypermethylation [107-110]. Several candidate genes of cancer-relevant signalling pathways have been identified. This is the case of the wingless and integration site (Wnt) signaling pathway target genes such as secreted frizzled-

related protein (*SFRP*) members (*SFRP1*, *SFRP2*, *SFRP4*), *DKK2*, *WNT3A* and *SOX17* [106]. Another hypermethylated gene in CCA is suppressor of cytokine signaling 3 (*SOCS3*), which downregulation is responsible for sustaining the interleukin-6/signal transducer and activator of transcription 3 (IL6/STAT3) signaling and for enhancing the expression of the prosurvival gene myeloid cell leukemia (*MCL1*), which results in survival of CCA cells [111].

According to these data, new epigenetic therapeutic strategies have been studied in order to reduce the DNA hypermethylation pattern in CCA. The most studied approach is the inhibition of DNA methyltransferase (DNMT) 1 activity [112]. The archetypal drugs used to inhibit DNMTs and thus promote genomic DNA demethylation are the azanucleosides azacytidine (5-azacytidine) and decitabine (2'-deoxy-5-azacytidine) [113]. Thus, DNMT1 inhibitors have successfully been used to revert in some CCA cell lines the expression of some downregulated genes, such as *SFRP1*, *SFRP2*, *SFRP4*, *DKK2*, *WNT3A*, SOX17[106] *and SOCS3* [111]. The recovery of SOCS3 expression, for example, resulted in a reduction of CCA cell survival [111].

Histone acetylation is another epigenetic mechanism altered in CCA [107]. Some histone deacetylases (HDACs) appear to be upregulated, and induce cell proliferation [114]. Combined pharmacological and molecular treatment with 5-FU and HDAC inhibitors (i.e. valproic acid, suberoylanilide hydroxamic acid) reduced the tumor capacity of some CCA cell lines [114]. In particular, overexpression of HDAC6 has been reported to promote the shortening of the primary cilium and the subsequent hyperproliferation in CCA, and experimental (shRNA) and pharmacological (tubastatin-A) inhibition restored the primary cilium and decreased CCA cell growth [115].

Some miRNAs contribute to cholangiocarcinogenesis through inhibition of tumor suppressor genes or by acting as oncogenes themselves [116]. Upregulation of miRs let-7a, 21, 26a, 34a, 421 and 494 has been reported in CCA, promoting cell proliferation mechanisms [40, 117, 118]. On the other hand, miRs 144 and 138 are downregulated in CCA, and their overexpression attenuate cell proliferation, migration and invasion [119]. Additionally, miR-148a and miR-152, reduced in CCA cells, decrease DNMT-1 expression, which may inhibit cell proliferation [120].

Epigenetic changes are early events in the tumorigenesis. Therefore, novel approaches approaches for early detection and treatment are necessary.

I.3.5.3. Developmental pathways involved in cholangiocarcinogenesis

Different developmental pathways become activated during the process of cholangiocarcinogenesis and play a key role in the proliferation, migration and survival of the tumor cells. The Wnt/β-catenin and TGFβ1 pathways are among those with high activity.

The Wnt/β-catenin signaling pathway has been described to be relevant in the development of the hepatobiliary system [5]. The canonical Wnt/β-catenin pathway is activated by the binding of Wnt ligands to frizzled receptors (Fzd) [121]. This interaction creates a chain reaction by which β-catenin activates through the phosphorylation of residues threonine (Thr) 41 and serine (Ser) 45 (Figure I.11) [122]. Thus, β-catenin enters the nucleous to initiate the transcription of its target genes, which are related to proliferation, differentiation, migration, and so on [122]. However, when the pathway is repressed by wnt

ligand inhibitors (SFRPs, DKKs,…) or other mechanisms [123], β-catenin is also phosphorylated but in residues Ser33, Ser37 and Thr41, which enables its proteasomal degradation [122].

Different Wnt ligands bind to Fzd receptors favoring the cytoplasm accumulation and nuclear translocation of β-catenin [124], which leads to the formation of a complex of proteins that promotes the transcription of genes involved in carcinogenesis [125]. β-catenin is overexpressed in CCA [126] and intrinsic activating mutations have been described in few patients (8,3%: 2 of 24 iCCA patients analyzed) [127, 128]. The high expression of Wnt ligands (i.e. Wnt3a, Wnt5a, Wnt7b, Wnt10a) in the inflammatory microenvironment of CCA is due, at least in part, by their secretion by activated macrophages [129, 130]. Thus, experimental inhibition of Wnt ligands release from macrophages reduces CCA tumor growth in a mouse xenograft model [130].

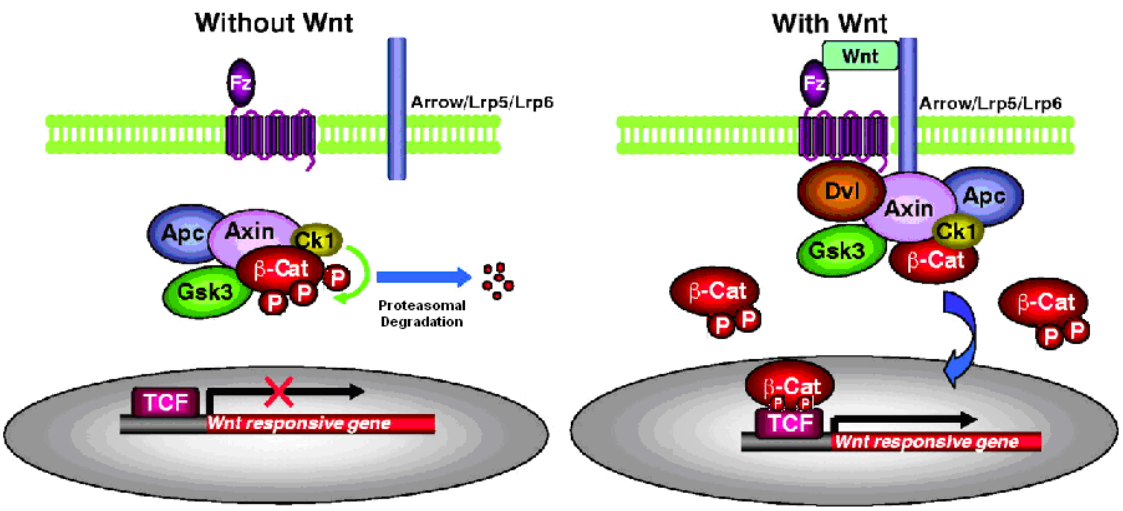

Figure I.11. Scheme of the Wnt/β-catenin signaling pathway (modified from He X, 2004, Development).[131]

The activity of TGFβ, similarly to Notch, Wnt, bone morphogenetic protein (BMP) and FGF, is necessary for the formation of cholangiocytes from hepatoblasts in embryonary development [5]. TGFβ proteins, for instance, are known to be ligands for serine-threonine kinase receptors I (TβRI) and II (TβRII) [132]. They are extracellularly secreted in an inactive state as prohormone, and utterly activated by cleavage due to the action of integrin-αvβ6, mannose-6-phosphate receptors (MPRs), plasmin, metalloproteinases (MMPs 2 and 9), and thrombospondin-1 (TSP1) [132]. The activated TGFβ proteins bind to their receptors and activate a Smad-protein phosphorylation-cascade, which leads to the final activation of the transcription of their target genes (Figure I.12) [132]. Those target genes are implicated in the regulation of the deposition of the extracellular matrix (ECM), fibrogenesis, cellular growth, differentiation and modulation of immune response [132].

Among the TGFβ proteins the TGFβ1 plays a key role in the fibrogenesis of some liver cancers, such as HCC and hepatoblastoma [133, 134]. In adition, TGFβ1 promotes cell growth, invasion and metastasis of CCA [135, 136]. In CCA, TGFβ1 decreases the expression of miR-29a, which reduces cell growth and metastasis by inhibiting HDAC4 [135]. Moreover, in a thioacetamide (TAA) drug-induced rat model of CCA, TGFβ1 neutralization by anti-TGFβ-monoclonal antibodies reduces CCA growth [137].

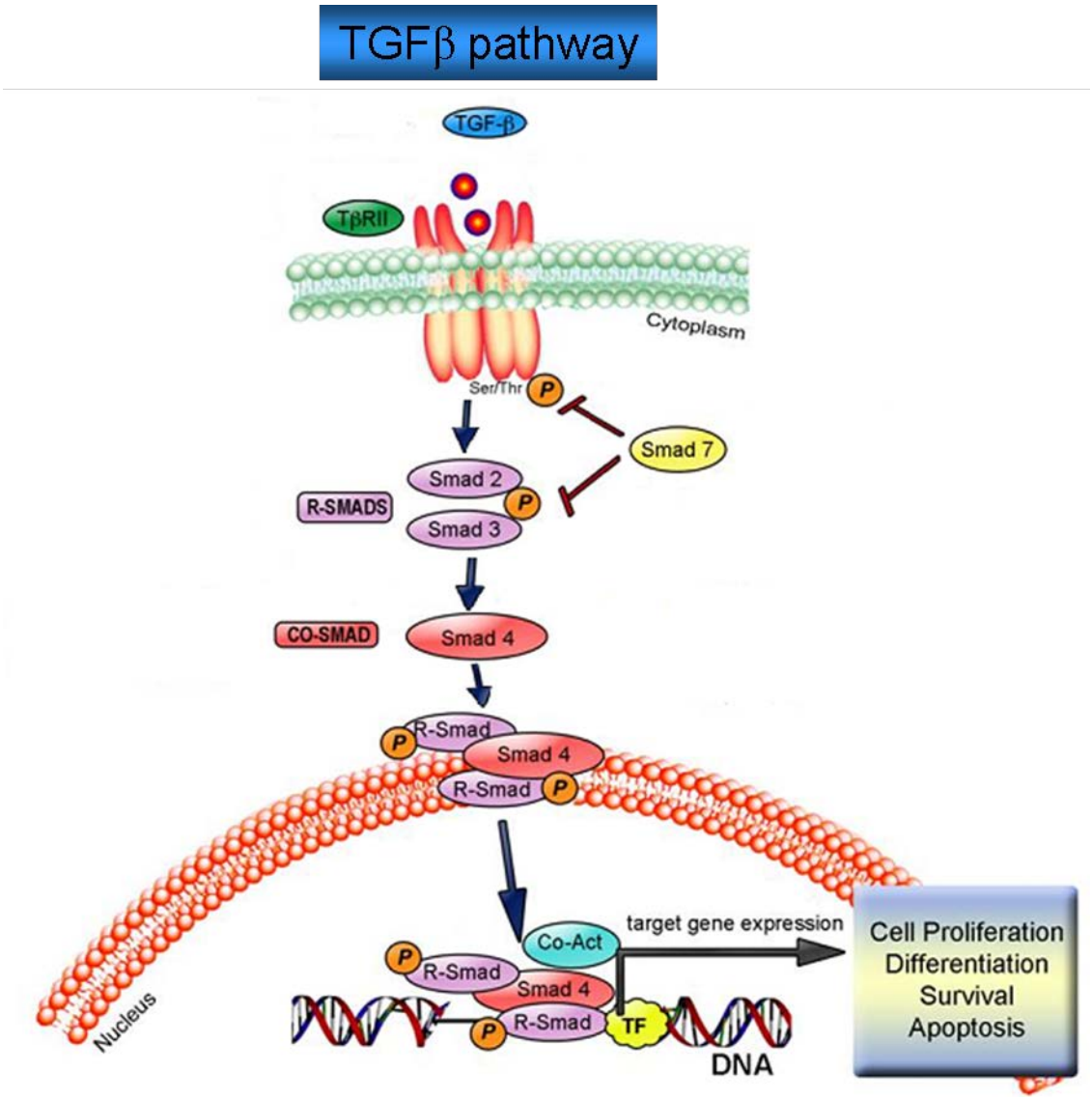

Figure I.12. Scheme of the TGFβ signaling pathway (modified from the website of www.intechopen.com/books, Villapol S *et al*, 2013, DOI: 10.5772/53941).

I.4. The transcription factor *SOX17*

I.4.1. SOX proteins: general features

The "sex-determining region of the Y-chromosome" (*SRY*) was the first *SOX* gene discovered in humans and mice [138, 139]. SRY protein presents a "high-mobility group" (HMG) key for DNA-binding and common in all *SOX* family members [140]. The evolutionarily conserved HMG box is a 79 amino acid (aa)

DNA-binding motif [140] that mediates DNA-binding on a common consensus site [i.e. (A/T)(A/T)CAA(A/T)G] but with different levels of efficiency [141]. The HMG box of SOX proteins contains two independent nuclear localization signals and one leucine-rich nuclear export signal, which regulate the dynamic nucleo-cytoplasmic shuttling of SOX proteins and result in the diverse subcellular distribution of SOX proteins during development [142-144]. In vertebrates, the SOX family includes more than 20 genes that are phylogenetically grouped in different subclasses (A-H) (Figure I.13) [145, 146].

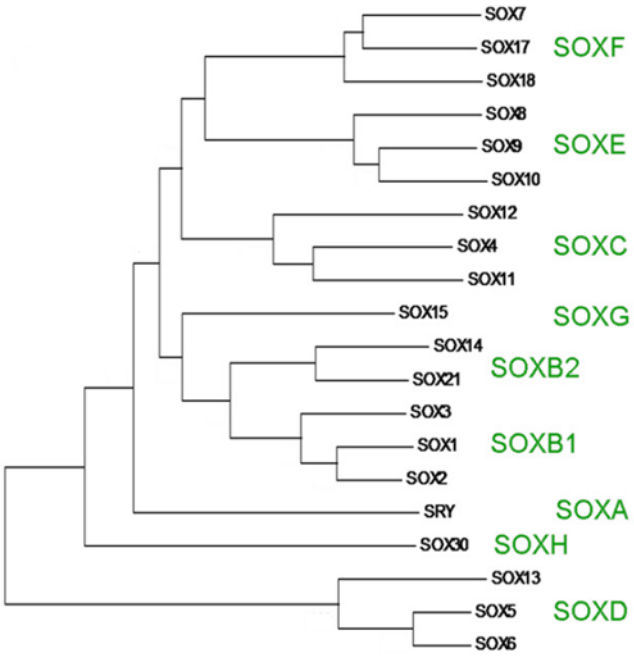

Figure I.13. A rooted phylogeny for the human SOX full-length aminoacid sequences [147].

Evidence from gain-of/loss-of-function studies in *SOX* genes revealed that they play key roles in tissue homeostasis, organogenesis and cell fate decision from embryonic to adult stages (Figure I.14) [147-150]. SOX proteins may also be regulated at 3 main levels: *i*) gene expression, which is cell-type and time specific within the developmental stages [149], *ii*) post-transcriptional and/or

post-translational modifications, altering their transactivation/transrepression features [151], and *iii*) regulation of recruited partner proteins, which not only influence the specific recognition of the binding sites of SOX-partner complexes on the target genes, but also determine transcription activities and significantly enhance the activation/repression potential [149, 152].

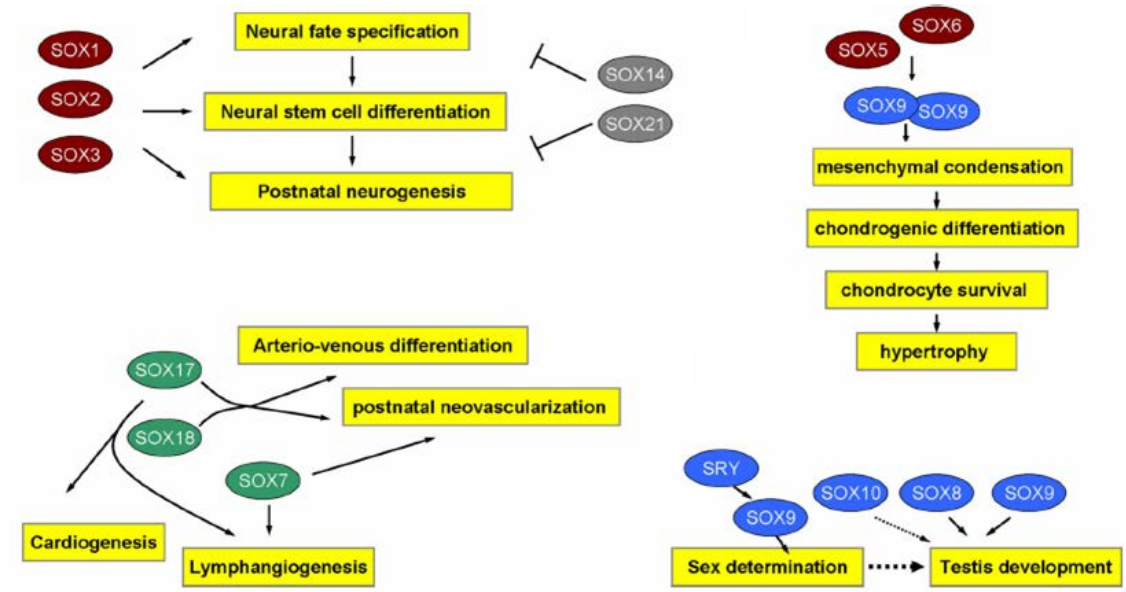

Figure I.14. The multiple roles of SOX proteins during development [147].

I.4.2. SOX proteins and cancer

Many of the proteins governing the embryonic development are also involved in carcinogenesis. Similarly, different genes primarily described as crucial for carcinogenesis (i.e. oncogenes and tumor suppressor genes) are now also identified as essential for embryogenesis, indicating that both processes are intimately related [153]. Some examples of these events are the signal transduction pathways sonic hedgehog (Shh), TGFβ, Wnt/β-catenin and Notch, among others [153]. This close relationship has led to the proposition of the lineage-dependency theory, which argues that the cellular mechanisms that

govern lineage proliferation and survival during development might also underlie tumorigenic mechanisms [154]. Such a model could also be applied to the SOX family genes (Figure I.15) [153, 155].

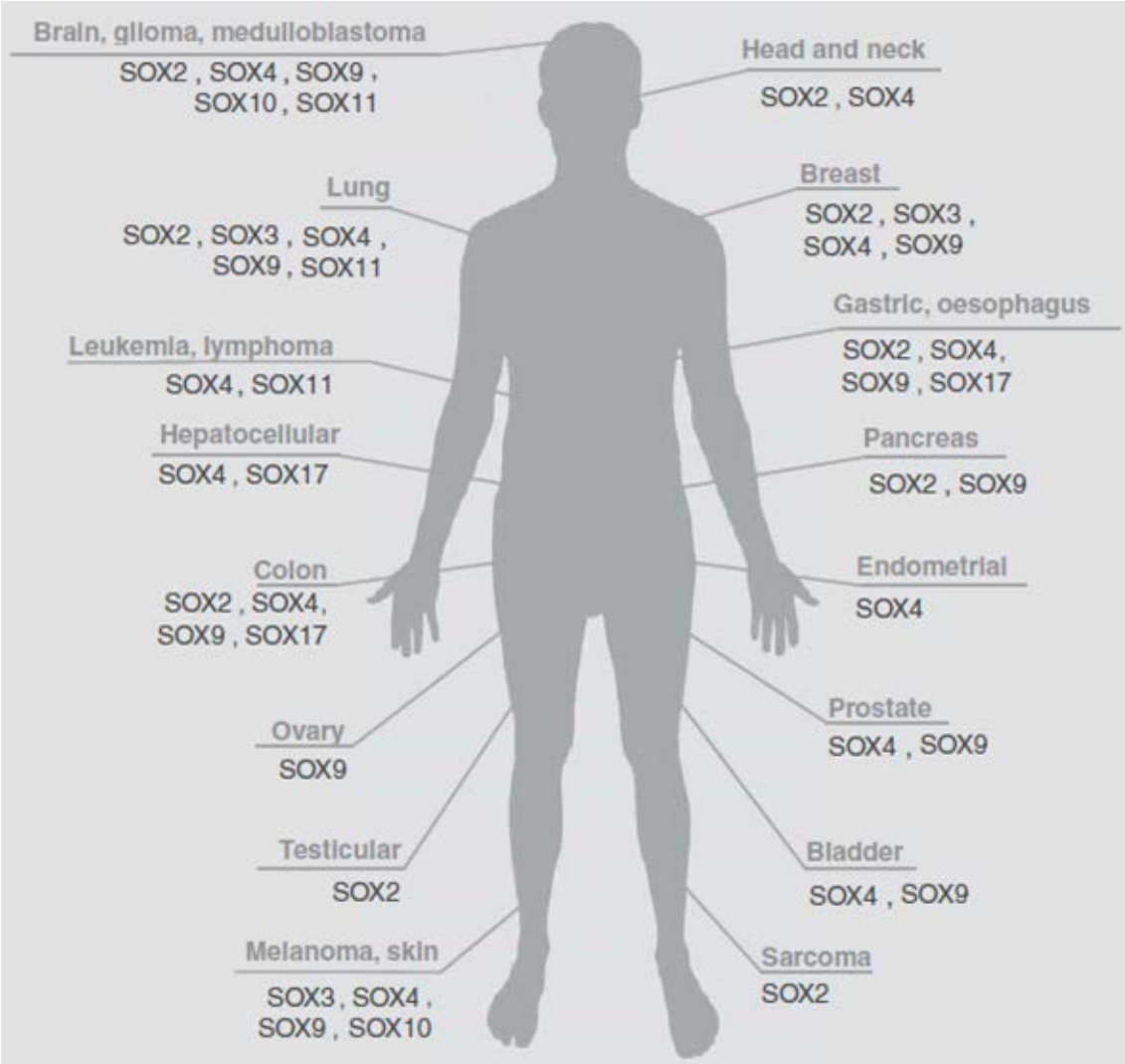

Figure I.15. Schematic representation of the *SOX* genes envolved in various cancer [153].

I.4.2.1. Oncogenic SOX proteins

SOX family members may act as oncogenes or tumor suppressor genes, and sometimes as both depending on the cellular context.

A subset of tumor cells, termed cancer stem cells (CSCs), has the ability to self-renew and to generate the diversity of cell types comprising the tumor. Accordingly, these cells carry stem-like properties and have the ability to sustain tumorigenesis continually [156]. CSCs are characterized by high levels of SOX2 expression, which is a major stemness marker. SOX2 expression has been reported in different solid tumors, such as cervical carcinomas, sarcomas, gliomas, and breast and colorectal cancer [157-160]. SOX2 confers a dedifferentiated phenotype and may promote metastasis [158].

SOX4 was found among the set of genes uniquely upregulated in most cancer types relative to the normal tissues from which they arise, thereby contributing to a general gene expression signature of cancer [161]. SOX4 is upregulated in human acute leukemia [162], bladder tumors [163], lung cancer [164], in colorectal oncogenesis and is correlated with poor outcome in these patients [165, 166]. Interestingly, experimental knock-down of SOX4 induces apoptosis and growth suppression of certain tumor cells [167, 168].

SOX9 is overexpressed in several human malignancies, such as brain, pancreas, colon, lung and prostate cancer [169]. The tumorigenicity of this transcription factor is, in part, due to its capability of regulating the CSC phenotype, preferentially in breast and brain tumors [170, 171]. In breast cancer cells, a high expression of SOX9 promotes the epithelial-to-mesenchymal transition (EMT) and metastases, and is associated with a poorer patient survival [170]. In spite of these observations, the role of SOX9 in oncogenesis is controversial and could be dependent on the cell context, even within the same type of cancer. This controversy may also be observed in breast cancer [172],

melanoma [173, 174], prostate cancer [175, 176], and bladder cancer [177, 178].

SOX11 appears to be a highly specific marker for mantle cell lymphoma (MCL), which is potentially useful for the differential diagnosis of MCL from other B-celllymphomas [179, 180]. Additionally, SOX11 is also overexpressed in lung cancers [181]. However, its role in glioma is controversial; some authors reported that SOX11 expression in the adult brain is reactivated during tumorigenesis [182], whereas others indicated that SOX11 inhibits tumorigenesis by inducing neuronal differentiation [183].

I.4.2.2. Tumor suppressor SOX proteins

Different SOX proteins have also a tumor suppressor ability. In particular, SOX7 acts as a tumor suppressor gene in prostate, colon, lung, and breast cancers through its involvement in cell death, movement, invasion and proliferation [184]. SOX15 (also known as SOX20) has also been identified as a potential tumor suppressor gene that inhibits the Wnt/β-catenin pathway in pancreatic ductal adenocarcinoma (PDAC) [184].

On the other hand, In mesenchymal breast cancer and in melanoma cells ectopic expression of SOX3 promotes the mesenchymal-to-epithelial transition (MET) program and impairs the cell mobility and invasion, suggesting that SOX3 has a tumor supressor role [185].

The role of SOX17 in cancer has been less extensively studied, but its potential role as tumor suppressor has been indicated in some tumor types.

I.4.3. SOX17

The human SOX17 gene is located in a region of the chromosome 8p11.23 and has a length of ~3,900 base pairs [186]. Two DNA exons comprise the mRNA product with a coding region of 2,300 base pairs [186]. The promoter region of the *SOX17* gene contains a frequently methylated CpG island that plays a role in regulating *SOX17* gene expression [186]. The human SOX17 protein length is composed by 414 aa, characterized by an N-terminal HMG domain (67-138 aa) and a C-terminal transactivation domain (195-413 aa) (Figure I.16) [186].

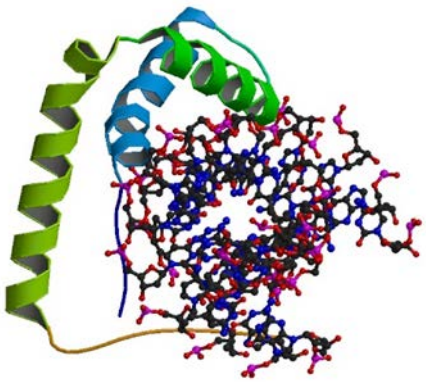

Figure I.16. Three-dimensional structural representation of the SOX17 protein bound to DNA (acquired from the website of Research Collaboratory for Structural Bioinformatics Protein Data Bank, RCSB PDB, www.rcsb.org).

I.4.4. SOX17 and biliary system development

During embryogenesis, *SOX17* is transiently expressed in the definitive endoderm during the initial phase of differentiation from mid-streak (7-day of gestation) to the early somite stages [187]. Interestingly, during the early somite (8.5-day of gestation) stages, *SOX17* is re-expressed in the posterior-ventral foregut, where the progenitors of the gallbladder/bile duct are found [188] and is

maintained in the gallbladder primordium during the perinatal period [189]. In mice, *Sox17*-null embryos show a drastic reduction in endodermal cell population, and fail to develop beyond 10.5-day of gestation [187]. Cell-autonomous Sox17 function in the foregut endoderm is required for the specification and differentiation of gallbladder/bile duct progenitors during foregut morphogenesis [16, 188]. *Sox17* haploinsufficiency causes tissue-autonomous defects in the morphogenesis and maturation of gallbladder and bile duct epithelia in mice, leading to congenital biliary atresia and subsequent acute hepatitis in late fetal stages [189]. The loss of *Sox17* expression, not only produces gallbladder agenesia, but it also induces ectopic development of pancreatic tissue in the common bile duct [16, 188]. On the other hand, excessive *Sox17* expression induces an ectopic biliary system development in positive PDX1 domains [16].

I.4.5. Other SOX17 functions

SOX17 promotes the inhibition of the pluripotency of the embryonic stem cells. When embryonic stem cell pluripotency is achieved, octamer-binding transcription factor 4 (Oct4) switches from the Sox2 to the Sox17 promoter [190]. This switch allows the cells to turn off the pluripotency and generate a subset of endoderm-expressing Sox17 and Hex cardiac fate cells [190]. Additionally, SOX17 has an essential function in vascularization and arterial development. Sox17 is essential for the acquisition and maintenance of arterial identity, through Notch signaling activation (Figure I.17) [191].

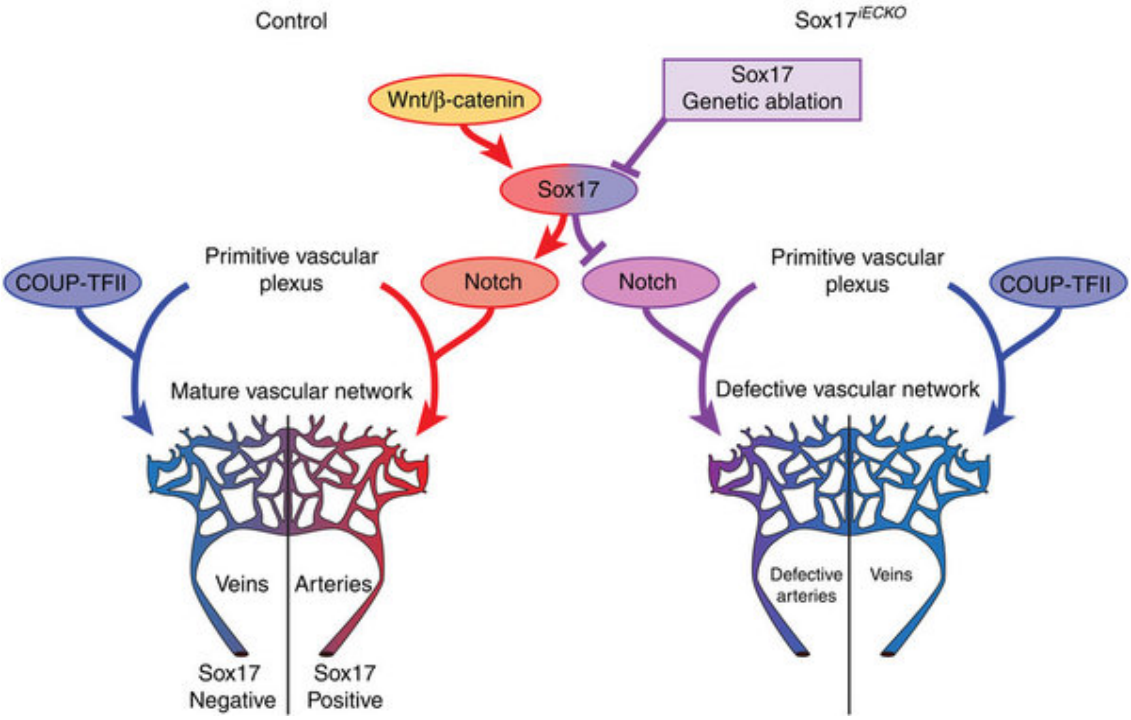

Figure I.17. SOX17 regulation of Notch signaling and artery development [191].

I.4.6. SOX17 and diseases

Abnormalities of *SOX17* expression are not only relevant for the development of the biliary system, they are also important in several pathologies. Some mutations have been observed in *SOX17*, which induce *SOX17* misregulation and diverse diseases. Congenital anomalies of the kidney and the urinary tract (CAKUT) represent a major source of morbidity and mortality in children and present the *SOX17* mutation c.775T>A (p.Y259N), which promotes hyperactivation of the Wnt/β-catenin signaling pathway [192]. Additionally, a heterozygous *SOX17* mutation (p.L194P) was also found in a sporadic colorectal cancer (CRC) cell line [193]. As in CRC, downregulation of *SOX17* expression is also found in other cancers, mostly due to promoter hypermethylation [194-196]. *SOX17* downregulation triggers oncogenic signals in tumors such as colon [166] and breast cancer [194].

The expression of *SOX17* is induced during the Wnt/β-catenin activation in the early stage of gastrointestinal tumorigenesis, and becomes downregulated by promoter methylation during malignant progression [197]. Hypermethylation of *SOX17* promoter has been reported in different gastrointestinal tumors such as HCC [198], gastrointestinal carcinoma [197], CRC [196] and CCA [106]. However, the particular role of SOX17 in the pathogenesis of these tumors remains unknown.

On the other hand, SOX17 is negatively related to kinesin family member 14 (KIF14) expression in HCC tissues, and thus, by downregulating KIF14 expression, SOX17 inhibits HCC cell proliferation and migration [199]. Moreover, *SOX17* expression may also be downregulated by microRNAs, such as miR-141 in esophageal cancer [200] and miR-151 in prostate cancer [201]; on the other hand, *SOX17* expression might be upregulated when miR-371-5p is overexpressed in CRC cell lines [202].

I.4.7. SOX17 and Wnt/β-catenin signaling pathway

Accumulating evidence indicates that activation of Wnt/β-catenin signaling is one of the direct causes of tumorigenesis for several types of cancer. One of the SOX17 tumor suppressor activities is its potential capacity to antagonize the Wnt/β-catenin signaling [198]. In contrast to other factors that repress the Wnt signaling, such as SFRPs and DKKs, SOX17 may inhibit this pathway at a nuclear level [166]. SOX17 can interact with the transcriptional factors T-cell factor/lymphoid enhancer factor (TCF/LEF) and/or with β-catenin [195], repressing the transcription of cell cycle and proliferation related genes, and so,

inhibiting the function of Wnt signaling pathway [203, 204]. SOX17 contains both a transactivation domain in the C-terminal and a short functional motif (DxxEFD/EQYL) thought to be involved in the interaction with β-catenin [205]. SOX17 may also promote the degradation of both TCF and β-catenin proteins [166]. In relation with this last one, SOX17 allows the triple phosphorylation of β-catenin at Ser33, Ser37 and Thr41, which enables its proteasomal degradation [206]. Furthermore, SOX17 might promote the expression of SFRP1, a Wnt ligand inhibitor, which impedes Wnt ligands to bind to the Wnt signaling Frizzled receptors [203].

II. HYPOTHESIS AND OBJECTIVES

The working hypothesis of this dissertation is that the transcription factor SOX17 may play a key role in the regulation of the biliary differentiation, and its downregulation may promote cholangiocarcinogenesis. These premises are based on the fact that: *i*) *SOX17*$^{-/-}$ mice show premature death due to alterations in the formation of the endoderm and severe biliary disorders (i.e. perinatal biliary atresia) [189], *ii*) *SOX17* promoter was found hypermethylated in CCA tissue [106], *iii*) SOX17 acts as a tumor suppressor in different cancers (i.e. breast [194], gastrointestinal [197], hepatocarcinoma [198], etc.), and *iii*) SOX17 may inhibit the protumorigenic Wnt/β-catenin pathway [198]. Thus, regulation of *SOX17* expression in CCA could have potential therapeutic value. Based on this hypothesis, the following aims of study were proposed:

I. Role of SOX17 in the differentiation of iPSC into mature cholangiocytes and in the regulation of the biliary phenotype.

II. Analysis of SOX17 expression in CCA human tissue and cell lines compared to normal controls.

III. Role of SOX17 in the pathogenesis of CCA and determination of the molecular mechanisms implicated using *in vitro* and *in vivo* (i.e. CCA xenografts in immunodeficient mice) experimental models.

IV. Role of Wnt and TGFβ ligands in the *SOX17* expression in cultured normal human cholangiocytes and molecular mechanisms involved.

V. Restauration of *SOX17* expression in CCA cells by using molecular and pharmacological demethylating tools.

III. MATERIALS AND METHODS

M.1. Human samples

Human liver samples were obtained from the Biobank of the Donostia University Hospital. The research ethical protocol was approved by the *Ethical Committee for Clinical Research of Gipuzkoa* and all patients signed a written consent for the use of their samples for biomedical research. In our study, we employed: 13 CCA human biopsies (i.e. 11 iCCAs, 1 pCCA, 1 dCCA) as well as 14 normal human gallbladder tissues.

Human liver samples were anonymously numbered and stored at -80ºC for further ribonucleic acid (RNA) isolation, and/or fixed in formaldehyde solution and embedded in paraffin for immunofluorescence analysis.

M.1.1. Total RNA extraction

Total RNA was isolated from small liver biopsies with Tri-Reagent® (Sigma). Briefly, 1 mL of Tri-Reagent® was added to every sample and homogenized by pipetting. Then samples were frozen at -80ºC. After 24 h, samples were thawed and 200 µL of chloroform (Sigma) were added to each tube. Tubes were vigorously shacked with a vortex for 30 seconds and incubated at room temperature for 10 min. Then, samples were centrifuged at 14,500 rpm for 15 min at 4°C. Subsequently, the aqueous phase was transferred into a new tube and the bottom phase was discarded. 0.5 mL of 2-propanol (Sigma) was added to the aqueous phase and incubated at room temperature for 10 min. Samples were centrifuged at 14,500 rpm for 10 min at 4°C and then the supernatant was removed. The pellet was washed with 1 mL of 75% ethanol (Sigma), briefly vortexed, and centrifuged at 14,500 rpm for 5 min at 4°C. After discarding the

supernatant, the pellet was left to dry at room temperature for 30 min. Finally, pellets were resuspended in 200 µL of *Ultrapure™ DNase/RNase-free distilled water* (Invitrogen). RNA quantification was performed by ultraviolet (UV) spectrophotometry using the NanoDrop® V3.7 spectrophotometer (Thermo Scientific, ND-1000).

M.1.2. Reverse transcription (RT)

The RNA isolated from liver biopsies was converted into cDNA by using the *SuperScript® VILO™ cDNA Synthesis Kit* (Life technologies) in a *C1000™ Thermal Cycler* (Bio-Rad). Briefly, 1 µg of total RNA was incubated in a solution containing 2 µL of 10X *SuperScript® Enzyme Mix*, 4 µL of 5X *VILO™ Reaction Mix* and up to 20 µL final volume of *Ultrapure™ DNase/RNase-free distilled water*. The RT was performed in three steps: *i*) 10 min at 25ºC, *ii*) 1 h at 42ºC, and *iii*) 5 min at 85ºC. The resultant cDNA was diluted with *Ultrapure™ DNase/RNase-free distilled water* to a final concentration of 10 ng/µL.

M.1.3. Histology

Human liver biopsies we fixed in 4% formaldehyde solution (Sigma) for 24 h and afterwards embedded in paraffin (Merk Millipore). The resultant blocks were cut in 3-5 µm slices with a microtome and used for immunofluorescence techniques (see section M.5. Immunofluorescence).

M.2. Cell cultures

M.2.1. Isolation and reprogramming of human myofibroblasts into cholangiocytes

The following studies were carried out in collaboration with Dr. Robert C. Huebert at the Mayo Clinic (Rochester, Minnesota, USA). The research protocol was approved by the *Ethical Committee for Research of Mayo Clinic* and all patients signed a written consent for the use of their samples for biomedical research.

Human myofibroblasts were isolated from biopsy specimens and then cultured and reprogrammed as previously described [207]. Briefly, isolated human myofibroblasts were transfected with vectors expressing *OCT4*, *SOX2*, kruppel-like factor 4 (*KLF4*) and myc protoncogene protein (c*MYC*) in order to induce stem cell pluripotency based on the *Sendai system* [208]. The induced pluripotent stem cells (iPSCs) were seeded in culture plates pre-coated with 0.1% Matrigel (R&D systems) and with Nutristem xeno-free/feeder free (XF/FF) culture medium (Stemgent) supplemented with 16% mTeSR1 basal medium (Stemcell Technologies), mTeSR1 5X Supplement, 50X StemGS (ScienCell Research Laboratories) and 1% Penicillin/Streptomycin (P/S).

The stepwise differentiation towards iPSC-derived cholangiocytes (iDCs) was performed by a process of temporal exposure to biliary morphogens. iPSCs were induced to definitive endoderm (DE) for 4 days using advanced Roswell Park Memorial Institute (RPMI) medium changed and supplemented daily with addition of 50 ng/mL Activin A and 50 ng/ml Wnt3a in the presence of Matrigel. For hepatic specification (HS), DE cells were treated daily with 10 ng/mL

fibroblast growth factor 2 (FGF2), 20 ng/mL bone morphogenic protein 4 (BMP4) and 50 µg/mL sonic hedgehog (SHH) for 4 days. HS cells were induced to hepatic progenitor (HP) cells for 4 days with daily exposure to 50 µg/mL SHH and 100 µg/ml recombinant Jagged-1 (JAG1). To generate iDC, HP cells were treated for 4 days with H69 media (hormone-supplemented medium in the presence of NIH/3T3 fibroblast coculture) [209] changed and supplemented daily with 100 µg/mL TGFβ, and Matrigel was replaced by collagen. All growth factors were purchased from R&D Systems.

M.2.2. Isolation of normal human cholangiocytes

Normal human cholangiocytes (**NHC**) were isolated from bordering tissue samples obtained during surgery dissection of a local hepatic adenoma at the Mayo Clinic (Rochester, MN, USA); only tissue pieces informed as normal by an experienced pathologist were employed.

The procedure to isolate and culture NHC was carried out according to a novel protocol described by our group [210]. Briefly, liver tissue was cut in small pieces (approximately 1 mm^3) and placed in a 50 mL tube. Samples were digested for 30 min in a shaker bath at 37ºC with 25 mL of Dulbecco's modified Eagle's medium/Ham's F-12 nutrient mixture (DMEM/F-12) medium (Invitrogen) supplemented with 3% of fetal bovine serum (FBS), 1% of P/S (both from Invitrogen), 0.1% of bovine serum albumin (BSA), 17 mg pronase, 12.5 mg type IV collagenase and 3 mg DNase (all three from Sigma). Digested tissue was sequentially filtered through 100 µm and 40 µm nylon meshes (Millipore, Bedford, MA). Trapped fragments between both meshes were collected, placed

in a new 50 mL tube and incubated again for another 30 min with the aforementioned solution, but substituting pronase with 13 mg hyaluronidase (Sigma). Afterwards, a second series of sequential filtrations were performed and intrahepatic bile duct units ranging from 40 µm to 100 µm were resuspended in fully supplemented DMEM/F-12 medium, named “FLASK medium” (Table M.1) and seeded on collagen-coated Cellstar flasks (Greiner Bio-One).

M.2.3. Cholangiocarcinoma human cells

We used 3 different CCA human cell lines in our experimental process:

- **EGI1** cell line was generated from a solid tumor of a 52-year-old Caucasian man with advanced malignant extrahepatic bile duct carcinoma and obtained from the “DSMZ German Collection of Microorganism and Cell Cultures”.
- **TFK1** cell line was generated from a surgical specimen of a 63-year-old Japanese man with extrahepatic bile duct carcinoma and obtained from the “DSMZ German Collection of Microorganism and Cell Cultures”.
- **Witt** cell line (also known as SK-ChA-1) was generated from a malignant ascites of a patient with primary adenocarcinoma of the extrahepatic biliary tree [211], and so, can be considered as a metastatic extrahepatic CCA cell line [212].

M.2.4. Cell culture conditions

Normal (NHC) and tumor (EGI1 and Witt) human cholangiocytes were cultured in “FLASK medium” (Table M.1). As exception, TFK1 cells were grown in a less enriched medium, which contained DMEM/F12+Glutamax™ (Gibco) with 10% FBS (Gibco) and 1% P/S (Gibco), for a better growth.

Table M.1. Composition of the FLASK medium

Reagent	Concentration	Company
DMEM/F12+Glutamax	89% (v/v)	Gibco
Fetal bovine serum	5% (v/v)	Gibco
MEM non-essential aa	1% (v/v)	Gibco
Lipid mixture 1000X	0.1% (v/v)	Sigma
MEM vitamin solution	1% (v/v)	Gibco
Penicillin/Streptomycin	1% (v/v)	Gibco
Soybean trypsin inhibitor	0.05 mg/mL	Gibco
Insulin transferrin selenium	1% (v/v)	Gibco
Bovine pituitary extract	30 µg/mL	Gibco
Dexamethasone	393 ng/mL	Sigma
T3 (3,3' 5-triiodo-L-thyronine)	3.4 µg/mL	Sigma
Epidermal growth factor	25 ng/mL	Gibco
Forskolin	4.11 mg/mL	Ascent-Scientific

All the cell types were cultured on collagen-coated 25 or 75 cm^2 flasks (Corning®) with their corresponding culture medium at 37°C and 5% CO_2. Medium was refreshed every 48 h. When cells reached confluence, the cellular passage was performed as follows: 10 mL of Dulbecco's phosphate buffered saline "DPBS" (Gibco) 1X were employed to wash the cells, prior to the addition of 1 mL of Trypsin-ethylenediaminetetraacetic acid (Trypsin-EDTA) 0.05% (Gibco) and subsequent incubation for 10 min at 37°C and 5% CO_2. Afterwards, the solution containing cholangiocytes was centrifuged at 1,500 rpm for 5 min at 4°C and the pellet resuspended in corresponding medium for subsequent seeding or in FBS with 10% dimethyl sulfoxide (DMSO) for freezing proceedings. Frozen vials were placed in a liquid nitrogen chamber for future needs.

M.2.5. Whole cell extract processing

M.2.5.1. Total RNA extraction

300,000 cells were seeded on collagen-coated 6-well plates (Life technologies) and cultured with the corresponding cellular medium for 24 h at 37ºC and 5% CO_2. Then, cells were washed with phosphatase buffered saline (PBS) 1X and 1 mL of Tri-Reagent® was added into each well. The whole cell extract was collected and stored at -80ºC. The RNA extraction method was similar to that one employed for tissue samples and previously explained in section M.1.1. The only difference relies on the resuspension water type and volume. The extracted RNA from cells was resuspended in 10 µL of DNase/RNase Free water.

M.2.5.2. Reverse transcription (RT)

1 µg of RNA was introduced in a 0.2 mL eppendorf tube. cDNA was obtained via RT with the M-MLV-RT protocol in a *C1000™* Thermal Cycler (Bio-Rad). Briefly, RNA underwent DNase treatment (1 µL of DNase I Amplification Grade + 1 µL of 10X DNase I Reaction Buffer) (Invitrogen) for 20 min at 37°C and then 1 µL of 25 mM ethylene-diamine-tetra-acetic acid (EDTA; Invitrogen) was added to each tube (10 min at 65°C, 1 min at 90°C and kept at 4°C). Then, 30 µL of RT Mix [i.e., Buffer 5X, 8 µL; Random primers (RP, 100 ng/µL), 4 µL; deoxynocleoside triphosphates (dNTPs), 4 µL; dithiothreitol (DTT), 2 µL; RNase OUT (Invitrogen), 1.2 µL; M-MLV-RT (Invitrogen 1.2 µL; dH_2O 9.6 µL)] were added to each tube and incubated under the following conditions: 37°C for 60 min, 95°C for 1 min and kept at 4°C. The cDNA obtained was finally diluted to a final concentration of 10 ng/µL.

M.3. Quantitative polymerase chain reaction

The quantitative polymerase chain reaction (qPCR) was performed in a *7300 Real-Time PCR System* (Applied biosystems) with *iQ™ SYBR® Green Supermix* (170-8880, Bio-Rad). Primers were purchased from Sigma (Table M.2). The mRNA expression level of every particular gene was determined by qPCR using 3 µL of cDNA (30 ng). Briefly, 0.6 µL of a 10 µM dilution of each primer (forward and reverse) and 10 µL of iQ™ SYBR® Green Supermix were added to the cDNA, and dH_2O until reaching a final volume of 20 µL. The amplification was performed following the standard protocol:

i) cDNA denaturation and activation of the enzyme at 95°C for 10 min.

ii) 40 cycles of 3 steps: cDNA denaturation at 95°C for 15 s, primers binding at 60°C for 30 s, and sequence extension at 72°C for 45 s.

iii) acquisition of the melting or dissociation curve (95°C for 15 s and 60ºC for 1 min).

The expression of the glyceraldehyde-3-phosphate dehydrogenase (*GAPDH*) gene was used as housekeeping and the control group was related to 100% of expression.

Table M.2. Human primers used in qPCR.

Primers	Sequence 5'-3'
CDK4 FW CDK4 RV	ATGGCTACCTCTCGATATGAGC CATTGGGGACTCTCACACTCT
Cytokeratin 7 FW Cytokeratin 7 RV	ATCTTTGAGGCCCAGATTGC TTGATCTCATCATTCAGGGC
Cytokeratin 19 FW Cytokeratin 19 RV	CAACGAGAAGCTAACCATGC ATTGGCTTCGCATGTCACTC
E-cadherin FW E-cadherin RV	AATCCCCAAGTGCCTGCTTT ACCCCTCAACTAACCCCCTT
Fibronectin FW Fibronectin RV	GGGCAACTCTGTCAACGAAG CACACCATTGTCATGGCACC
GAPDH FW GAPDH RV	CCAAGGTCATCCATGACAAC TGTCATACCAGGAAATGAGC
HDAC6 FW HDAC6 RV	CGATGGACTTGGATGGTCTC GATGCTGACTACCTAGCTGC
p16 FW p16 RV	GGGGGCACCAGAGGCAGT GGTTGTGGCGGGGGCAGTT
p21 FW p21 RV	CGATGGAACTTCGACTTTGTCA GCACAAGGGTACAAGACAGTG
S100A4/FSP-1 FW S100A4/FSP-1 RV	ACGTGTTGATCCTGACTGCT CCTGTTGCTGTCCAAGTTGC
SFRP1 FW SFRP1 RV	CTACTGGCCCGAGATGCTTA GCTGGCACAGAGATGTTCAA
SOX17 FW SOX17 RV	GTGGACCGCACGGAATTTG GGAGATTCACACCGGAGTCA
ZO-1 FW ZO-1 RV	CGGTCCTCTGAGCCTGTAAG GGATCTACATGCGACGACAA

(FW: Forward; RV: Reverse)

M.4. Western blotting

Cells were seeded in a 6-well plate and left overnight (O/N) in quiescent medium (DMEM/F12+Glutamax, Gibco). The following day, cells were scrapped with 80 µL of radio-immunoprecipitation assay (RIPA) lysis buffer [150 mM sodium chloride (NaCl), 50 mM Tris pH 7.5, 0.1% SDS, 1% Triton-100X, 0.5% sodium deoxycholate, protease inhibitor cocktail tablet (Roche) and phosphatase inhibitors [1 mM ortovanadate, 10 mM sodium fluoride (NaF), 100 mM β-glycerophosphate] and incubated at -80ºC O/N for cell lysis and protein extraction. Afterwards, cells were centrifuged at 14,500 rpm for 10 min at 4°C. Supernatant was employed for protein measurement.

The protein concentration was measured using the *Pierce™ bicinchoninic acid (BCA) protein assay kit* (ThermoFisher Scientific) according to the manufacturer´s instructions. Briefly, a 1/5 dilution of each sample (or just RIPA as a negative control) in dH_2O was performed and placed in a 96 well plate. At the same time, a calibration curve was prepared [ranging from 0 to 1 mg/mL of BSA (Sigma)] and placed in the same plate. Afterwards, A and B reagents were mixed (in a 1:50 proportion respectively) and 200 µL were added to each well. The plate was incubated at 37°C for 30 min in darkness and subsequently measured in a *Microplate Reader Multiscan Ascent®* spectrophotometer (ThermoFisher Scientific) at a wavelength of 570 nm.

Changes in protein expression were detected by immunoblotting using 20 µg of protein from whole cell extract in 7.5 or 12.5% sodium dodecyl sulfate polyacrilamide gel electrophoresis (SDS-PAGE), and electro-transferred to a nitrocellulose membrane (BioRad). Once blocked with 0.5% skim milk powder/ tris-buffered saline-5% tween (TBS-Tween) (Milk) or 0.5% BSA/TBS-Tween

(BSA), membranes were incubated O/N at 4°C with the appropriate primary antibody (Table M.3) at 1:1000 dilution in blocking solution (Milk or BSA). Horseradish peroxidase-conjugated secondary antibodies (Cell Signaling) at 1:5000 dilution in blocking solution (Milk or BSA) were incubated for 2 h at room temperature and the *Novex® enhanced chemoluminiscence (ECL) horseradish peroxidase (HRP) Chemiluminiscent Substrate Reagent Kit* (Invitrogen) used for further band visualization and quantitation with the *ChemiDoc™ MP System* (Bio-Rad). The β-actin protein expression, or GAPDH in few cases, was used to normalize both the protein loading and expression. In some cases *Ponceau S BioReagent* (Sigma) was used to visualize the bands of the loaded proteins.

M.5. Immunofluorescence

M.5.1. Immunofluorescence in liver tissue samples

Paraffin-embedded tissue samples were heated at 60ºC for 30 min and de-waxed in xylene. Afterwards, rehydration was carried out in decreasing grades of ethanol (100%, 96%, 70% and 50%). Antigenic unmasking was performed by boiling the tissue samples in Citrate Buffer for 15 min. Samples were incubated O/N at 4ºC with the primary antibody in DPBS (1:100; Table M.3) or DPBS only as negative control. That step was followed by the incubation of the fluorescent secondary antibody (1:200) for 2 h and washed 3 times with DPBS. Finally, slides were mounted with a drop of *VECTASHIELD™ mounting medium with 40,6-diamidino-2-phenyindole* (DAPI, Vector laboratories). Pictures were taken with a *Nikon Digital Sight* camera under a fluorescence microscope *(Eclipse 80i, Nikon)* with the *NIS-elements AR 3.2* software or *with a Zeiss LSM 510* confocal microscope [11].

Table M.3. Antibodies used for western blot and/or immunofluorescence.

Antibody	Company	Reference	Use
Goat polyclonal anti-SOX17	R&D	AF1924	WB, IF
Mouse monoclonal anti-acetylated α-tubulin	Sigma-Aldrich	T7451	IF
Mouse monoclonal anti-CK7	Santa Cruz	sc-23876	WB
Mouse monoclonal anti-p-p53 (Ser15)	Cell signaling	#9286	WB
Rabbit polyclonal anti-β-actin	Cell signaling	#4967	WB
Rabbit polyclonal anti-β-catenin	Cell signaling	#9581	WB, IF
Rabbit polyclonal anti-γ-tubulin	Abcam	ab11320	IF
Rabbit polyclonal anti-GAPDH	Abcam	ab22555	WB
Rabbit polyclonal anti-KRT19 (CK19)	ARP	10-P1335	WB
Rabbit polyclonal anti-p21	Abcam	ab7960	WB
Rabbit polyclonal anti-p53	Novocastra (Leica)	NCL-p53-CM1	WB
Rabbit polyclonal anti-p-β-catenin (Ser33/37/Thr41)	Cell signaling	#9561	WB
Rabbit polyclonal anti-pSAPK/pJNK (Thr183/Tyr185)	Cell signaling	#9251S	WB
Rabbit polyclonal anti-SAPK/JNK	Cell signaling	#9252	WB
Rabbit polyclonal anti-SOX17	Abcam	ab89954	IF
Anti-rabbit IgG, HRP-linked Antibody	Cell signaling	#7074	WB
Anti-mouse IgG, HRP-linked Antibody	Cell signaling	#7076	WB
Donkey anti-goat IgG-HRP	Santa Cruz	sc-2020	WB
Chicken anti-Goat IgG (H+L) Secondary Antibody, Alexa Fluor® 488 conjugate	ThermoFisher	A21467	IF
Donkey anti-Goat IgG (H+L) Secondary Antibody, Alexa Fluor® 568 conjugate	ThermoFisher	A11057	IF
Donkey anti-Mouse IgG Secondary Antibody, Alexa Fluor® 568 conjugate	ThermoFisher	A10037	IF
Donkey anti-Rabbit IgG (H+L) Secondary Antibody, Alexa Fluor® 488 conjugate	ThermoFisher	A21206	IF

Abbreviations: WB: western blot; IF: immunofluorescence

M.5.2. Immunofluorescence in cell cultures

Cells were cultured on collagen-coated coverslips (Menzel-Gläser) in 24-well plates. Then, they were fixed with 1 mL of methanol for 10 min at -20ºC. Samples were washed 3 times with antigen retrieval solution (0.5% Triton-100X/PBS 1X) and incubated for 20 min with this solution at room temperature. Next, cells were incubated with blocking solution (5% FBS/1% BSA/PBS1X) for 30 min at room temperature and them with the primary antibody (1:100) (Table M.3) in 0.1% Triton-100X/1% BSA solution for 1 h. Afterwards, cells were washed 3 times with 1% BSA/PBS 1X solution and incubated under darkness with the corresponding fluorescent secondary antibody (1:1000) diluted in that same solution for 1.5 h. Finally, cells were washed 3 times with DPBS and coverslips were placed onto a microscope slide appropriate for immunofluorescence (Thermo Scientific) with a drop of *VECTASHIELD™ mounting medium with DAPI* (Vector laboratories). Immunofluorescence images were obtained with a *Nikon Digital Sight* camera under a fluorescence microscope (*Eclipse 80i, Nikon*) with the *NIS-elements AR 3.2* software or with a *Zeiss LSM 510* confocal microscope [11]. Immunofluorescence of ciliary-associated proteins was performed in the same conditions but in cells under 7 days of confluence.

M.6. Viral vectors and small interfering RNAs

M.6.1. SOX17 knock-down with lentiviruses (Lent-shRNA-SOX17)

The expression of *SOX17* was knocked-down in NHC with lentiviruses that constitutively express short hairpin RNAs (shRNAs) against *SOX17* mRNA

(Lent-shRNA-SOX17; Santa Cruz Biotechnologies) and that contain the gene of resistance to puromycin. As a negative control, lentiviruses that constitutively express a shRNA-Control sequence (Santa Cruz) were used. The Lent-shRNA-SOX17 contains a pool of three different expression constructs, each encoding target specific 19-25 nt (plus the hairpin sequence) designed to knock-down *SOX17* gene expression (Table M.4).

Table M.4: Sense and antisense sequences composing the pool of Lent-shRNA-SOX17 constructs.

shRNA-SOX17	Sequence 5'-3'
Sc-38429-VA	
Sense	GCACGGAAUUUGAACAGUATT
Antisense	UACUGUUCAAAUUCCGUGCTT
Sc-38429-VB	
Sense	GUCUGCCACUUGAACAGUUTT
Antisense	AACUGUUCAAGUGGCAGACTT
Sc-38429-VC	
Sense	CCCAUAGUUGGAUUGUCAATT
Antisense	UUGACAAUCCAACUAUGGGTT

M.6.2. SOX17 overexpression with lentiviruses (Lent-prEF1a-SOX17)

Lentiviruses overexpressing SOX17 were produced in collaboration with the group of Prof. José Juan G. Marín (University of Salamanca, Salamanca, Spain). Briefly, human *SOX17* open reading frame (ORF) was amplified from total RNA isolated from NHC cells by reverse transcription followed by high-fidelity PCR using *AccuPrime Pfx* DNA polymerase (Life Technologies), specific primers (Table M.5) and an *Eppendorf Mastercycle ep gradient S* Thermal Cycler (Thermo Fisher). SOX17 cDNA was cloned into the *Pac*I site of the pWPI lentiviral vector under the regulation of the constitutive elongation factor 1α

promoter. The identity of the cloning was confirmed by sequencing. The pWPI lentiviral vector also contains the enhanced green fluorescent protein (*eGFP*) gene. Recombinant lentiviruses were produced in HEK293T cells (ATCC american type culture collection: CRL-11268) and using a standard polyethylenimine (PEI; Sigma) protocol. Thus, HEK293T cells were transfected with the pWPI-SOX17 vector or with the pWPI vector (negative control) and the packaging plasmids psPAX2 and pMD2.G. To form complexes PEI:ADN 6 μg of pWPI-SOX17 (or empty pWPI), 6 μg of psPAX2 and 4.5 μg of pMD2.G were dissolved in 1.2 mL of saline solution and 60 μL of PEI. After 20 min of incubation at room temperature, the mixture was added in the HEK293T culture. The following 3 days the supernatant was collected, and finally was filtered (0.45 μm pore size) and ultracentrifuged (53,000 g, 120 min, 16ºC). The lentivirus concentration was determined by infecting HEK293T cells with serial dilutions of the viral solution and the following analysis of eGFP-positive cells by a *FACSCalibur* flow cytometer (BD Biosciences).

Table M.5. Primers used to *SOX17* ORF amplification.

***SOX17* primers**	**Sequence 5'-3'**
Forward	CCAAGGTTCCTTAATTAAGCCAAGATGAGCAGCCCGGATGCG
Reverse	GGAACCTTGGTTAATTAACTGTCACACGTCAGGATAGTTGCAGT

M.6.3. Cellular lentiviral infection

NHC were infected by lentiviruses carrying shRNA against *SOX17* (Lent-shRNA-SOX17) or Control (Lent-shRNA-control) at a MOI (multiplicity of

infection) of 1. After 24 h of incubation, media was changed and cell selection was performed with *Puromycin dihydrochloride (from Streptomyces alboniger) suitable for cell culture* (5 µg/mL; Sigma) (Figure M.5). On the other hand, CCA human cells (i.e. EGI1) were infected with lentiviruses carrying *SOX17* (Lent-SOX17) or empty viruses (negative control, Lent-control), at different MOIs (1, 3, 5, 10, 15) and the appropriate MOI (3) was selected (Figure M.6). For Lent-SOX17 and controls, once lentiviruses were added into the cell culture medium, the culture plate was centrifuged for 90 min at 32ºC and 1,800 g and the lentiviruses were kept in the culture medium overnight at 37ºC. In both cases (Lent-shRNA-SOX17 or Lent-SOX17), the infection was performed in the presence of *Polybrene*® (5 µg/mL, Santa Cruz).

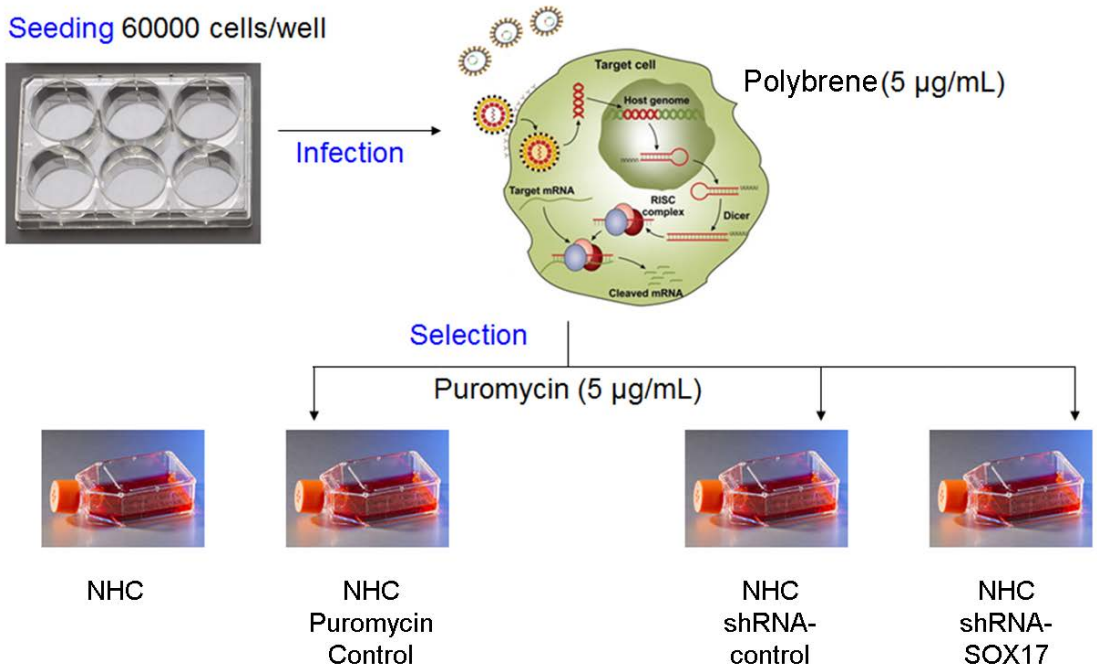

Figure M.5. Workflow for lentiviral infection with shRNA and selection of infected cells.

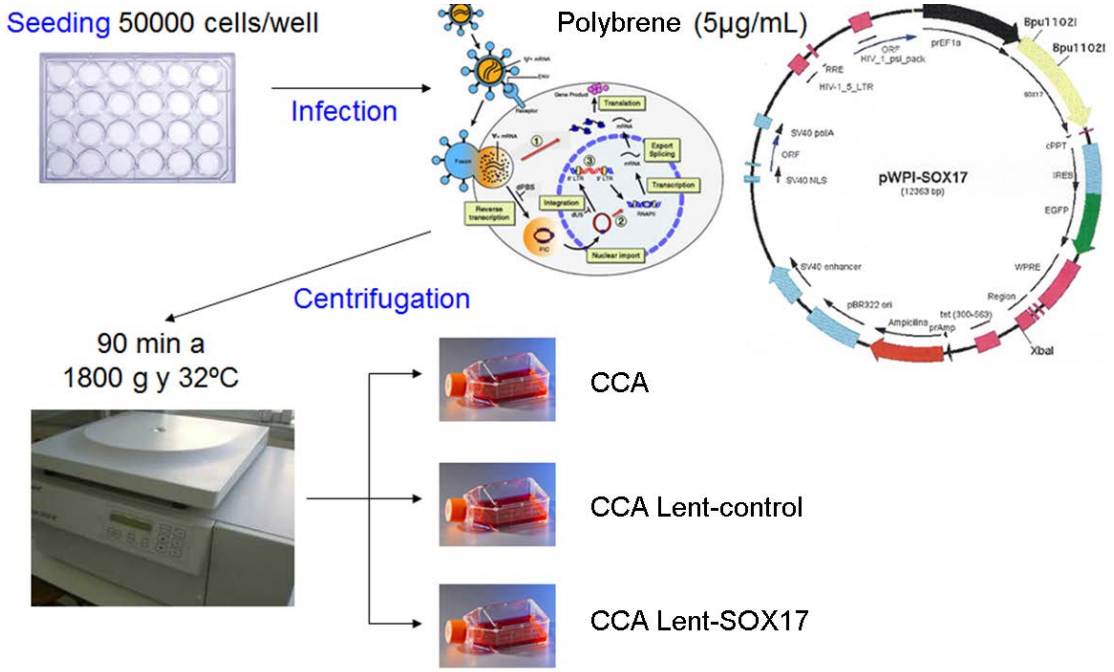

Figure M.6. Workflow for SOX17 overexpression in CCA cells using lentiviral infection.

M.6.4. Inhibition of DNMT1 mRNA expression with siRNAs in normal human cholangiocytes and cholangiocarcinoma cells

The *DNMT1* mRNA expression was inhibited in both NHC and CCA (EGI1) human cells by using specific small interference RNA (siRNA) oligos against *DNMT1* mRNA (siRNA-DNMT1; sc-35204, Santa Cruz Biotechnologies). In parallel, negative control siRNAs (siRNA-Control-A; sc-37007, Santa Cruz Biotechnologies) were also used. Cells were seeded in 12-well collagen-coated plates (100,000 cells/well) and transfected with siRNA-DNMT1 or siRNA-Control using *Lipofectamine RNAiMAX* (Invitrogen). The transfection protocol was performed according to the manufacturer´s instructions. This transfection mixture was incubated O/N with the cells and the following day was replaced by FLASK-medium. NHC were treated, 24 h after transfection, with TGFβ1 (5 ng/mL, R&D systems) or Wnt3a (100 ng/mL, R&D systems) in 1% P/S-DMEM

for 48 h and then cells were collected for RNA analysis. On the other hand, CCA (EGI1) human cells were collected 48 h after siRNA (siRNA-DNMT1 or siRNA-Control) transfection for RNA analysis.

M.7. CCA xenograft animal model

Immune-deficient nu/nu mice (Crl:NU-*Foxn1*^{nu}; strain 088, homozygous) were purchased from Charles River Company to carry out CCA xenografts studies. These hairless animals (i.e. nude) are unable to produce T-cells because they have no thymus. All experimental procedures were approved by the *Ethical Committee for Animal Experimentation* of the "Diputación de Gipuzkoa" and were used in conformity with our institution's guidelines for the use of laboratory animals.

CCA (EGI1) human cells (100,000 cells in 100 µL of 1X PBS) were subcutaneously injected in the back of immune-deficient nu/nu mice. Three different conditions were studied:

i) **EGI1 wild-type cells (CCA)** were injected in both flanks of one mouse.

ii) **EGI1 cells infected with Lent-pWPI-Control (CCA Lent-control)** were injected in the left flank of eight mice.

iii) **EGI1 cells infected with Lent-pWPI-SOX17 (CCA Lent-SOX17)** were injected in the right flank of the same previously mentioned eight mice.

One month after the subcutaneous injection of the cells in immune-deficient nu/nu mice the first tumors started to be visible. Then, we measured the tumor size (length and wide) every three/four days and the tumor volume was calculated as described [213]:

$$\text{Tumor Volume} = (D \times d^2) / 2$$

Where “D” represents the largest diameter measured, and “d” the shortest

Tumor measurements were carried out for 21 days, and animals were sacrificed when one of the mice showed a tumor volume of ~1.5 cm^3 (maximum allowed by the *Ethical Committee for Animal Experimentation*). Tumors were extracted and the size compared after taking a picture with an *Olympus SP-590UZ* camera (Olympus Imaging Corporation).

All experimental procedures (i.e. injection of the cells, tumor measurements and sacrifice) were performed after anesthetizing the animals with isofluorane (2.5% in oxygen at a flow of 0.3 L/min) using an *Inhalation Anesthetizing Equipment* (Ohmeda).

M.8. Cell death analysis

Cell death was determined by using three different flow cytometry-based assays:

i) **Annexin-V** (Alexa Fluor® 594 conjugate, Invitrogen)

ii) **Propidium Iodide** (Ex/Em=535/617, Invitrogen)

iii) **Caspase-3 activity** (Phiphilux-G2D2, OncoImmunin® Inc)

All fluorochromes did not interfere with the pWPI vector-derived lentivirus. All three assays were performed according to the manufacturer’s instructions and cells were equally seeded and infected. Briefly, 50,000 CCA (EGI1) and NHC

cells were seeded in each well of a collagen-coated 24-well plate, and infected with Lent-control or Lent-SOX17. Some cells were kept uninfected as controls.

M.8.1. Annexin-V and propidium iodide

48 h after infection, cells from each well were separated into two tubes for *Annexin-V* or *Propidium Iodide staining*. Then, they were centrifuged at 1,500 rpm for 5 min at room temperature and washed once with cold PBS 1X at 1,500 rpm for 5 min. The resulting pellet was incubated with 25 µL Annexin-V mixture for 15 min or 25 µL Propidium Iodide mixture for 30 min at room temperature. Finally, cells were resuspended in PBS 1X to a maximum volume of 160 µL (200-300 cells/µL) and analyzed by flow cytometry with the *GUAVA EasyCyte 8HT Benchtop* flow cytometer (MerkMillipore).

M.8.2. Caspase-3 activity

48 h after infection, cells were centrifuged at 1,500 rpm for 5 min at room temperature and then incubated with 10 µL of *Phiphilux-G2D2* for 30 min at 37ºC. Next, they were washed once with Flow Cytometry Buffer at 1,500 rpm for 5 min at room temperature. Finally, cells were resuspended in the same buffer to a maximum volume of 160 µL and analyzed with the *Guava 8HT Benchtop* flow cytometer.

M.9. Cell proliferation

50,000 CCA (EGI1) cells were seeded in each well of a collagen-coated 24-well plate, and infected with Lent-control or Lent-SOX17. Some cells were kept uninfected as controls. 48 h after infection, cells were reseeded in a 96-well plate (5,000 cells per well). Cell proliferation was evaluated in the presence or absence of *recombinant human Wnt3a protein* (R&D systems) for 48 h by using the *Cell Proliferation WST-1 Assay* (Roche). Briefly, reseeded cells were incubated O/N at 37ºC in Flask medium. Next, cells were incubated with different doses of Wnt3a (ranging from 0 to 400 ng/mL) in DMEM/F12+Glutamax, 1% FBS and 1% P/S for 48 h. Then, 10 µL of *water soluble tetrazolium salt 1* (WST-1) were added to each well, incubated at 37ºC for 1 h and the colorimetry read at a wavelength of 450 nm in a *Multiskan Ascent* spectrophotometer.

M.10. Cell senescence

20,000 NHC cells (at passages ~5, ~10 and ~15, and passage 5 NHC uninfected or infected with Lent-shRNA-SOX17 or Lent-shRNA-control) were seeded in each well of a collagen-coated 24-well plate. After 48h of incubation, cells were washed with PBS 1X and the senescence *β-galactosidase kit* (Cell signaling) protocol was followed according to the manufacturer's instructions. Briefly, cells were fixed with 1X fixation solution for 10-15 min at room temperature, washed two times with PBS 1X and incubated with β-gal staining solution O/N at 37ºC in darkness in the absence of CO_2. Finally, cell staining

images were obtained with a *Nikon D90* camera coupled to an *Eclipse TS100 light* microscope (Nikon).

M.11. Cell migration

50,000 CCA (EGI1) cells were seeded in each well of a collagen-coated 24-well plate, and infected with Lent-control or Lent-SOX17. Some cells were kept uninfected as controls. After cell death was observed, the remaining living cells were reseeded (200,000 cells/well) in a collagen-coated 6-well plate with DMEM/F12+Glutamax and 1% P/S. Once cells reached confluence, three longitudinal scratches were done to the surface of each well with a 10 µL pipette tip and cell migration was monitored every four hours with a *Nikon Eclipse TS-100* light microscope. At 24 h cells were fixed and stained with crystal-violet (Sigma) in 4% formaldehyde and images were obtained with a *Nikon D90* camera coupled to a *Nikon Eclipse TS-100* light microscope. Finally, the well surface not covered with cells was compared in each condition by using the *Image J* software.

M.12. Cell redox stress

Levels of oxidative stress were determined in both NHC and CCA (EGI1) cells, after inhibiting (Lent-shRNA-SOX17) or overexpressing SOX17 (Lent-SOX17), by using the *CellROX® "Deep Red" Flow Cytometry Assay Kit* (Invitrogen) according to the manufacturer's instructions. Briefly, 50,000 cells were seeded in collagen-coated 24-well plates and infected with the corresponding lentivirus for 48 h. Then, cells were trypsinized and centrifuged at 1,500 rpm for 5 min at

room temperature. The pellet of cells was resuspended with 250 µL of 250 µM *CellROX Deep Red*, incubated for 30 min at 37ºC and centrifuged at 1,500 rpm for 5 min at room temperature. Finally, cells were resuspended in PBS 1X to a maximum volume of 160 µL (200-300 cells/µL) and analyzed by flow cytometry with the *GUAVA EasyCyte 8HT Benchtop* flow cytometer. As a negative control, cells were incubated at 37ºC with 5 mM of the antioxidant N-acetylcysteine (NAC) for 1 h, and as a positive control cells were incubated at 37º C with 800 µM (NHC) or 2 mM (EGI1) of the oxidative stress inducer ter-butyl hydroperoxide (THBP) for 30 min.

M.13. Illumina mRNA expression array

Illumina_human_v6.2 gene expression arrays were carried out in NHC and CCA (EGI1) cells in collaboration with Dr. Ana María Aransay and Dr. Jose Luis Lavín (Genome Analysis Platform of CICBigune, Zamudio). NHC uninfected or infected with Lent-shRNA-SOX17 or Lent-shRNA-control (as described in section M.6.3) were collected 1 week after infection. On the other hand, CCA cells, both uninfected and infected with Lent-SOX17 or Lent-control (as described in section M.6.3) were collected 6 h after infection.

M.13.1. Total RNA isolation protocol

The *miRNeasy Micro kit* (Qiagen) was used for total RNA isolation following the manufacturer's instructions. Briefly, cells were incubated with 1 mL of Qiazol and then collected into a 1.5 mL Eppendorf tube. Cell extracts were homogenized with a vortex for 1 min and incubated at room temperature for 5

min. Then, 140 µL of chloroform were added and the tube was shacked vigorously for 15 s and incubated at room temperature for 2 additional min. Tubes were centrifuged at 12,000 g at 4ºC and the upper colorless phase transferred into a new tube. Afterwards, absolute ethanol was added and mixed thoroughly. The resultant solution was transferred into an *"RNeasy MinElute" spin column* introduced in a 2 mL collection tube and then centrifuged of 8,000 g for 15 s at room temperature. The flow-through solution was discarded and the RNA trapped into the column was washed with 350 µL of *Buffer RWT* (prepared with isopropanol) by centrifugation at 8,000 g for 15 s at room temperature. The column was then treated with 80 µL of *DNase I/Buffer RDD* for 15 min at room temperature and after washed twice with 500 µL of *Buffer RWT* (prepared with isopropanol) at 8,000 g for 15 s at room temperature and with 500 µL of *Buffer RPE* at 8,000 g for 15 s at room temperature. For the last washing step, 500 µL of 80% ethanol were added onto the *RNeasy MinElute spin column*, centrifuged for 2 min at 8,000 g. The column-membrane was dried by centrifugation at full speed for 5 min and then 15 µL of RNase-free water was added directly to the center of the spin column membrane and centrifuged for 1 min at full speed to elute the RNA. This last step was repeated twice to recover a higher amount of RNA.

M.13.2. Illumina gene expression array

The whole human genome expression was evaluated in NHC and CCA (EGI1) cells total RNA by using the *Illumina_human_v6.2 gene expression array* (Illumina Inc.). The RNA to use in the arrays required a high level of quality. That is why several quality controls were performed: *i*) 260/280 nm wavelength

ratio, to determine the purity of the sample, and *ii*) RNA Integrity Number (RIN) measurement in a *RNA Nano Chip Bioanalyzer* (Agilent Technologies), to determine the degradation level of the sample. The total RNA isolated from the cells had a 260/280 nm wavelength ratio between 1.8 and 2.0, and showed a RNA integrity number (RIN) over 8.0, meaning no degradation. The concentration of the total RNA was evaluated by a *Qubit® 2.0 Fluorimeter* (ThermoFisher Scientific), and 200 ng of each sample RNA were used for the array. The cRNA synthesis, amplification, labeling and hybridization of the samples were performed following the *Whole-Genome Gene Expression Direct Hybridization* protocol (Illumina Inc.).

The cRNA of the samples were hybridized to the diverse gene-probes of the array and the differential gene expression levels in the diverse samples were detected by a *HiScan* scanner (Illumina Inc.). The crude data acquired from the scanner was uncodified with a *GenomeStudio* analysis and exported as a *spp2.txt* file for its further statistical analysis performed at the Genome Analysis Platform of CICBigune (Zamudio).

M.13.3. Volcanoplots and heatmaps

In statistics, a volcanoplot is a type of scatter-plot that is used to quickly identify changes in large datasets composed of replicate data [214]. It plots log10 statistical significance (log10 p-value) *versus* log2 fold-change on the y- and x-axes, respectively [214]. These result in datapoints with low p-values (highly significant) appearing toward the top of the plot, and expression changes toward the right and left sides of the plot equidistant from the center [215].

Meaning, the volcanoplots show the genes significantly upregulated or downregulated in one sample in comparison with another one.

Heatmap is a graphical 2-dimentional representation of data where the individual values contained in a matrix are represented as colors. Higher values are represented by small dark red squares, lower values by blue squares and medium values as white squares. The results of a cluster analysis displayed by permuting the rows and the columns of a matrix to place diverse genes with similar values near each other according to the clustering.

M.13.4. Gene expression analysis

The RNA array statistical analysis provides three lists of the expression levels according to the different gene-probes present in the array plate. The first list is a representation of all the expression levels of the whole pool of gene-probes, and is called **Table**. Another list is filled by all the gene-probes which represented the best p-value of the expression compared between the samples, and is called **Table_BestP**. However, to have the best p-value does not mean that the gene represented by that probe is significantly differentially expressed. The last list shows the real differentially expressed genes, both the upregulated and downregulated ones, and is called **Table_WonNR**. This list, by an algorithm, considers both the fold-change and the adjust p-value of each sample in order to verify the real expression differences.

The gene function analysis was performed with diverse database programs such as Panther (WebGestalt, String), Pubmed, Uniprot and Genecards. Moreover, we used Gene Ontology and Kegg programs to test potential

association of the differentially-expressed genes on metabolic pathways and/or intracellular interactions.

M.14. Statistical analysis

All results of the study were collected in *MS Excel* tables for subsequent statistical analysis using the *GraphPad* program. For comparisons between two groups, statistical parametric *t Student* test or non-parametric *Mann-Whitney* test were used. For comparisons between more than two groups, nonparametric *Kruskal-Wallis* test followed by *a posteriori Dunns test* or the parametric test *One-Way ANOVA* followed by *a posteriori Bonferroni test* were used. The differences are considered significant when $p<0.05$.

IV. RESULTS

R.1. The reprogramming of induced pluripotent stem cell (iPSC) into cholangiocytes is dependent on SOX17

In the last years, iPSC reprogramming has emerged as a potential tool for regenerative medicine [216, 217]. Very recently, human myofibroblats were genetically modified to produce iPSCs, and then further reprogrammed into normal cholangiocytes [207]. In this context, human myofibroblasts were differentiated into a pluripotent phenotype by transient-forced expression of the transcription factors OCT4, SOX2, KLF4 and c-MYC to obtain iPSCs, and then these cells were reprogrammed into normal cholangiocytes (i.e. induced differentiated cholangiocytes, “iDCs) by using a multistep process with exposure to biliary morphogens. As indicated in the Material and Methods section, this protocol contains five subsequent steps: *i*) iPSCs, *ii*) definitive endoderm (DE), *iii*) hepatic specification (HS), *iv*) hepatic progenitor (HP) and *v*) iDCs (Figure R.1.A). These iDCs recapitulate different biliary features such as the mRNA and protein expression of CK7, CK19, polycystic kidney disease 2 (PKD2), cystic fibrosis transmembrane conductance regulator (CFTR) and anion exchanger 2 (AE2), as well as the presence of the cholangiocyte primary cilium [207].

In our approach, we found that SOX17 protein expression is highly induced in the last step of the reprogramming phase, similarly to the biliary markers CK7 and CK19, corresponding to the biliary differentiation (i.e. iDCs) compared to the previous steps (i.e. HS and HP) (Figure R.1.B). Based on these data, we evaluated the potential role of SOX17 in the regulation of the biliary differentiation. For this purpose, we knocked-down SOX17 expression in the three phases of the iDC reprogramming protocol (i.e. between DE-HS, HS-HP and HP-iDC) by using lentiviruses overexpressing shRNAs against *SOX17*

(Lent-shRNA-SOX17) (Figure R.1.A). On the other hand, we used Lent-shRNA-control or non-infected cells as controls (Figure R.1.A). Infection with Lent-shRNA-SOX17 downregulated the high induction of SOX17 protein expression in the iDC phase partially, but significantly. Notably, the knock-down of SOX17 protein expression resulted in decreased protein expression of CK7 and CK19 biliary markers (Figure R.1.B-C). These data strongly supported the hypothesis that SOX17 is a key transcription factor regulating cholangiocyte differentiation.

A

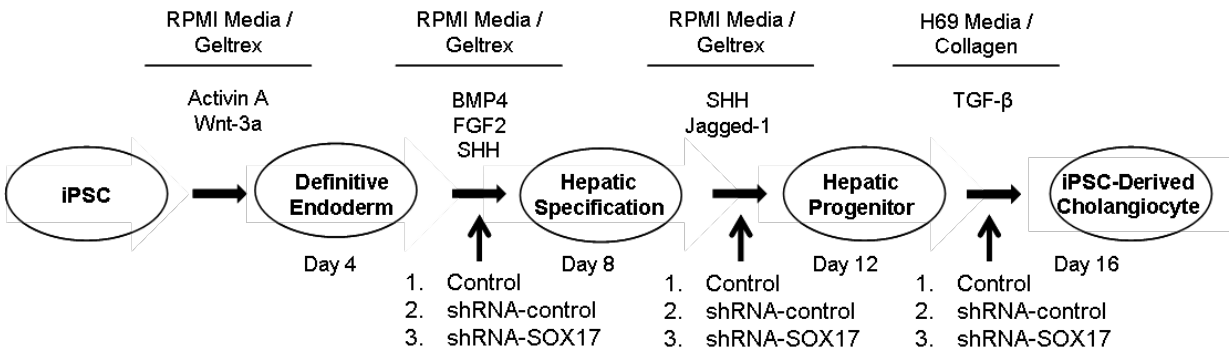

B

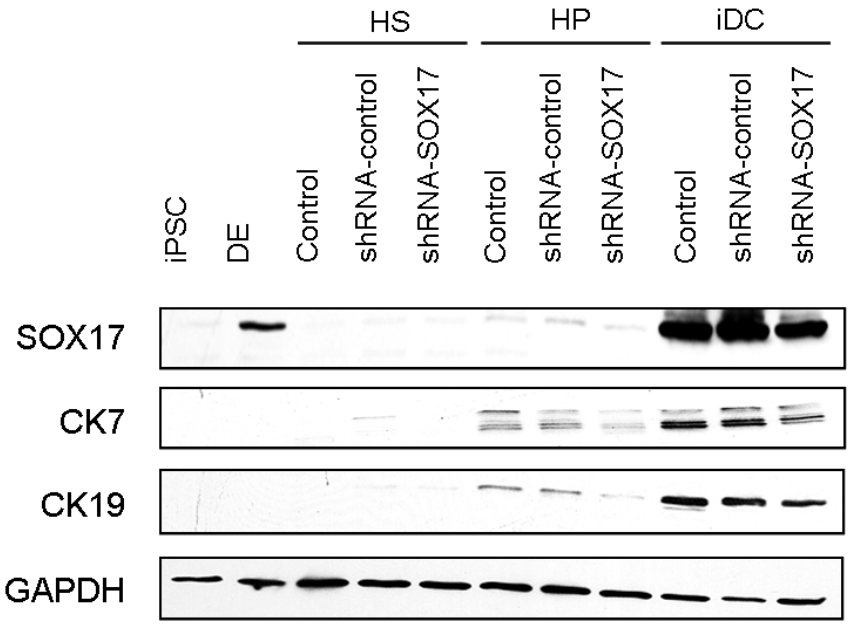

C

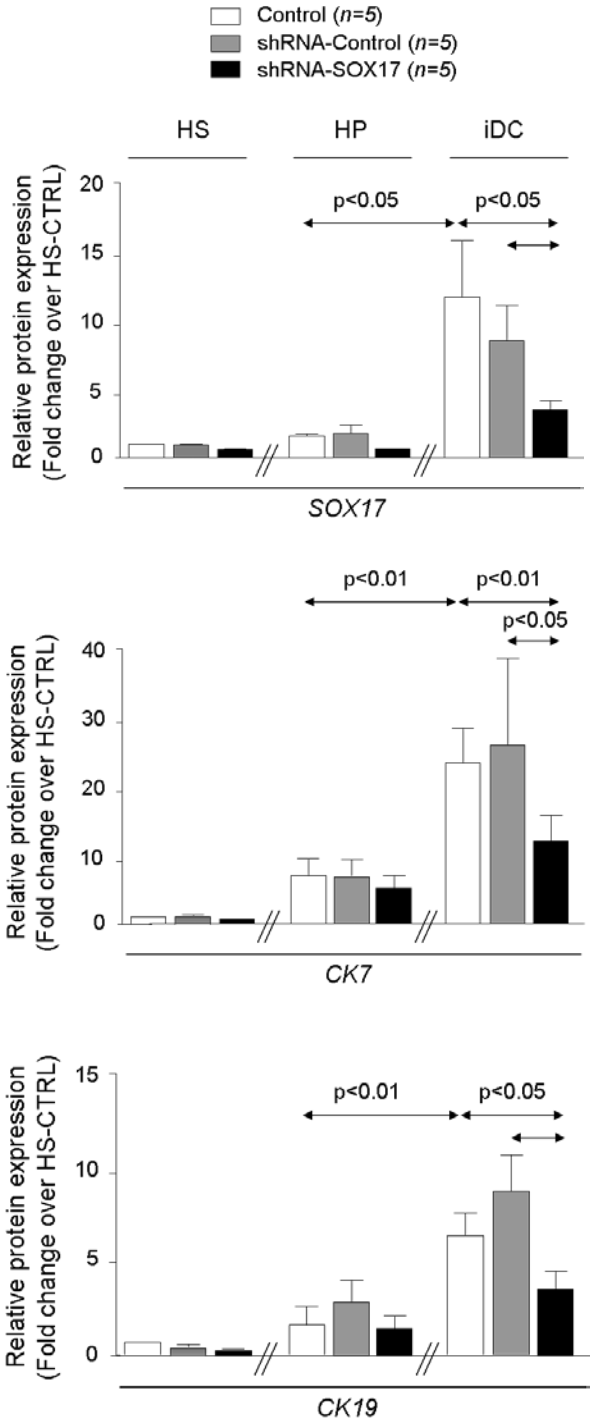

Figure R.1. Protein expression of biliary markers over the differentiation of iPSCs into iDCs. A) Workflow of iPSC differentiation into iDCs and timepoints of *SOX17* inhibition with Lent-shRNA-SOX17. B) western blot and C) densitometry quantitation showing SOX17, CK7 and CK19 protein expression. GAPDH was used as a normalizing loading control for the western blot.

R.2. The expression of SOX17, and other biliary markers, decreases in normal human cholangiocytes over the cellular passages *in vitro* and runs in parallel with increased cell senescence

Normal human cholangiocytes (NHC), similarly to other primary cultures, progressively lose epithelial markers of differentiation along cell passages and gradually enter in senescence [218]. The analyses of expression in NHC revealed that SOX17 mRNA (Figures R.2) and protein (Figures R.3) both decrease over cell passages *in vitro*. Similarly, the expression of specific cholangiocyte markers within the liver such as *CK7* and *CK19*, as well as the expression of the epithelial marker *E-cadherin*, all decreased in NHC over cell passages *in vitro* (Figures R.2).

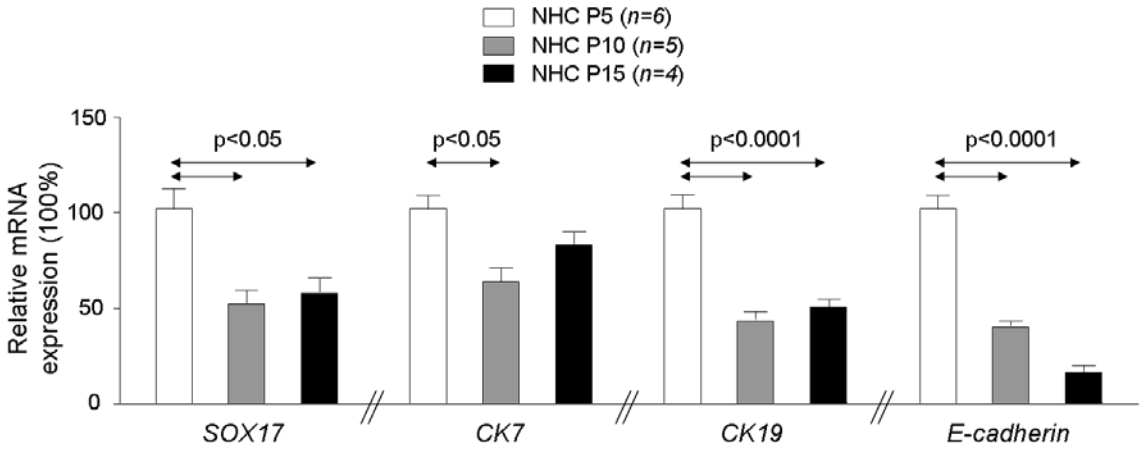

Figure R.2. Relative mRNA expression of biliary epithelial markers (*SOX17*, *CK7*, *CK19* and *E-cadherin*) in NHC over cell passages *in vitro*. P: number of cell passages *in vitro*. n=number of samples in each condition. *GAPDH* was used as housekeeping normalizing gene.

On the other hand, increased expression of senescence markers was observed in NHC over cell passages *in vitro*, which run in parallel with decreased expression of biliary epithelial markers. In particular, progressive

overexpression of the senescence marker p21 protein occurs together with the downregulation of SOX17 protein in NHC over cell passages *in vitro* (Figure R.3).

A

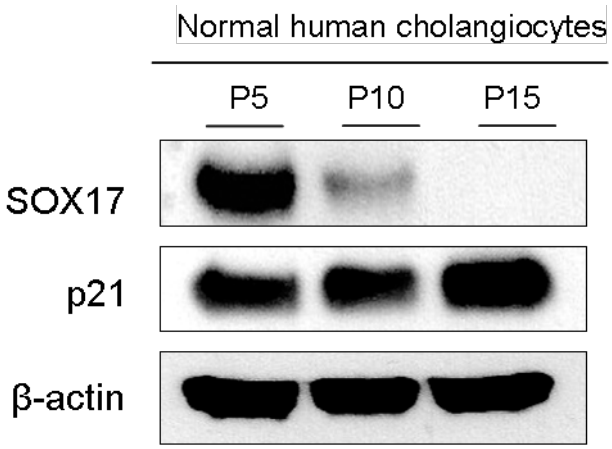

B

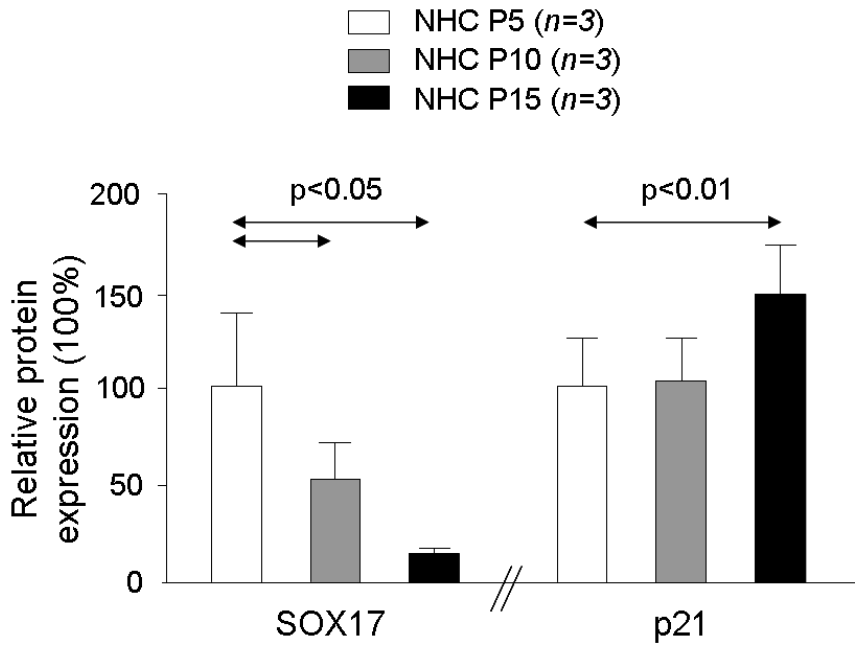

Figure R.3. Relative expression of SOX17 and p21 proteins in NHC over the cell passages *in vitro*. A) Representative western blot showing the expression of SOX17 and p21 proteins in NHC over cell passages (5, 10 and 15) *in vitro*. B) Relative SOX17 and p21 protein expression in NHC over cell passages (5, 10 and 15) *in vitro*. β-actin was used as normalizing loading control. P: number of cell passages *in vitro*. n=number of samples in each condition.

Additionally, the analysis of expression of cell cycle-related proteins that participate in the regulation of senescence was performed. Thus, the mRNA expression of the cyclin-dependent kinase 4 (*CDK4*), which promotes cell cycle and cell division, was found downregulated in NHC over cell passages *in vitro* (Figure R.4). In contrast, the expression of the *CDK4* inhibitor $p16^{INK4a}$, which inhibits cell cycle promoting senescence [219], increased in NHC over cell passages *in vitro* (Figure R.4).

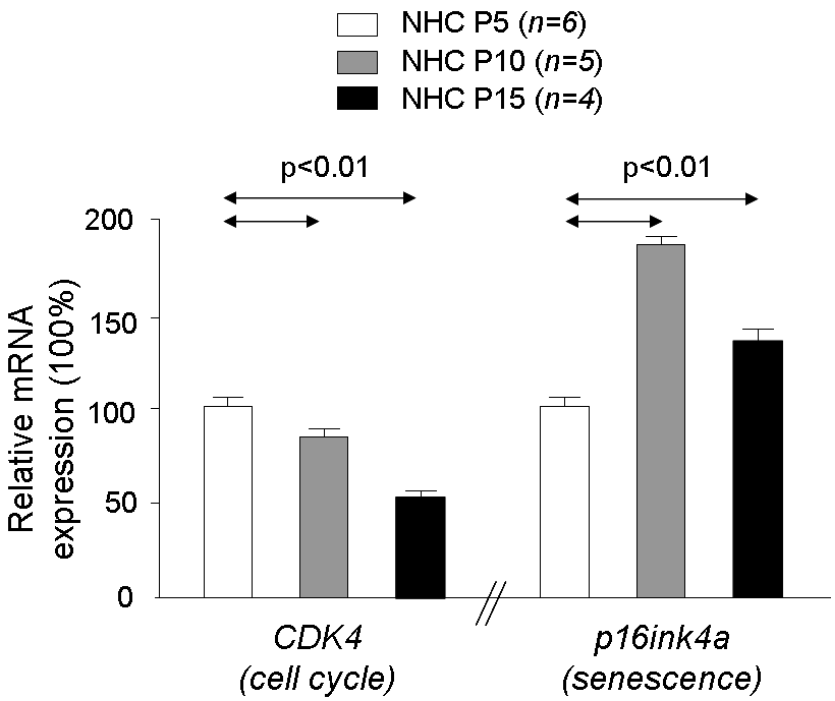

Figure R.4. Relative mRNA expression of *CDK4* and $p16^{ink4a}$, in NHC over cell passages *in vitro*. *GADPH* was used as housekeeping normalizing gene. P: number of cell passages *in vitro*. n=number of samples in each condition.

All these data were also associated with increased β-galactosidase activity in NHC over the cell passages *in vitro* (Figure R.5), which is also a marker of cell senescence [220].

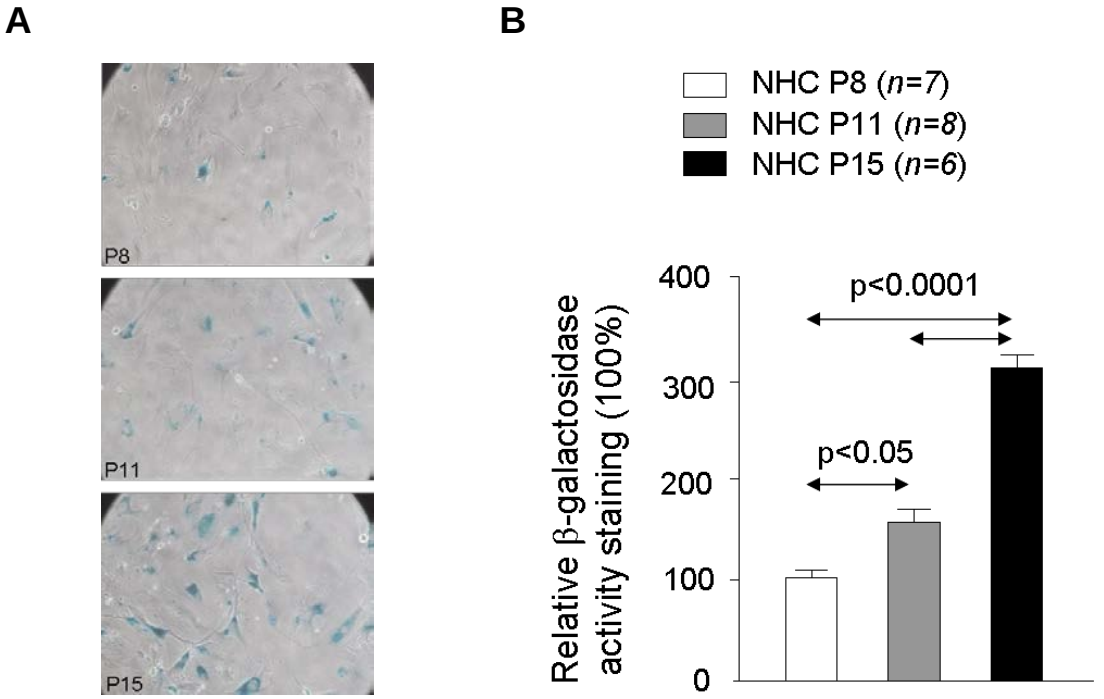

Figure R.5. Representative staining of β-galactosidase activity in NHC over the cell passages *in vitro*. A) Light microscopy images showing β-galactosidase activity in NHC in blue over the cell passages (8, 11 and 15) *in vitro*. B) Relative β-galactosidase activity in NHC over the cell passages (8, 11 and 15) *in vitro*. P: number of cell passages *in vitro*. n=number of samples in each condition.

R.3. SOX17 regulates CK7 and CK19 expression in normal human cholangiocytes but does not influence the senescence process

In order to further demonstrate the role of SOX17 as regulator of cholangiocyte differentiation, and to test its role in senescence, the expression of SOX17 was experimentally downregulated by infecting NHC low passages with Lent-shRNA-SOX17 (Lent-shRNA-control and non-infected cells were used as controls) as described in Materials and Methods (M.6.3 section). NHC low passages (between 5-8 passages) showed high basal expression levels of SOX17. Infection of NHC low passages with Lent-shRNA-SOX17 resulted in downregulation of both SOX17 mRNA and protein expression compared to cells infected with Lent-shRNA-control or non-infected cells (Figure R.6).

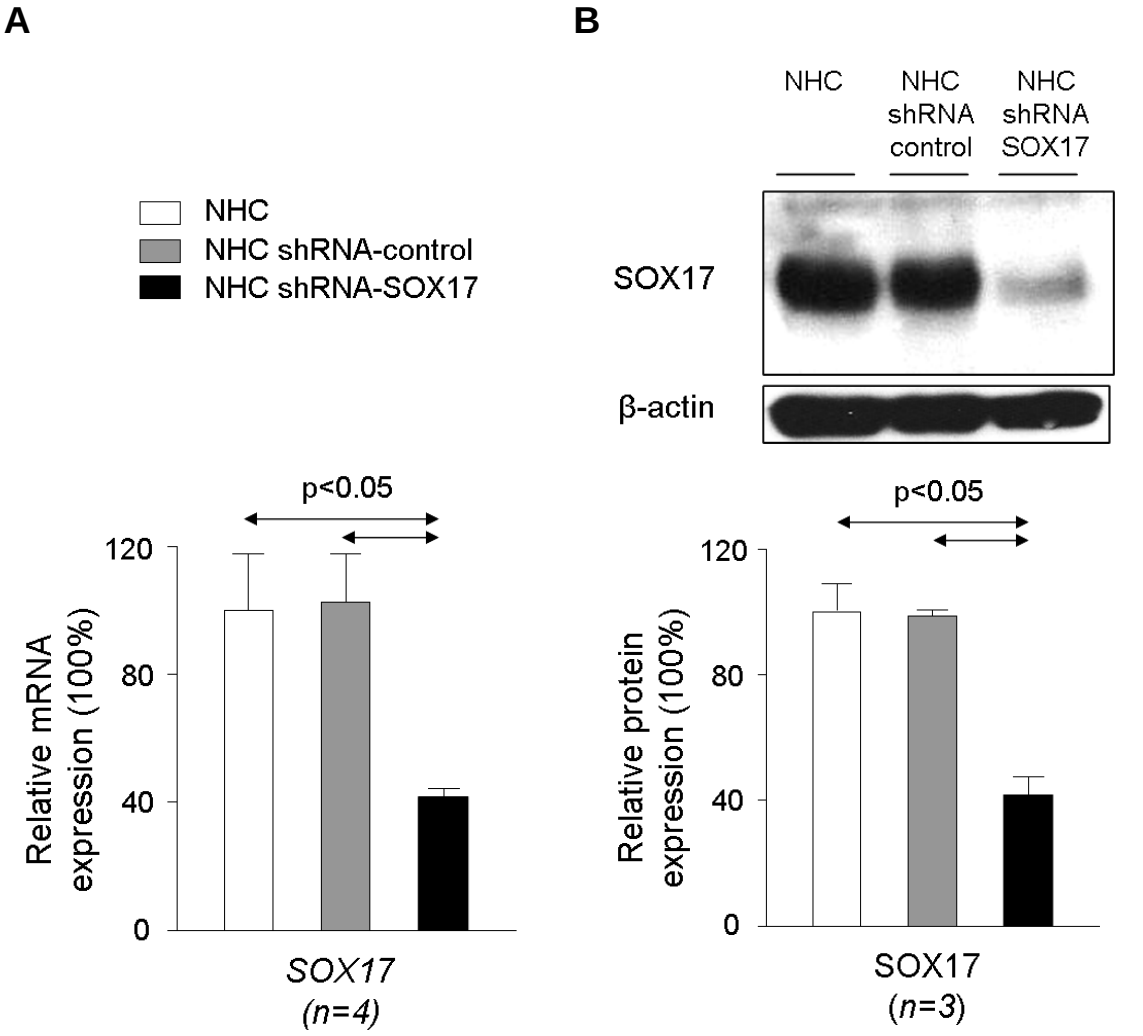

Figure R.6. Relative SOX17 expression in NHC low passages (between P5-8) infected with Lent-shRNA-SOX17, Lent-shRNA-control or non-infected. A) Relative *SOX17* mRNA expression. *GADPH* was used as housekeeping normalizing gene. B) Representative western blot of SOX17 and relative SOX17 protein quantification. β-actin protein was used as a normalizing loading control. n=number of samples in each condition.

In addition, experimental knock-down of SOX17 in NHC with Lent-shRNA-SOX17 prompted the downregulation of both *CK17* and *CK19* mRNA expression compared to the experimental control conditions (Figure R.7), indicating that SOX17 regulate the maintenance of expression of both biliary markers in NHC in culture.

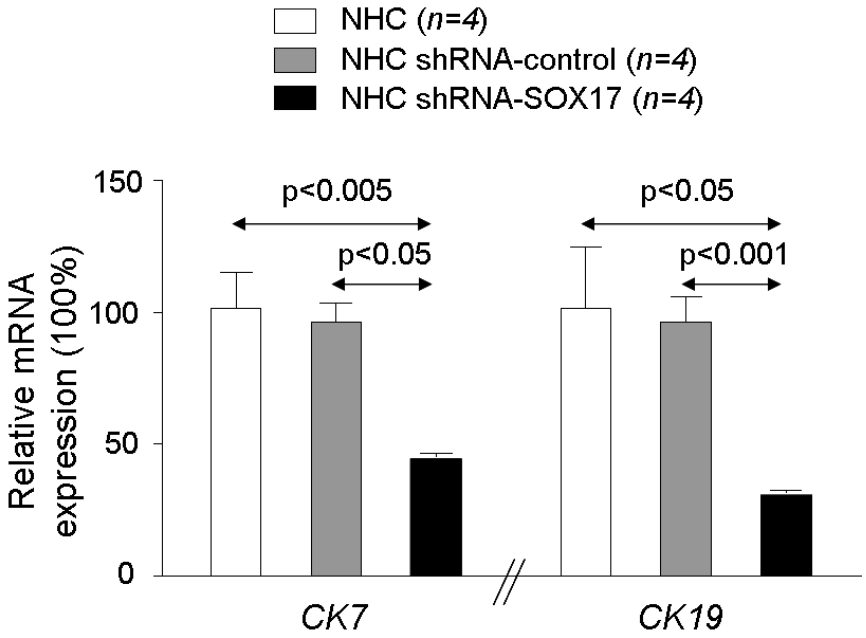

Figure R.7. Relative *CK7* and *CK19* mRNA expression in NHC low passages (between P5-8) infected with Lent-shRNA-SOX17, Lent-shRNA-control or non-infected. *GADPH* was used as housekeeping normalizing gene. n=number of samples in each condition.

In contrast, experimental knock-down of SOX17 in NHC with Lent-shRNA-SOX17 did not affect senescence, as no changes in p21 protein, β-galactosidase activity (Figure R.8), and *CDK4* or $p16^{INK4a}$ mRNA levels were observed compared to the experimental control conditions (Figure R.9). Additionally, only the lentiviral infection increased the p21 protein expression in NHC showing no differences between Lent-shRNA-control and Len-shRNA-SOX17 (Figure R.8).

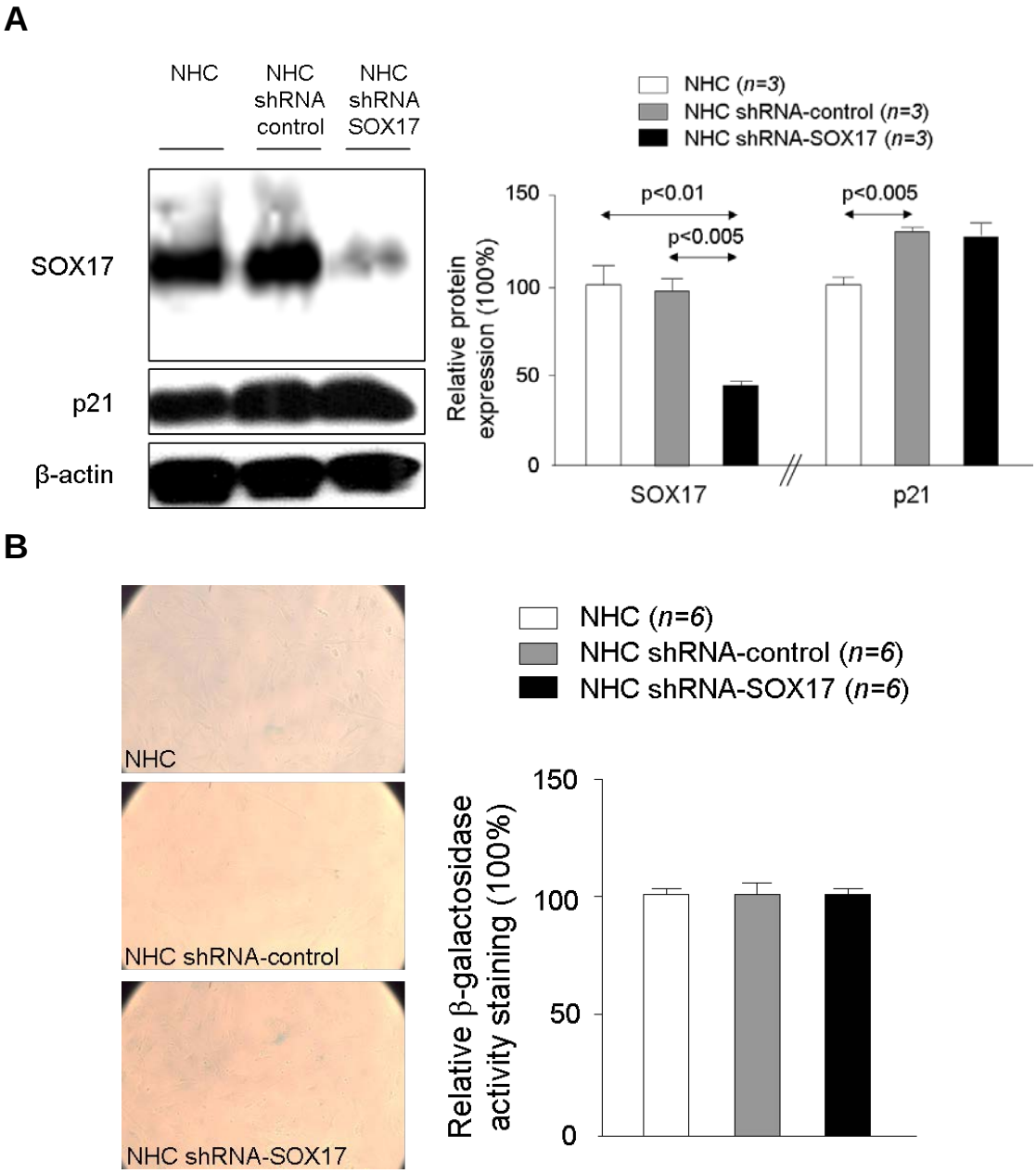

Figure R.8. SOX17 does not affect the senescence process of NHC in culture. A) Representative western blot (left) and relative expression (right) of SOX17 and p21 proteins in NHC infected with Lent-shRNA-SOX17, Lent-shRNA-control or non-infected. β-actin was used as normalizing loading control. B) Light microscopy images (left) and relative β-galactosidase staining activity (right) in NHC infected with Lent-shRNA-SOX17, Lent-shRNA-control or non-infected. n=number of samples in each condition.

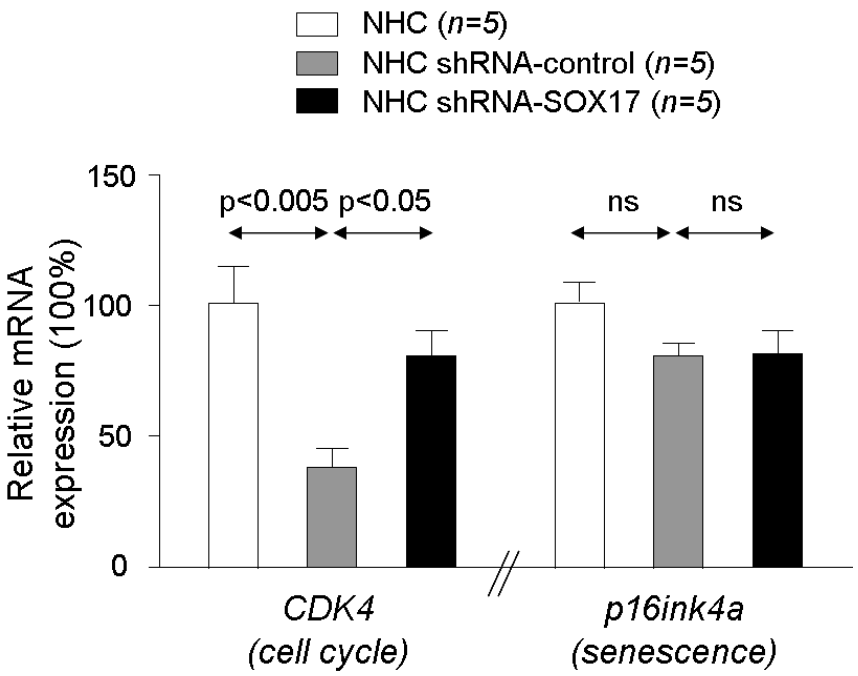

Figure R.9. Relative *CDK4* and *p16*^{INK4a} mRNA expression in NHC infected with Lent-shRNA-SOX17, Lent-shRNA-control or incubated with vehicle solution. *GADPH* was used as housekeeping normalizing gene. n=number of samples in each condition.

R.4. Experimental downregulation of SOX17 in normal human cholangiocytes promotes their Wnt-dependent proliferation.

Recent reports indicated that SOX17 could be involved in the negative regulation of the Wnt/β-catenin pathway [198]. Based on this data, we investigated the implication of SOX17 on the proliferation-regulating role of the Wnt/β-catenin pathway in NHC in culture. The inhibition of *SOX17* alone already induced NHC proliferation (Figure R.10.A). The presence of the Wnt3a ligand did not affect the proliferation of NHC infected with Lent-shRNA-control or non-infected. However, notably, the Wnt3a ligand promoted the proliferation of NHC previously infected with Lent-shRNA-SOX17 (Figure R.10.B); this event was

associated with decreased mRNA levels of *SFRP1*, a protein that binds to and inhibits the Wnt ligands (Figure R.11).

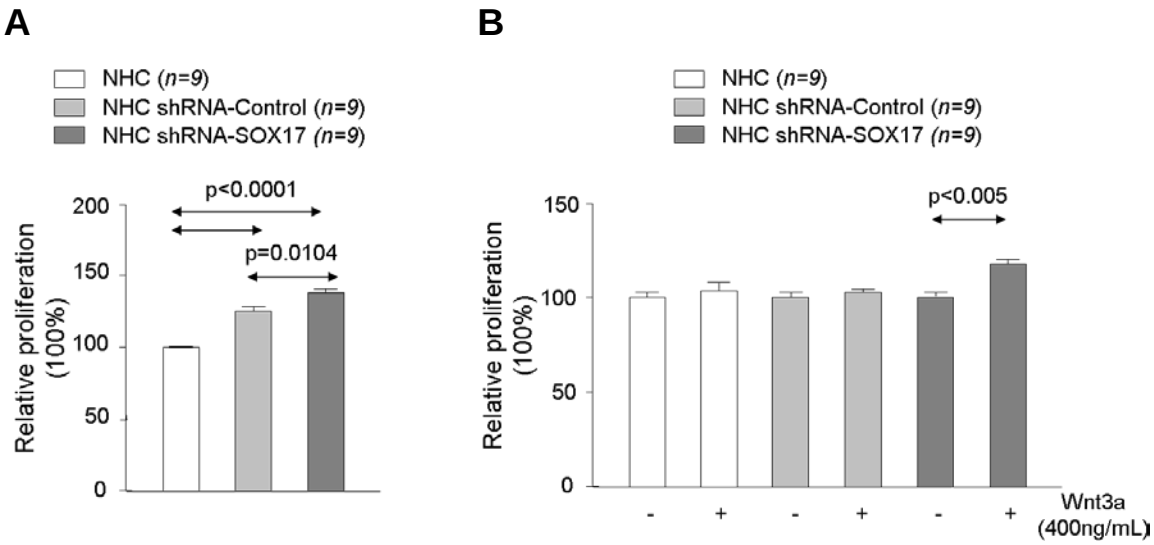

Figure R.10. A) Relative proliferation of NHC in NHC infected with Lent-shRNA-SOX17, Lent-shRNA-control or non-infected. B) Relative proliferation of NHC in NHC infected with Lent-shRNA-SOX17, Lent-shRNA-control or non-infected in the presence or absence of Wnt3a.

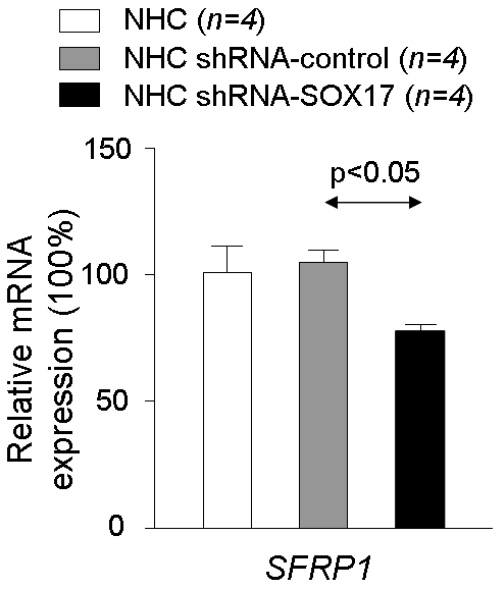

Figure R.11. Relative *SFRP1* mRNA expression in NHC infected with Lent-shRNA-SOX17, shRNA-control or non-infected. *GADPH* was used as housekeeping normalizing gene. n=number of samples in each condition.

R.5. SOX17 expression is reduced in CCA human tissue

Based on our aforementioned data demonstrating that SOX17 regulate cholangiocyte differentiation and the maintenance of the biliary phenotype, we evaluated the expression of SOX17 in CCA human samples compared to diverse controls. Since normal human liver biopsies are mainly composed of hepatocytes, which show very low expression of SOX17 [221], the *SOX17* mRNA levels in CCA human tissue were compared to both low passages of NHC and normal gallbladder human tissue (which is highly composed by cholangiocytes) [222]. Our data revealed that *SOX17* mRNA expression levels are lower in CCA human tissue than both NHC in culture and normal gallbladder human tissues (Figure R.12).

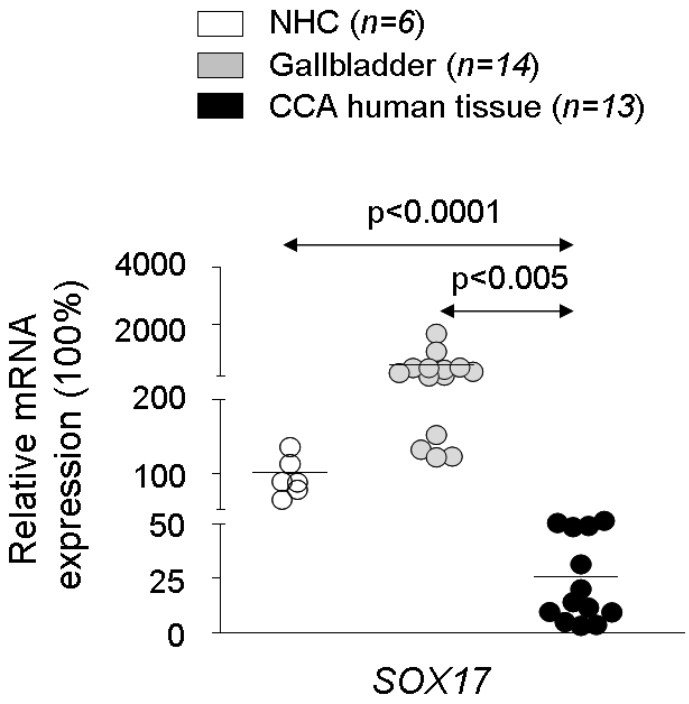

Figure R.12. Relative *SOX17* mRNA expression in NHC in culture, normal human gallbladder tissues and CCA human samples. *GAPDH* was used as housekeeping normalizing gene. Dots represent independent patient's samples and bars indicate the mean value.

In addition, SOX17 protein expression was evaluated by immunofluorescence in both normal human livers and iCCA human tissues. In normal human livers, CK19-positive cells (i.e. cholangiocytes) show high expression of SOX17 (Figure R.13). At the cellular level, SOX17 ewas present at the perinuclear and nuclear level. In contrast, the expression of SOX17 was found almost absent in human iCCA cells, which stained positively for CK19 (Figure R.13).

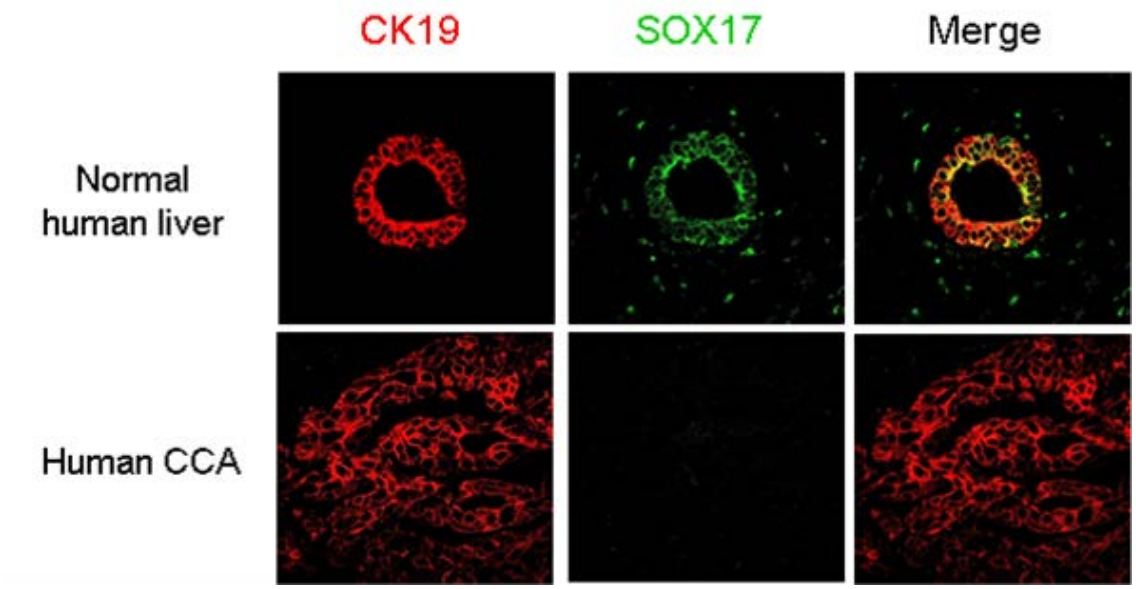

Figure R.13. Representative images of immunofluorescence showing SOX17 expression in normal human liver and iCCA human tissue. Expression of CK19 and SOX17 are indicated in red and green, respectively. Number of normal liver biopsies and iCCA human tumors analyzed = 5 in each condition.

R.6. CCA human cells show decreased SOX17 expression compared to normal human cholangiocytes in culture

We further evaluated the expression of SOX17 in three different CCA human cell lines (EGI1, TFK1 and Witt) compared to NHC in culture. Similarly to the previous observations using human liver and CCA samples, SOX17 mRNA and protein expression was found highly downregulated in all three types of CCA

human cells compared to NHC (Figure R.14). These data strongly indicated the potential role of SOX17 downregulation in cholangiocarcinogenesis and supported the study of this transcription factor in the etiopathogenesis of CCA.

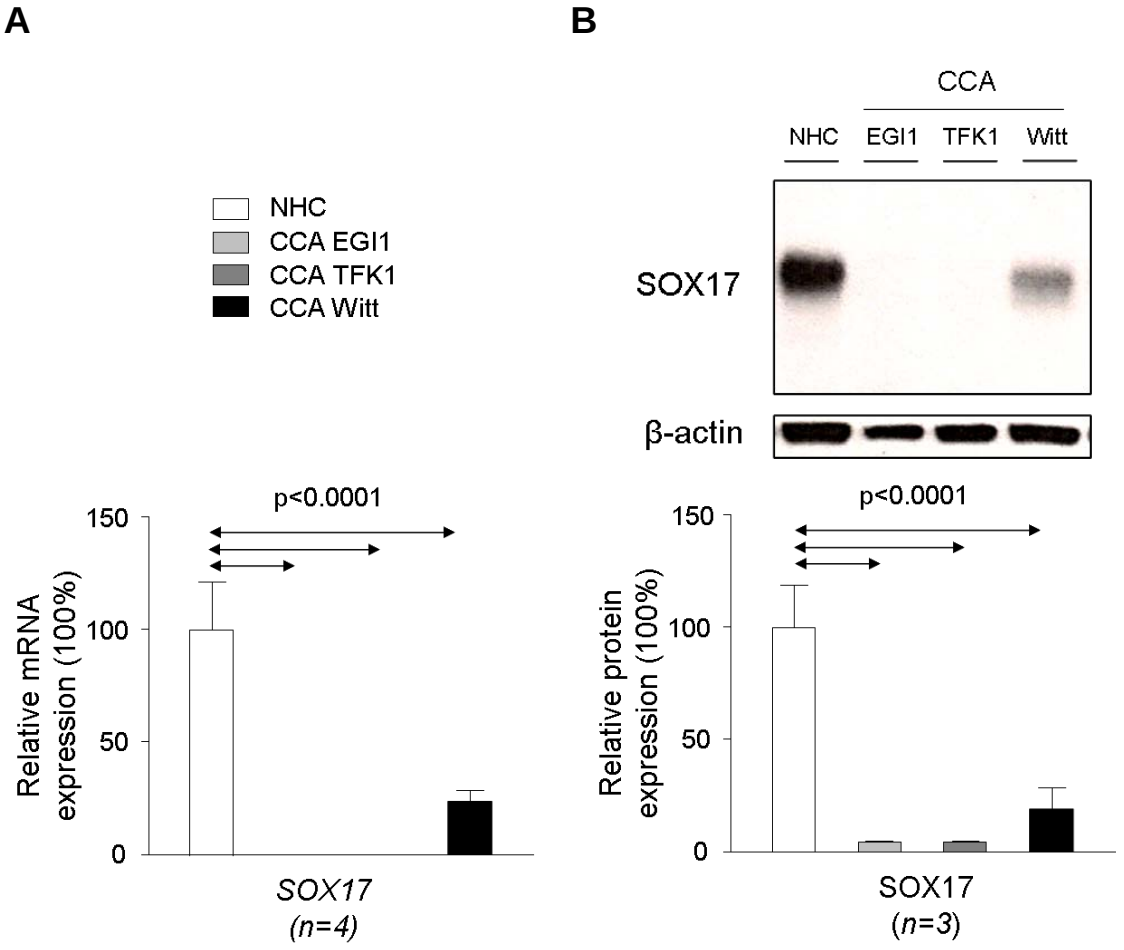

Figure R.14. Relative SOX17 expression in NHC and CCA human cell lines. A) *SOX17* mRNA levels in NHC and CCA human cell lines (EGI1, TFK1, Witt). *GADPH* was used as housekeeping normalizing gene. B) Representative western blot of SOX17 protein in NHC and CCA human cell lines (EGI1, TFK1, Witt). β-actin was used as normalizing loading control. n=number of samples in each condition.

R.7. Role of SOX17 in cholangiocarcinogenesis

In order to evaluate the role of SOX17 on biliary cancer we overexpressed this transcription factor in CCA human cells (EGI1) by using lentiviral vectors encoding the *SOX17* ORF.

R.7.1. Experimental overexpression of SOX17 in CCA human cells promotes its accumulation in the nucleus

Lentiviral vectors containing *SOX17* ORF (Lent-SOX17) under the regulation of the elongation factor 1α promoter were produced in collaboration with the group of Prof. José J. G. Marín (University of Salamanca, Salamanca, Spain), as described in the Materials and Methods section. First, we evaluated the multiplicity of infection (MOI) needed to overexpressed SOX17 in all CCA human cell lines *in vitro*. Thus, different MOIs (i.e. 1, 3, 5, 10 and 15) per cell were used. Western blot analysis for SOX17 revealed that 48 h after infection there is SOX17 overexpression, which is dependent on the MOI employed (Figure R.15).

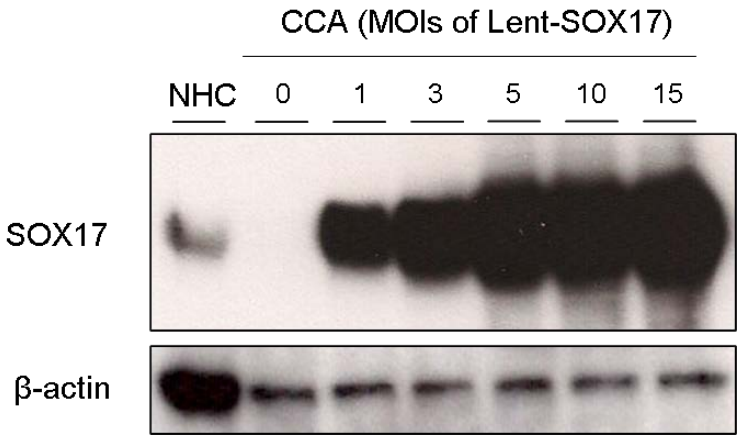

Figure R.15. Representative western blot showing SOX17 protein expression in CCA human cells infected with different MOIs of Lent-SOX17 compared to its basal levels in both NHC and CCA human cells. β-actin was used as a normalizing loading control.

Next, we performed immunofluorescence analysis to evaluate the proportion of CCA human cells showing SOX17 overexpression under the infection of different MOIs of Lent-SOX17 compared to CCA human cells infected with a Lent-control and to both NHC and CCA human cells under basal condition. Moreover, the location of SOX17 in the cells was investigated. In agreement with the western blot analysis, immunofluorescence also demonstrated that NHC possess higher basal levels of SOX17 protein than CCA human cells and this expression is mainly located in the nucleus of the cells but can also be found in the cytoplasm (Figure R.13). On the other hand, experimental overexpression of SOX17 in CCA human cells resulted in its accumulation in the nucleus, and the percentage of cell infection was dependent on the MOI employed (1, 3, or 5) compared to CCA human cells infected with Lent-control (MOI of 5) (Figure R.16). The MOIs of 3 and 5 resulted in the general infection (~100%) of CCA human cells and in the overexpression of SOX17 in the nucleus, whereas the MOI of 1 just infected a partial proportion (~40%) of the cells (Figure R.16). Based on these data, the MOI of 3 was used for further experiments of SOX17 overexpression as it is the minimal MOI by which all cells are infected and show non-saturating SOX17 overexpression.

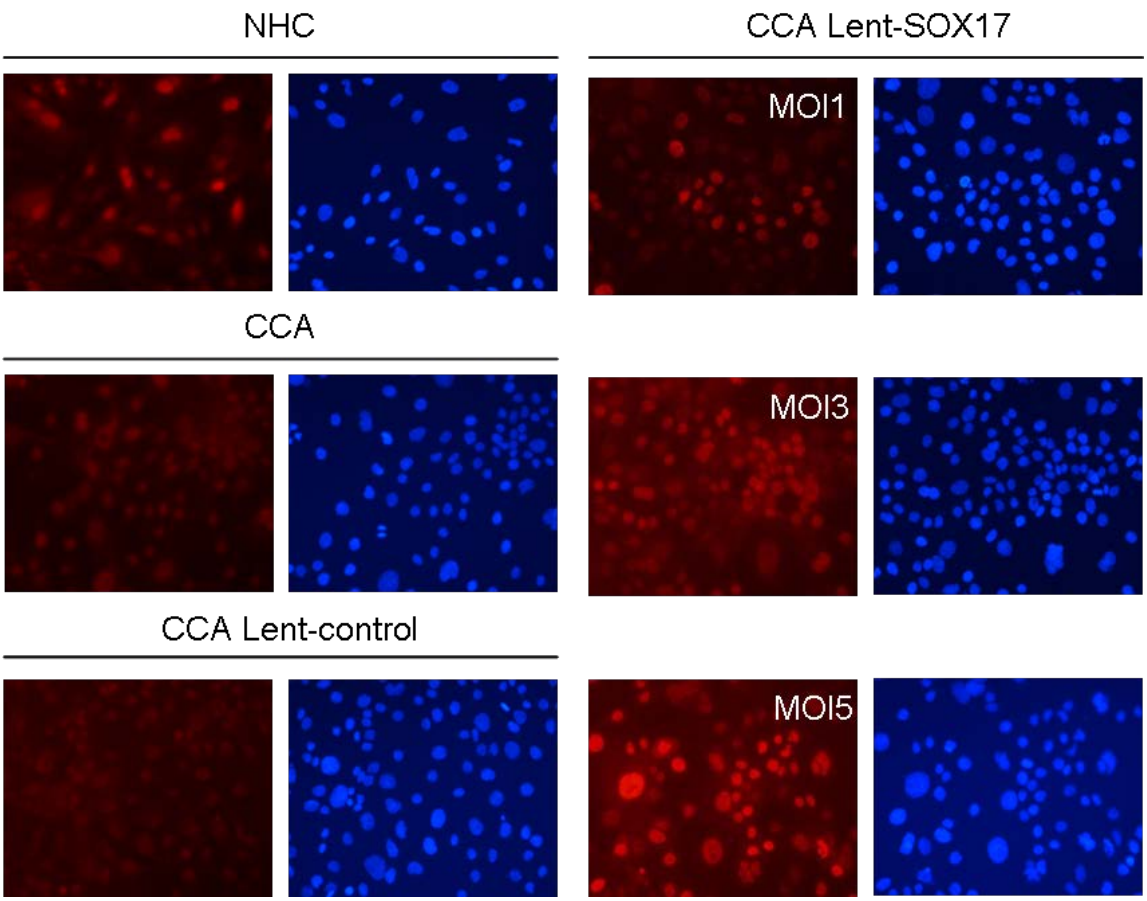

Figure R.16. Representative immunofluorescence of SOX17 protein expression (red) in CCA human cells infected with different MOIs of Lent-SOX17 (1, 3 and 5) or Lent-control (5), as well as in NHC and CCA human cells under basal conditions. Nuclei were stained with DAPI (blue).

R.7.2. Experimental overexpression of SOX17 in human CCA cells reduces their tumorigenic capacity *in vivo*

We evaluated the role of SOX17 on the tumorigenic capacity of CCA human cells *in vivo*. For this purpose, CCA human cells (10^5 cells) were infected subcutaneously into immunodeficient nude mice (*Crl:NU-Foxn1*^{nu}). In particular, CCA human cells, previously infected with Lent-control or Lent-SOX17 at a MOI of 3, were injected into the left or right flank of the back of eight immunodeficient mice, respectively (Figure R.17.A). Non-infected CCA human cells were injected in both flanks of an immunodeficient mouse as a control (data not shown).

The tumor size monitoring was initiated one month after cell injection and was carried out every 3-4 days for an additional month before of the sacrifice of the animals. The tumors generated from CCA human cells infected with Lent-control showed continuous lineal growth overtime (Figure R.17.B), which was similar to the non-infected CCA human cells (data not shown). In contrast, CCA human cells infected with Lent-SOX17 showed smaller subcutaneous tumors, or even absence of tumors, compared to those generated CCA from human cells infected with Lent-control (Figure R.17.A-C).

A

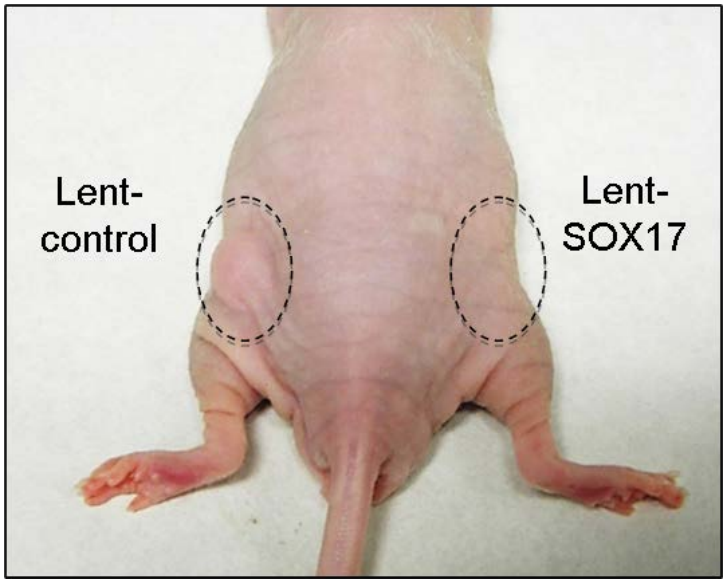

B

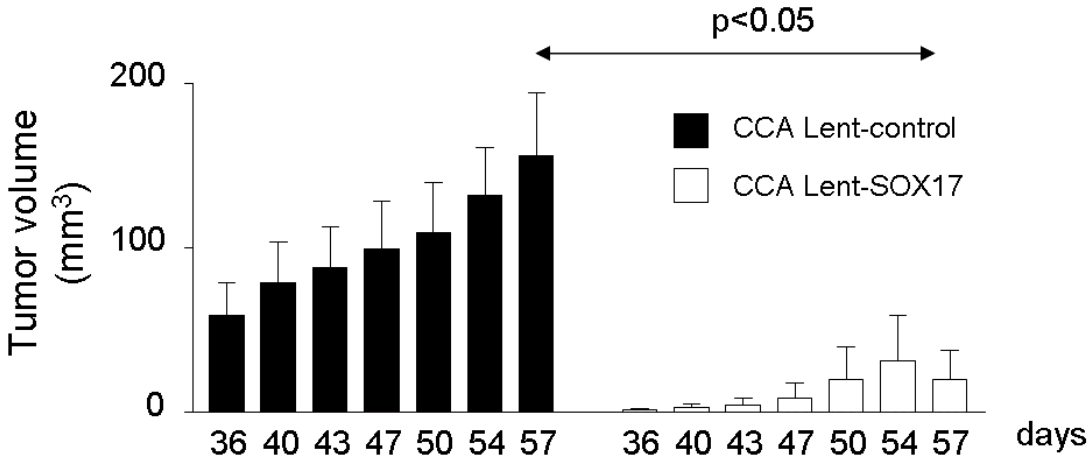

C

Figure R.17. Role of SOX17 in CCA tumor growth in immunodeficient mice. A) Representative images of an immunodeficient mouse before the sacrifice that received the injection of CCA human cells infected with Lent-control (left flank) and Lent-SOX17 (right flank). B) Tumor volume measurement over time. C) Image comparing in pairs the tumors isolated after the sacrifice of the immunodeficient mice.

R.7.3. Experimental overexpression of SOX17 promotes apoptosis in CCA human cells but not in normal human cholangiocytes

Since experimental overexpression of SOX17 in CCA human cells strongly reduced their tumorigenic capacity *in vivo*, we evaluated the molecular mechanism involved in this effect. First, we analyzed apoptosis in these cells. Our data indicated that experimental overexpression of SOX17 promotes cell death (i.e. apoptosis measured by Annexin V and Propidium Iodide) in CCA human cells in a MOI-dependent manner compared to cells infected with Lent-control and non-infected cells (Figure R.18). The MOI previously chosen for the *in vivo* experiment (MOI=3) showed a ~45% of apoptosis (by Annexin V and Propidium Iodide) (Figure R.18).

Since Lent-SOX17 increases the expression of SOX17 in CCA human cells beyond the basal expression levels of SOX17 in NHC, we evaluated the effect of the experimental overexpression of SOX17 on the NHC survival. Notably, in contrast to CCA human cells, experimental overexpression of SOX17 (MOIs 1, 3 and 5) in NHC did not affect their survival (Figure R.19).

A

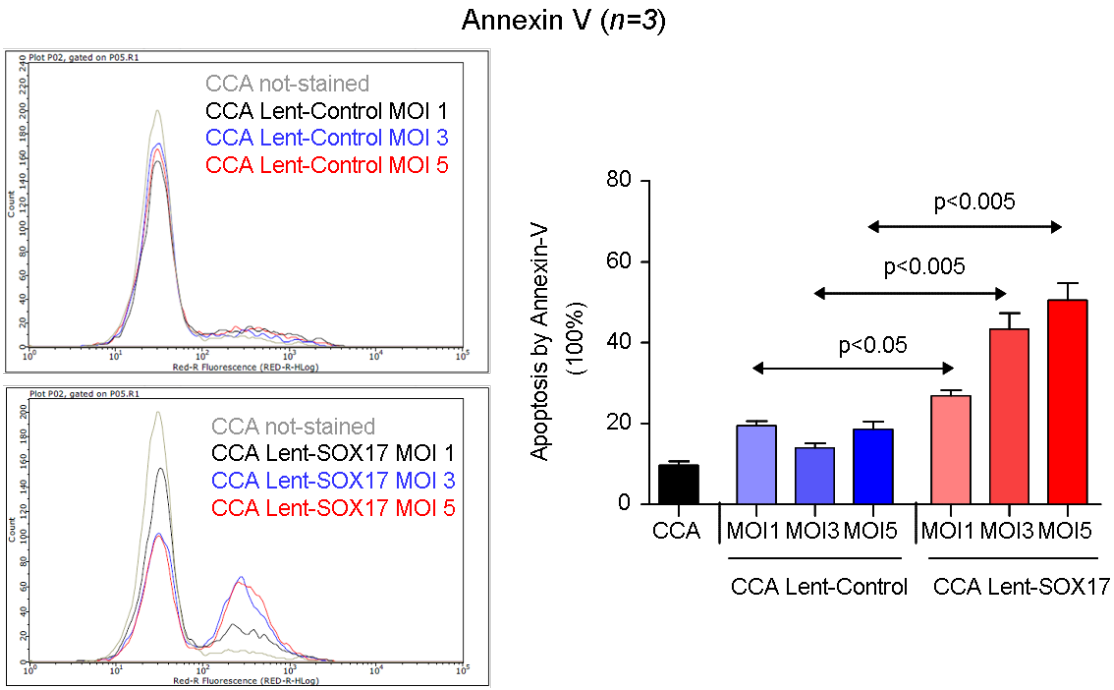

B

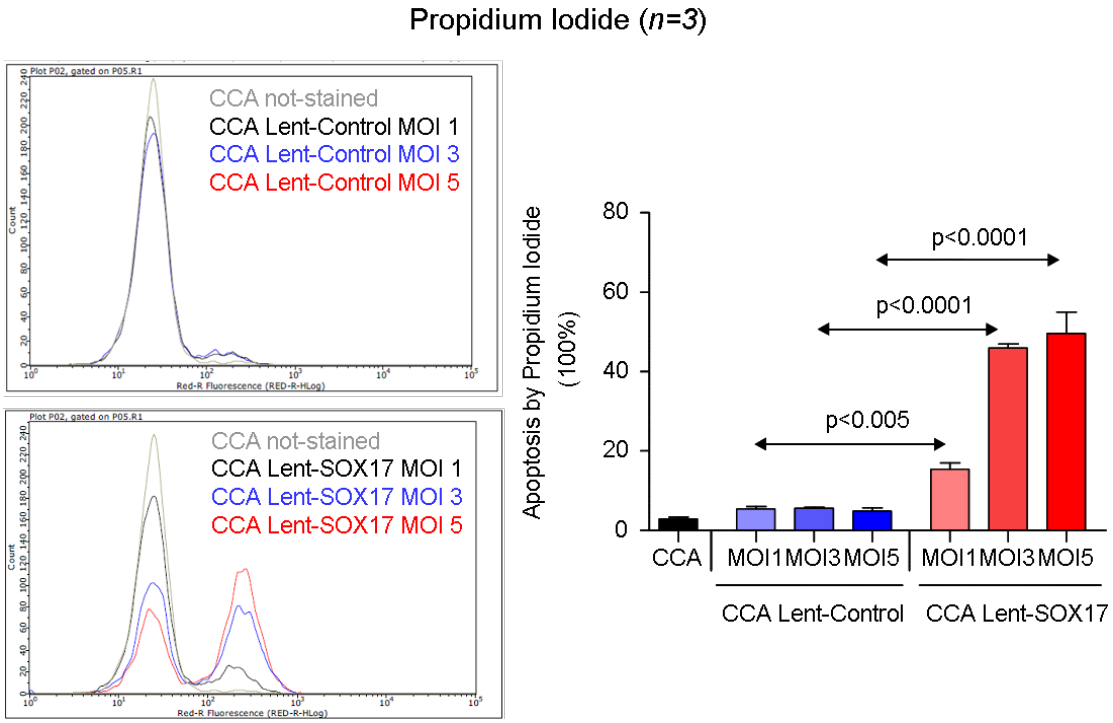

Figure R.18. Role of SOX17 in the survival of CCA human cells. Apoptosis was analyzed 48 h after CCA human cell infection with Lent-SOX17, Lent-control or in non-infected cells by flow cytometry for A) Annexin V and B) Propidium Iodide. A and B show representative histograms and percentage of apoptosis in each assay. n=number of samples in each condition.

A

Annexin V (*n=3*)

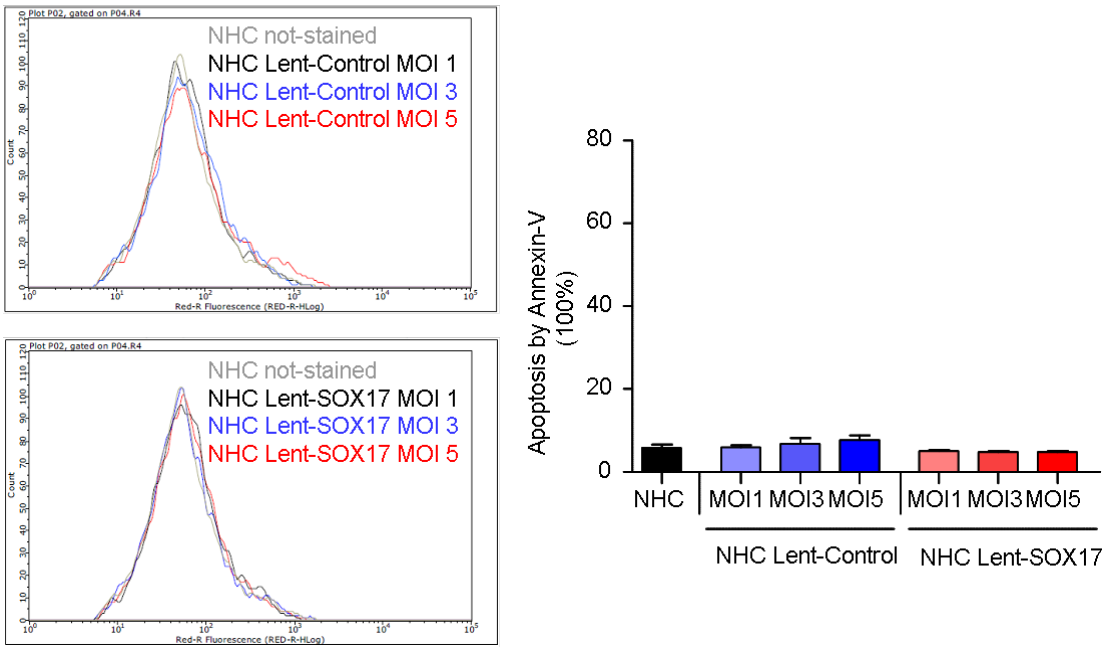

B

Propidium Iodide (*n=3*)

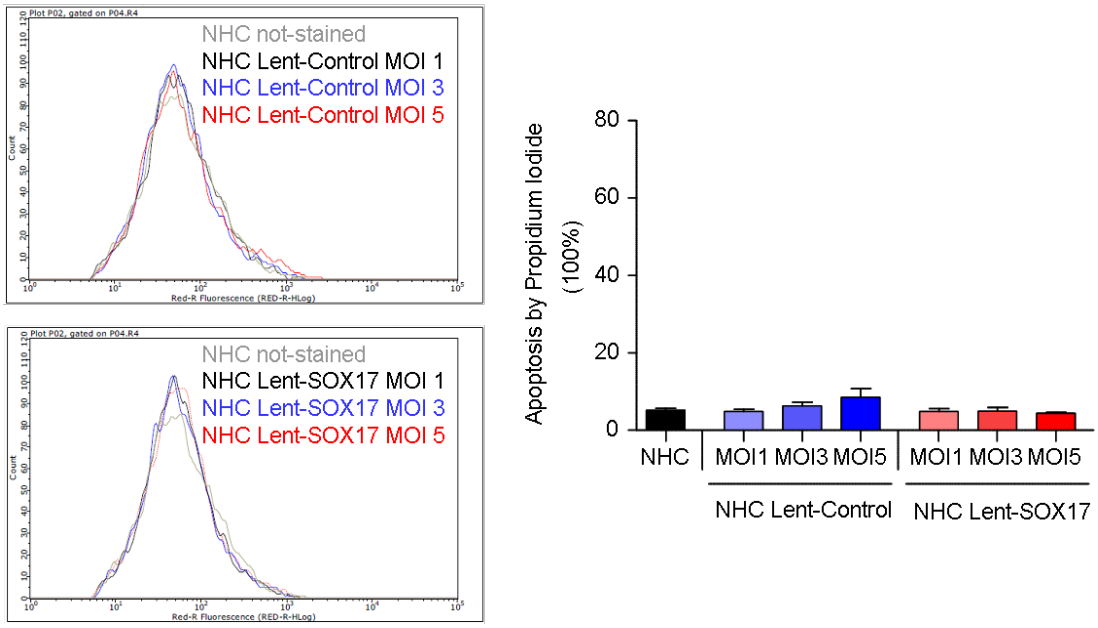

Figure R.19. Role of SOX17 experimental overexpression on NHC survival. Apoptosis was analyzed 48 h after NHC infection with Lent-SOX17, Lent-control or in non-infected cells by flow cytometry for A) Annexin V and B) Propidium Iodide. A and B show representative histograms and percentage of apoptosis in each assay. n=number of samples in each condition.

Next, we studied the molecular mechanisms triggering the apoptotic effect of SOX17 in CCA human cells (using a MOI of 3) by analyzing the caspase-3 activity. Caspase-3 activation may be the result of both mitochondrial-dependent and/or mitochondrial-independent apoptosis. Increased caspase-3 activity (measured by flow cytometry with the Phiphilux-G2D2 kit) was observed in CCA human cells infected with Lent-SOX17 for 48 h compared to cells infected with Lent-control or non-infected cells (Figure R.20).

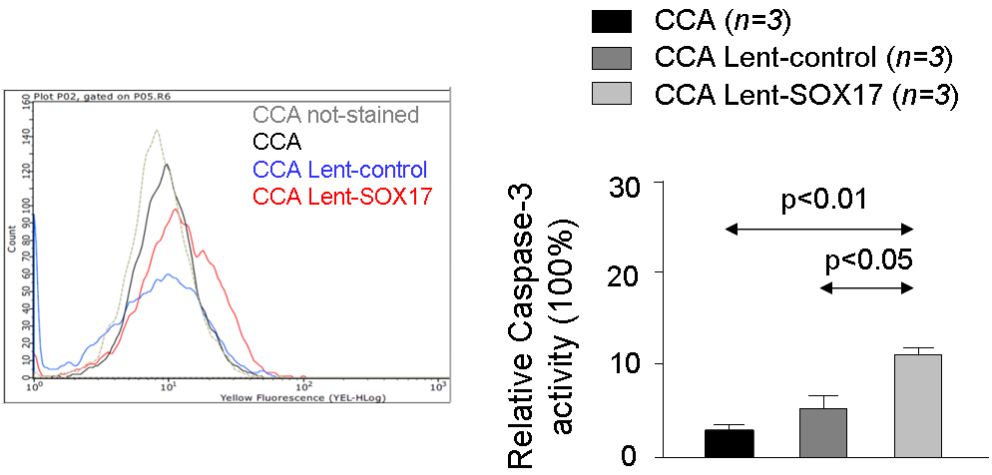

Figure R.20. Role of SOX17 in the caspase-3 activity of CCA human cells. Caspase-3 activity was measured by flow cytometry (Phiphilux-G2D2 assay) in CCA human cells 48 h after infection with Lent-SOX17, Lent-control or in non-infected cells. Representative histogram and percentage of caspase-3 activity in each assay. n=number of samples in each condition.

The apoptotic process may be promoted by the activation of different intracellular signaling pathways. Here, we evaluated the relevant pro-apoptotic JNK/p53 signaling pathway. In particular, the c-Jun N-terminal protein kinase (JNK) activates by phosphorylation the activity of the pro-apoptotic transcription factors c-Jun [223] and p53 [224], among others [225]. Our data showed that experimental overexpression of SOX17 in CCA human cells increased the

phosphorylation of both JNK and p53 compared to cells infected with Lent-control or non-infected (Figure R.21).

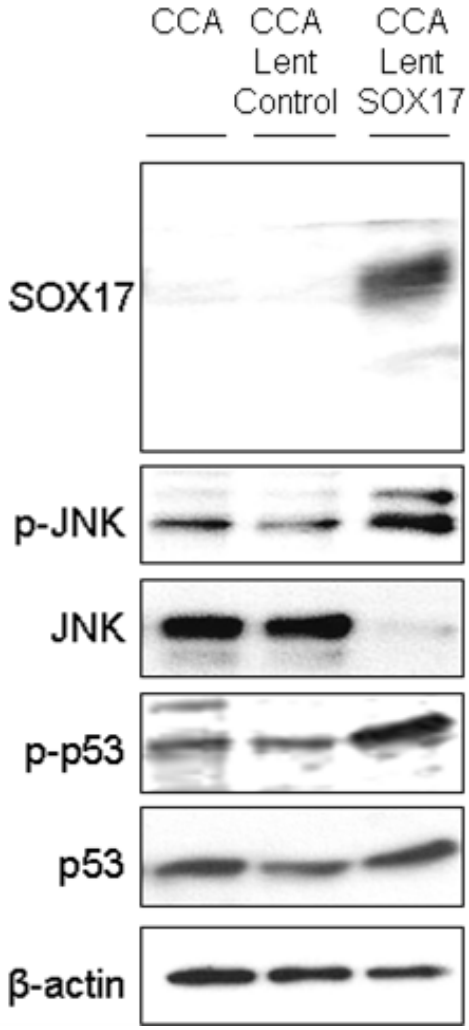

Figure R.21. Representative western blots of the expression and phosphorylation of the pro-apoptotic proteins JNK and p53 in CCA human cells infected for 48 h with Lent-SOX17, Lent-control or non-infected. β-actin was used as a normalizing loading control.

Since apoptosis may be the result of increased oxidative stress in the cell [226-228], we measured the levels of reactive oxygen species (ROS) in CCA human cells by using the CellROX assay kit based on the detection of ROS formation by flow cytometry. Experimental overexpression of SOX17 in CCA

human cells with Lent-SOX17 for 48 h increased the ROS levels compared to cells infected with Lent-control or non-infected cells (Figure R.22).

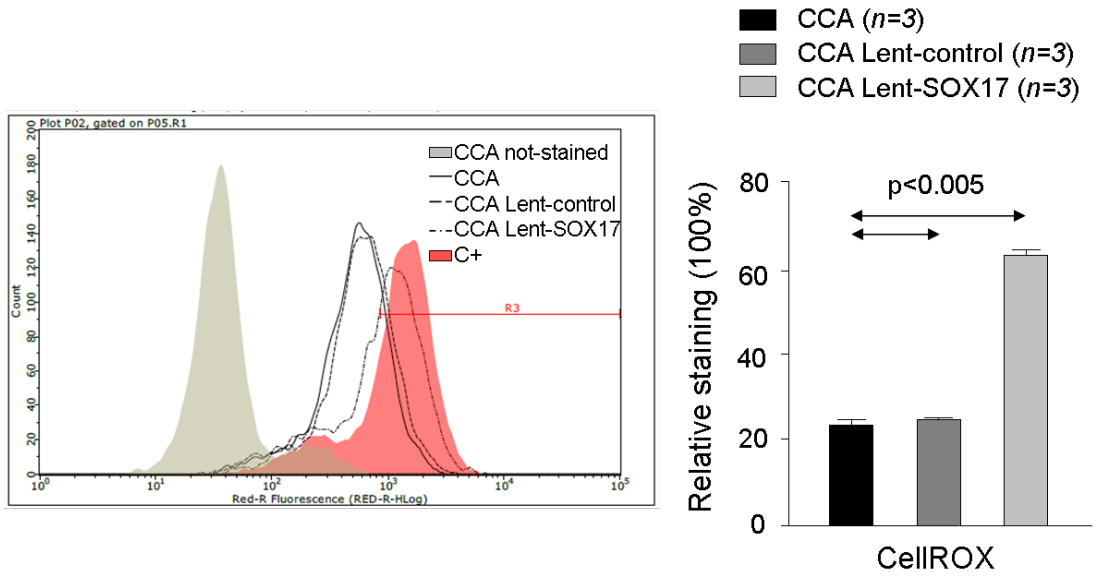

Figure R.22. Role of SOX17 in the oxidative stress CCA of human cells. ROS levels were analyzed by flow cytometry (CellROX Deep Red assay) in CCA human cells infected for 48 h with Lent-SOX17, Lent-control and non-infected. n=number of samples in each condition.

R.7.4. Experimental overexpression of SOX17 in CCA human cells inhibits the Wnt3a-dependent proliferation

The role of SOX17 was also studied on the proliferation of those CCA human cells that did not enter in apoptosis. In particular, we evaluated the pro-mitotic and pro-tumorigenic Wnt/β-catenin pathway, which participates in cholangiocarcinogenesis [229]. Our data showed that Wnt3a ligand promotes the proliferation of non-infected CCA human cells in a dose-dependent manner (Figure R.23.A). Interestingly, the Wnt3a (400ng/mL)-dependent proliferation was inhibited in CCA human cells infected with Lent-SOX17 compared to cells infected with Lent-control and non-infected cells (Figure R.23.B).

A

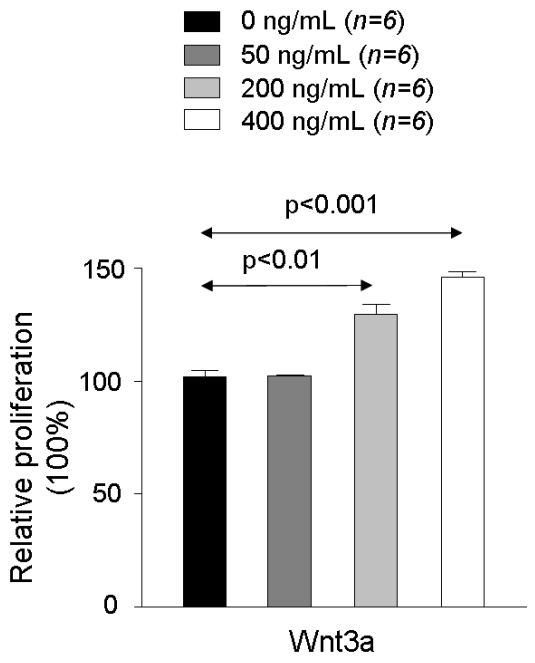

B

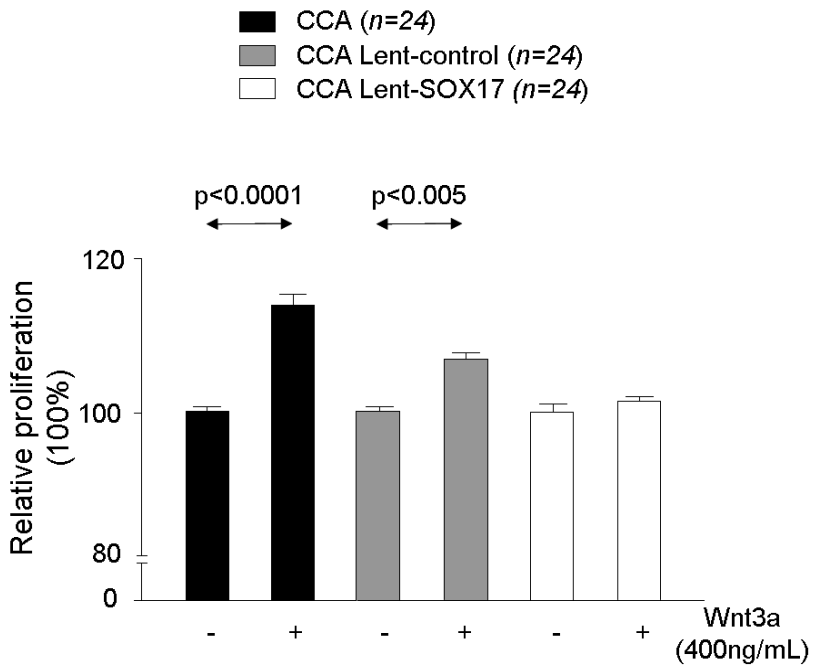

Figure R.23. Role of SOX17 in the Wnt3a-dependent proliferation of CCA human cells. A) Wnt3a ligand promotes the proliferation of CCA human cells in a dose-dependent manner. B) Wnt3a (400 ng/ml)-dependent proliferation is inhibited in CCA human cells infected with Lent-SOX17 compared to cells infected with Lent-control or non-infected cells.

In addition, we evaluated the expression and phosphorylation levels of β-catenin, which is a key effector in the Wnt signaling pathway. Different β-catenin residues may be phosphorylated determining its biological consequences. Thus, thr41/ser45 phosphorylation promotes a characteristic nuclear activation of β-catenin [122]. In contrast, phosphorylation of ser33/37/thr41 residues mediates the ubiquitin/proteasome-dependent degradation of β-catenin [230]. Our data showed that experimental overexpression of SOX17 in CCA human cells with Lent-SOX17 increased the ser33/37/thr41 phosphorylation of β-catenin compared to cells infected with Lent-control or non-infected cells (Figure R.24). These data indicated that SOX17 may inhibit the Wnt/β-catenin-dependent proliferation in CCA human cells by promoting the degradation of β-catenin.

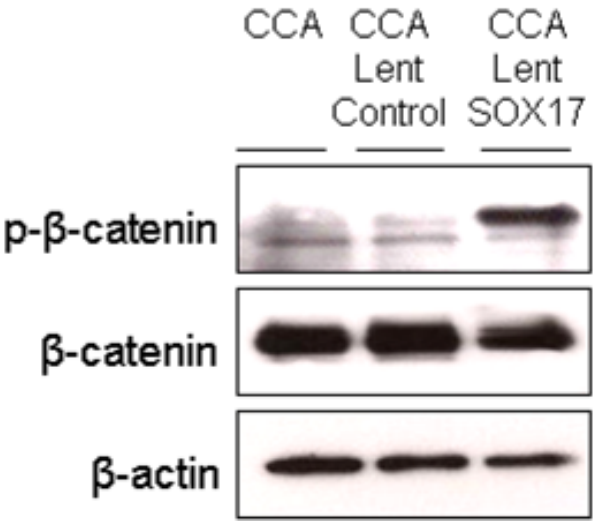

Figure R.24. Role of SOX17 in β-catenin (S33/37/T41) phospholylation. Representative western blots of p-β-catenin (S33/37/T41)/total β-catenin expression in CCA human cells infected with Lent-SOX17, Lent-control or non-infected cells. β-actin was used as normalizing loading control.

R.7.5. Experimental overexpression of SOX17 in CCA human cells inhibits cell migration

We also evaluated the role of SOX17 in cell migration. Thus, cell migration was determined by the scratch method using non-infected, Lent-control or Lent-SOX17 infected CCA human cells. Our data revealed that SOX17 overexpression diminished CCA human cell migration in comparison with non-infected or Lent-control infected CCA human cells (Figure R.25).

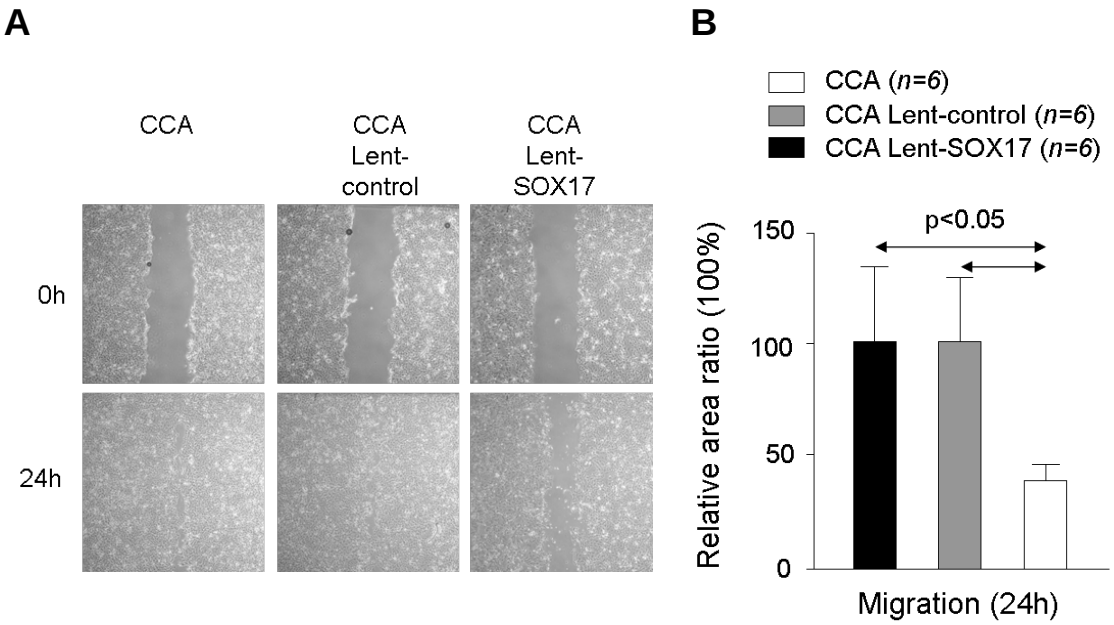

Figure R.25. A) Representative microscopic images of the scratch-migration assay at 0 and 24 h timepoints in CCA human cells infected with Lent-SOX17, Lent-control or non-infected cells. B) Relative area ratio 24 h after the scratch of the migrated CCA human cells infected with Lent-SOX17, Lent-control or non-infected cells. n=number of samples in each condition.

R.7.6. Experimental overexpression of SOX17 in CCA human cells increases the expression of biliary markers of differentiation

The role of SOX17 was studied on the expression of biliary epithelial markers of differentiation in those CCA human cells that did not enter in apoptosis. Thus, overexpression of SOX17 in CCA human cells increased the

mRNA levels of *CK7*, *FN* [231] and *zonula occludins* (*ZO-1*) [232] compared to cells infected with Lent-control or non-infected cells (Figure R.26). On the other hand, overexpression of SOX17 in CCA human cells downregulated the mRNA levels of the mesenchymal marker *S100A4* [233, 234], which becomes upregulated in cholangiocarcinogenesis during the EMT process, compared to cells infected with Lent-control or non-infected cells (Figure R.26).

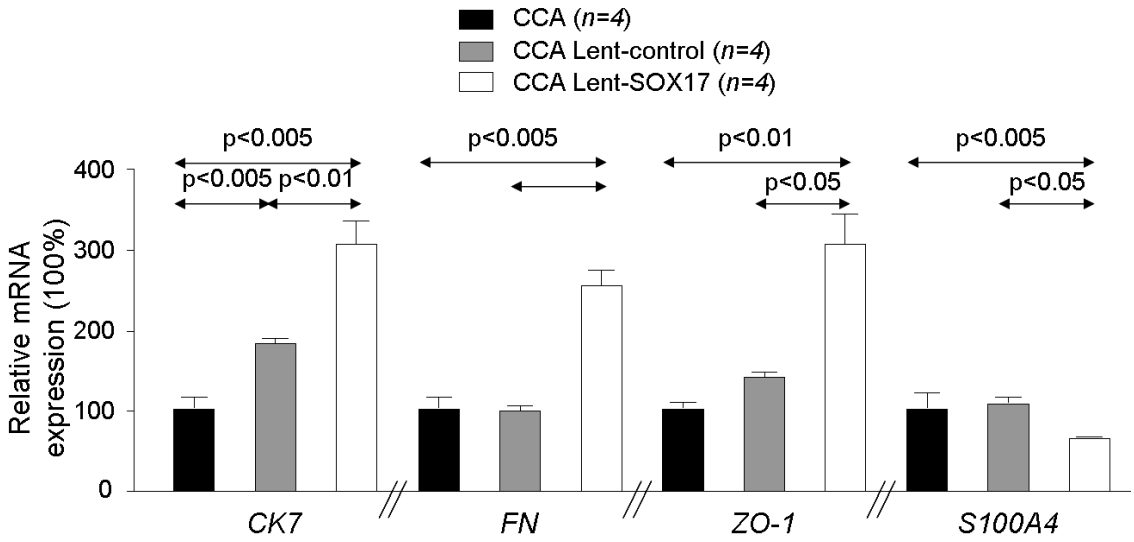

Figure R.26. Relative mRNA expression of biliary (*CK7*, *FN* and *ZO-1*) and mesenchymal (*S100A4*) markers in CCA human cells with SOX17 overexpression compared with Lent-control infected and non-infected cells. *GADPH* was used as housekeeping normalizing gene. n=number of samples in each condition.

R.7.7. Experimental overexpression of SOX17 in CCA human cells normalizes their diminished primary cilium length

The primary cilium is a sensory organelle key for cholangiocyte biology but also involved in the pathogenesis of different cholangiopathies like CCA [11, 115, 235]. In this regard, CCA human cells show morphological and functional ciliary abnormalities characterized by shorter or even absent primary cilia due to HDAC6 overexpression that de-acetylates ciliary α-tubulin [115]. Here, we

evaluated in collaboration with the group of Dr. Sergio Gradilone (Hormel Institute, University of Minnesota, Austin, MN, USA) the role of SOX17 in the primary cilium length of CCA human cells. Experimental overexpression of SOX17 in those CCA human cells that did not enter apoptosis showed after 7 days of confluence longer cilia than to those cells infected with Lent-control or non-infected cells (Figure R.27); this event was associated with decreased *HDAC6* mRNA levels (Figure R.28).

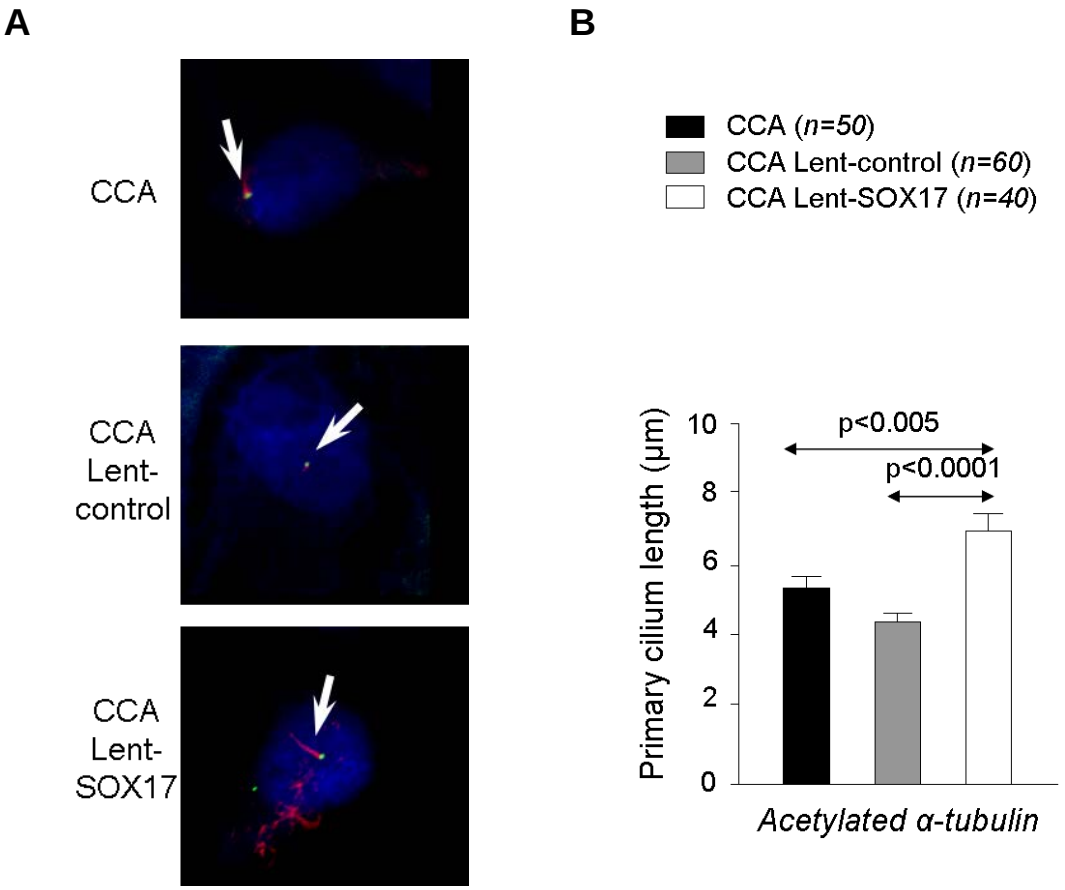

Figure R.27. A) Representative confocal fluorescence microscopy images of primary cilia stained with acetylated α-tubulin (axoneme: red) and γ-tubulin (centrioles that form from the basal body of the cilium: green). Nuclei were stained with DAPI. B) Relative primary cilium length (µm) quantified by acetylated α-tubulin immunofluorescence staining. n=number of samples in each condition.

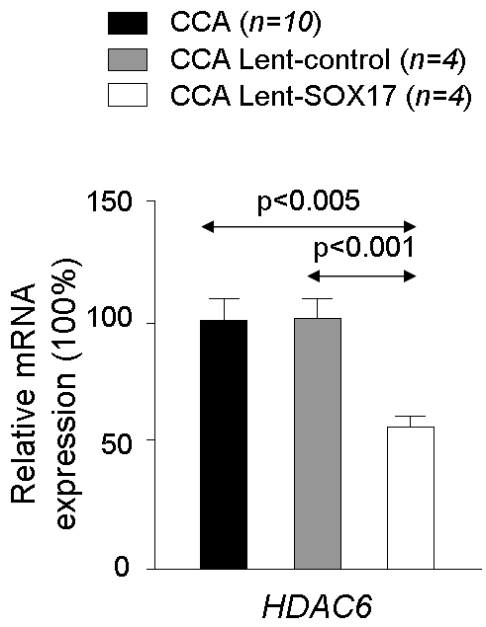

Figure R.28. Relative *HDAC6* mRNA levels in CCA human cells infected with Lent-SOX17, Lent-control or non-infected. *GADPH* was used as housekeeping normalizing gene. n=number of samples in each condition.

R.8. Gene expression analysis by "mRNA microarrays"

R.8.1. Samples

For the "mRNA microarrays", NHC both non-infected and infected, with Lent-shRNA-control or Lent-shRNA-SOX17, were used. Infected cells were selected with puromycin for one week and then the RNA was isolated from the cells. On the other hand, CCA human cells (EGI1) infected with Lent-control, Lent-SOX17 or non-infected were used and the RNA isolated after 6 h of infection. All these conditions are summarized as follows:

a) non-infected NHC (NHC)

b) NHC infected with Lent-shRNA-Control (N_shCtrl)

c) NHC infected with Lent-shRNA-shSOX17 (N_shSOX17)

d) non-infected CCA (CCA)

e) CCA infected with Lent-Control (C_Ctrl)

f) CCA infected with Lent-SOX17 (C_SOX17)

The mRNA expression profiles were determined by using the *Illumina_human_v6.2* microarray. The total mRNA was isolated by using the *miRNeasy Micro kit* (Qiagen) following the manufacturer's instructions, as was described in Materials and Methods section M.13.1.

R.8.2. Volvanoplots, heatmaps and gene functions

Four different comparisons were carried out in order to determine the differential mRNA expression profile between NHC and CCA human cells (EGI) after the experimental modulation of SOX17 expression levels:

i) **"N_shSOX17" vs "NHC and N_shCtrl"**: this condition determines the mRNA expression changes induced by knocking-down *SOX17* in NHC compared to those genes similarly expressed between "non-infected NHC" and "NHC infected with Lent-shRNA-control".

ii) **"N_shSox17 and CCA"** ***vs*** **"NHC and N_shCtrl"**: this condition determines the mRNA expression changes induced by knocking-down *SOX17* in NHC that are similar to CCA human cells (EGI1) but different to both "non-infected NHC" and "NHC infected with Lent-shRNA-control".

iii) **"C_SOX17"** ***vs*** **"CCA and C_Ctrl"**: this condition determines the mRNA expression changes induced by overexpressing SOX17 in CCA human cells (EGI1) compared to those genes similarly expressed between "non-

infected CCA human cells (EGI1)" and "CCA human cells (EGI1) infected with Lent-control".

iv) **"C_SOX17 and NHC"** ***vs*** **"CCA and C_Ctrl"**: this condition determines the mRNA expression changes induced by overexpressing SOX17 in CCA human cells (EGI1) that are similar to NHC but different to those genes similarly expressed between "non-infected CCA human cells (EGI1)" and "CCA human cells (EGI1) infected with Lent-control".

R.8.2.1. Comparison #1: "N_shSOX17" vs "NHC and N_shCtrl"

A *volcanoplot* analysis was performed to compare the gene expression (mRNA) profile between "N_shSOX17" and "NHC and N_shCtrl" groups (Figure R.29). Thus, the expression of those genes differentially expressed between "NHC cells under *SOX17* downregulation" and "NHC controls (NHC and NHC Lent-shRNA-control)" cells were compared.

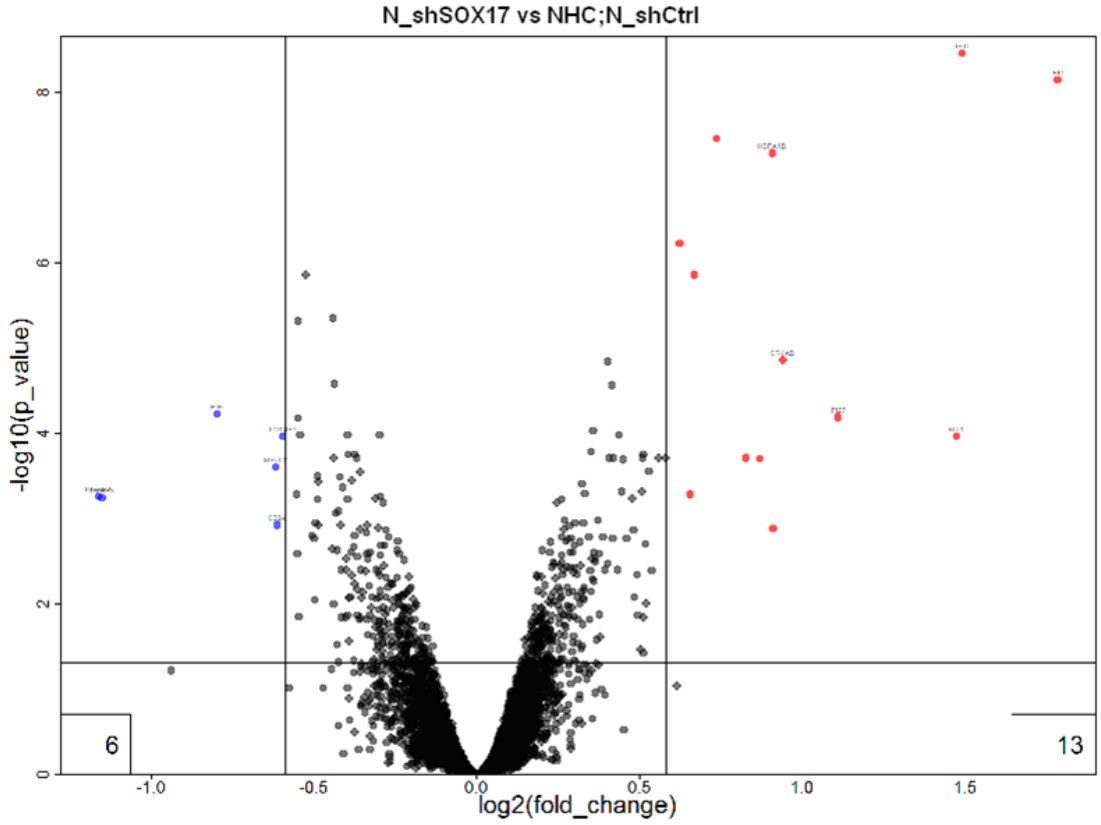

Figure R.29. *Volcanoplot* analysis comparing the mRNA levels "NHC Lent-shRNA-SOX17" cells against "NHC and NHC Lent-shRNA control" cells. Dots represent the expression of each particular gene. Blue dots represent genes downregulated (>-1.5-fold change; *p* value <0.05) and red dots represent genes overexpressed (>+1.5-fold change; *p* value <0.05). Statistical variables: Log2 (Fold change >+/- 1.5) and Log10 (*p* value <0.05).

Additionally, *heatmaps* showing the semi-quantitative expression of those genes differentially expressed (>+/<-1.5-fold change and *p* value <0.05) were generated (Figure R.30).

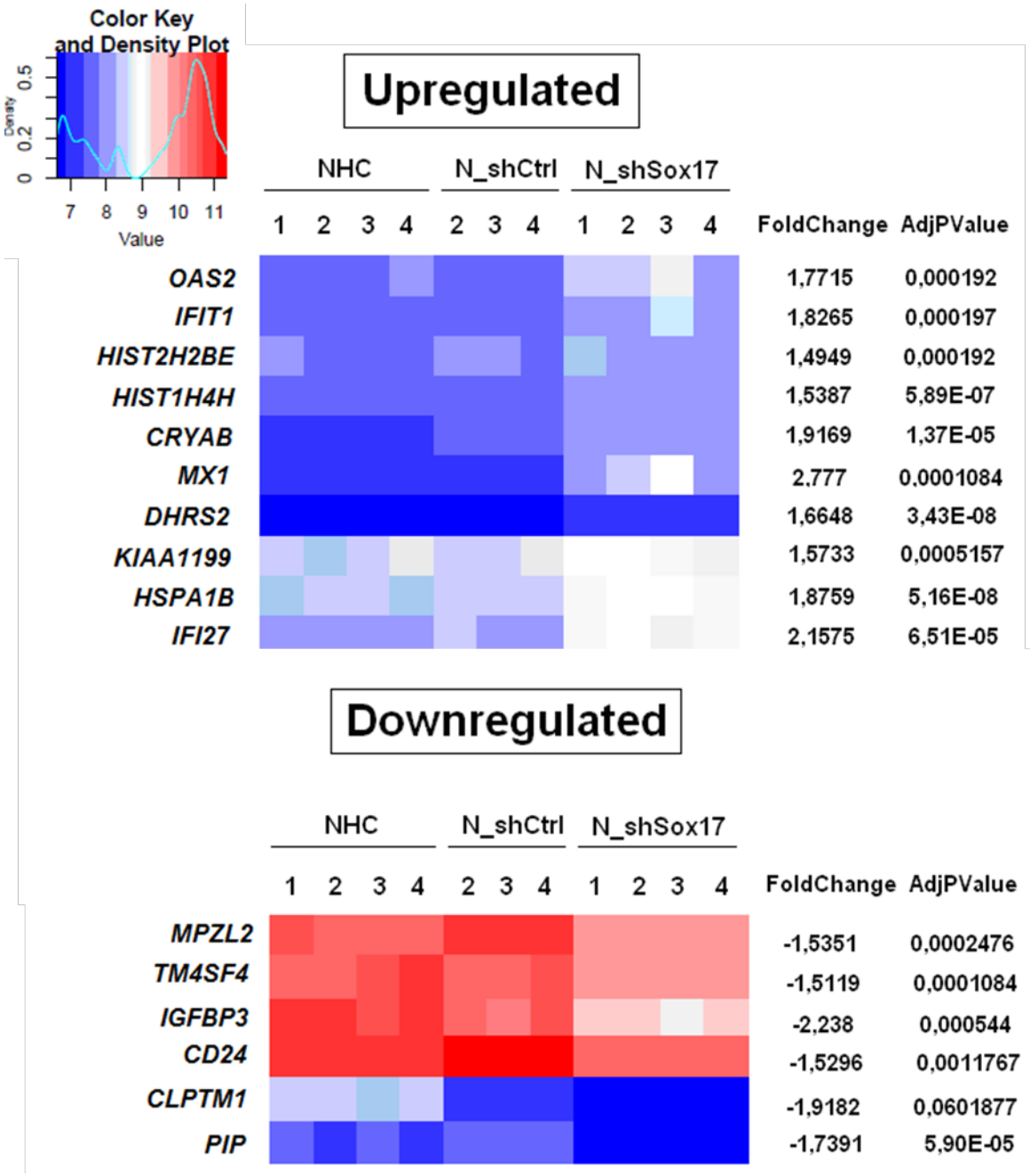

Figure R.30. *Heatmaps* showing those genes found upregulated (top) or downregulated (bottom) in "NHC Lent-shRNA-SOX17" cells compared to "NHC and NHC Lent-shRNA-Control" cells.

The functional analysis of the dysregulated genes revealed that they participate in processes of cell migration, proliferation and survival (Figure R.31). Thus, experimental downregulation of *SOX17* in NHC resulted in decreased expression of genes that inhibit cell migration/invasion [i.e *CD24*

[236, 237], *MPZL2* (also known as EVA1) [238] and *TM4SF4* [239]] and proliferation (i.e. *IGFBP3* [240]). On the other hand, these results were associated with overexpression of genes that promote tumorigenesis [i.e. *IFI27* [241], *IFI6* (also known as G1P3) [242], *IFIT1* [243] and *KIAA1199* [244, 245]] by regulating cell proliferation, migration and drug resistance. These data support the concept that SOX17 is a key regulator of NHC differentiation and its lack may promote tumorigenesis.

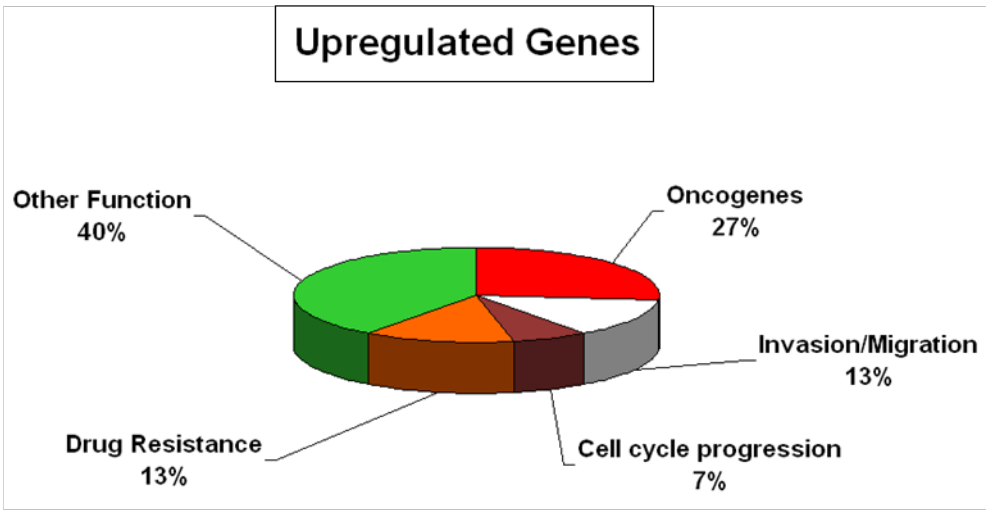

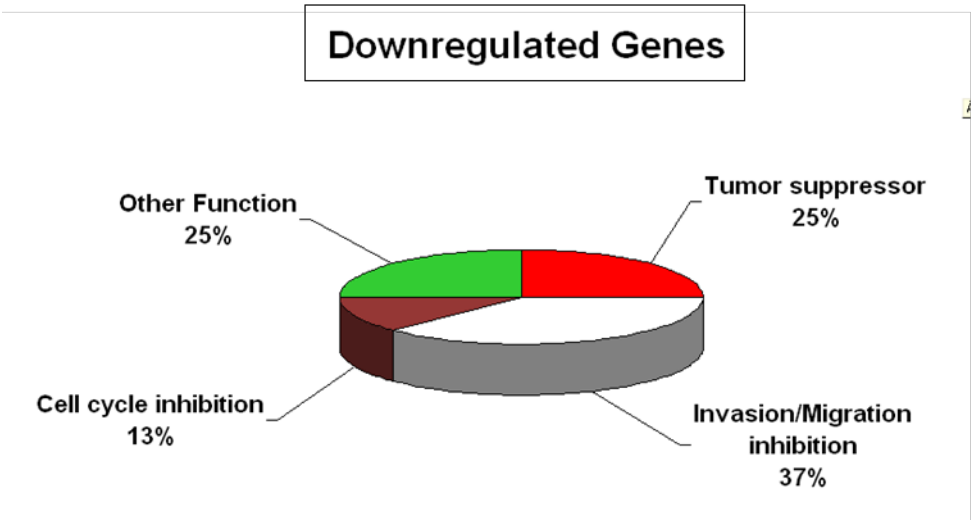

Figure R.31. Clustering by cellular function of those genes found upregulated (top) or downregulated (bottom) in “NHC Lent-shRNA-SOX17” cells compared to “NHC and NHC Lent-shRNA-control” cells. Gene information collected from Pubmed, Uniprot or Genecards.

R.8.2.2. Comparison #2: “N_shSOX17 and CCA” vs “NHC and N_shCtrl”

A *volcanoplot* analysis was performed to compare the gene expression (mRNA) profile between “N_shSOX17 and CCA” and “NHC and N_shCtrl” groups (Figure R.32). Thus, the expression of those genes similarly expressed between “NHC cells under *SOX17* downregulation” and “CCA human cells (EGI1)” were compared with the NHC controls, “NHC and NHC Lent-shRNA-control” cells.

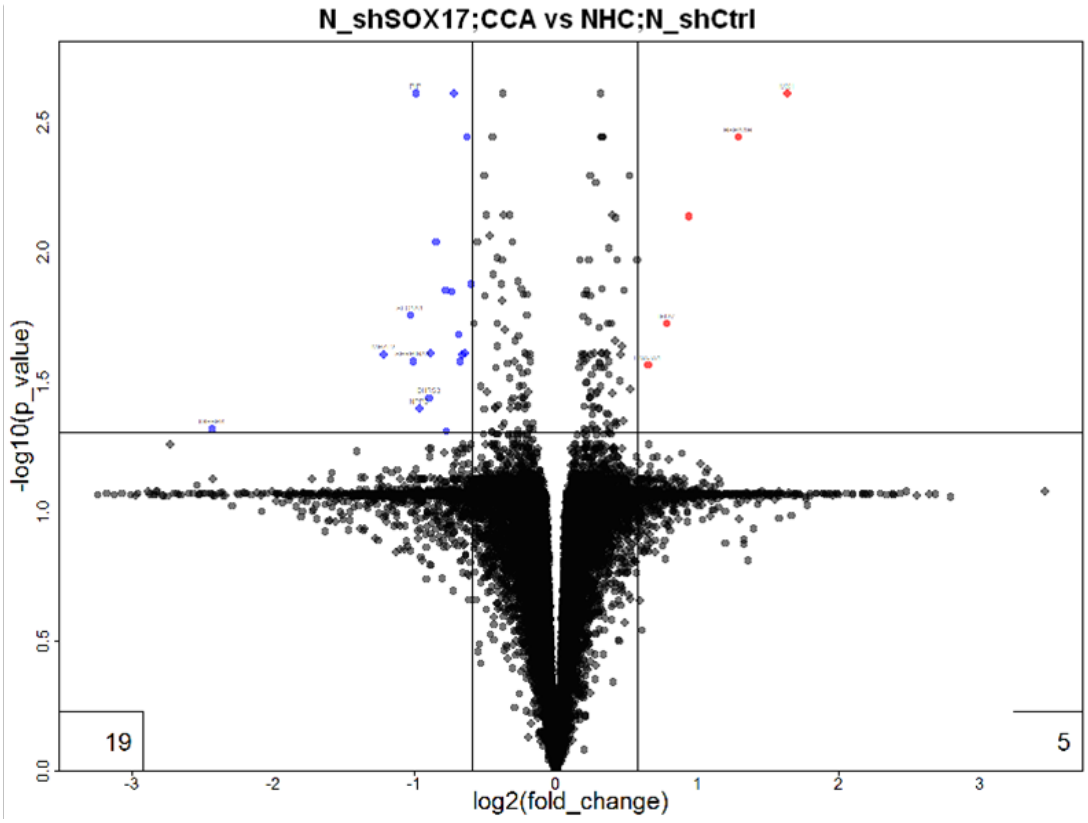

Figure R.32. *Volcanoplot* analysis comparing the mRNA levels between “NHC Lent-shRNA-SOX17 cells and CCA human cells (EGI1)” against “NHC and NHC Lent-shRNA-Control” cells. Dots represent the expression of each particular gene. Blue dots represent genes downregulated (>-1.5-fold change; *p* value <0.05) and red dots represent genes overexpressed (>+1.5-fold change; *p* value <0.05). Statistical variables: Log2 (Fold change >+/- 1.5) and Log10 (*p* value <0.05).

Additionally, *heatmaps* showing the semi-quantitative expression of those genes differentially expressed (>+/<-1.5-fold change and *p* value <0.05) were generated (Figure R.33).

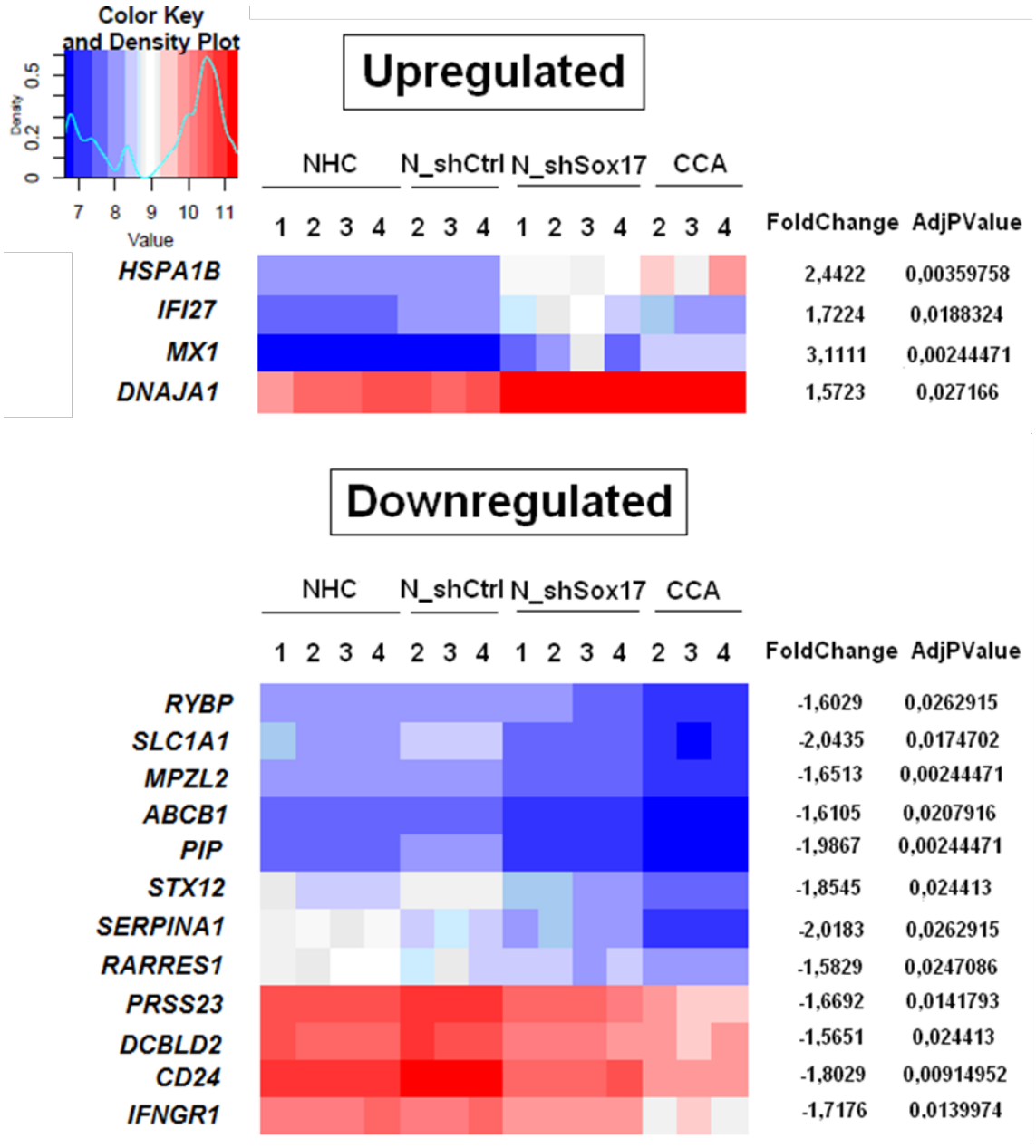

Figure R.34. *Heatmaps* showing those genes found upregulated (top) or downregulated (bottom) in "NHC Lent-shRNA-SOX17 cells and CCA human cells (EGI1)" compared to "NHC and NHC Lent-shRNA-Control" cells.

The functional analysis of the dysregulated genes revealed that they participate in processes of cell proliferation, migration and survival (Figure R.34). Those genes found downregulated in both “NHC Lent-shRNA-SOX17 cells” and “CCA human cells (EGI1)” are negative regulators of carcinogenesis; thus, they are involved in the inhibition of cell migration and invasion (i.e. *IFNGR1* [246], *MPZL2* [238], *RARRES1* [247], *RYBP* [248], *SERPINA1* [249], *STX12* [250]), tumor suppression (i.e.*DCBLD2* [251], *MPZL2* [238], RYBP [252]), inhibition of proliferation (i.e. *DCBLD2* [253], *IGFBP3* [240], *RARRES1* [247], RYBP [252]), stimulation of apoptosis (*IFNGR1* [246], RYBP [248]), and chemosensitivity [i.e. *MPZL2* [238], *RARRES1* [254], RYBP [248]). On the other hand, the genes found upregulated in these conditions may play a role (based on *gene ontology* program) in the ubiquitin-proteasome pathway (i.e. *DNAJA1* [255]), in degradation of protein-aggregates (i.e. *HSPA1B* [256]) and in the promotion of proliferation and tumorigenesis (i.e. *IFI27* [241]).

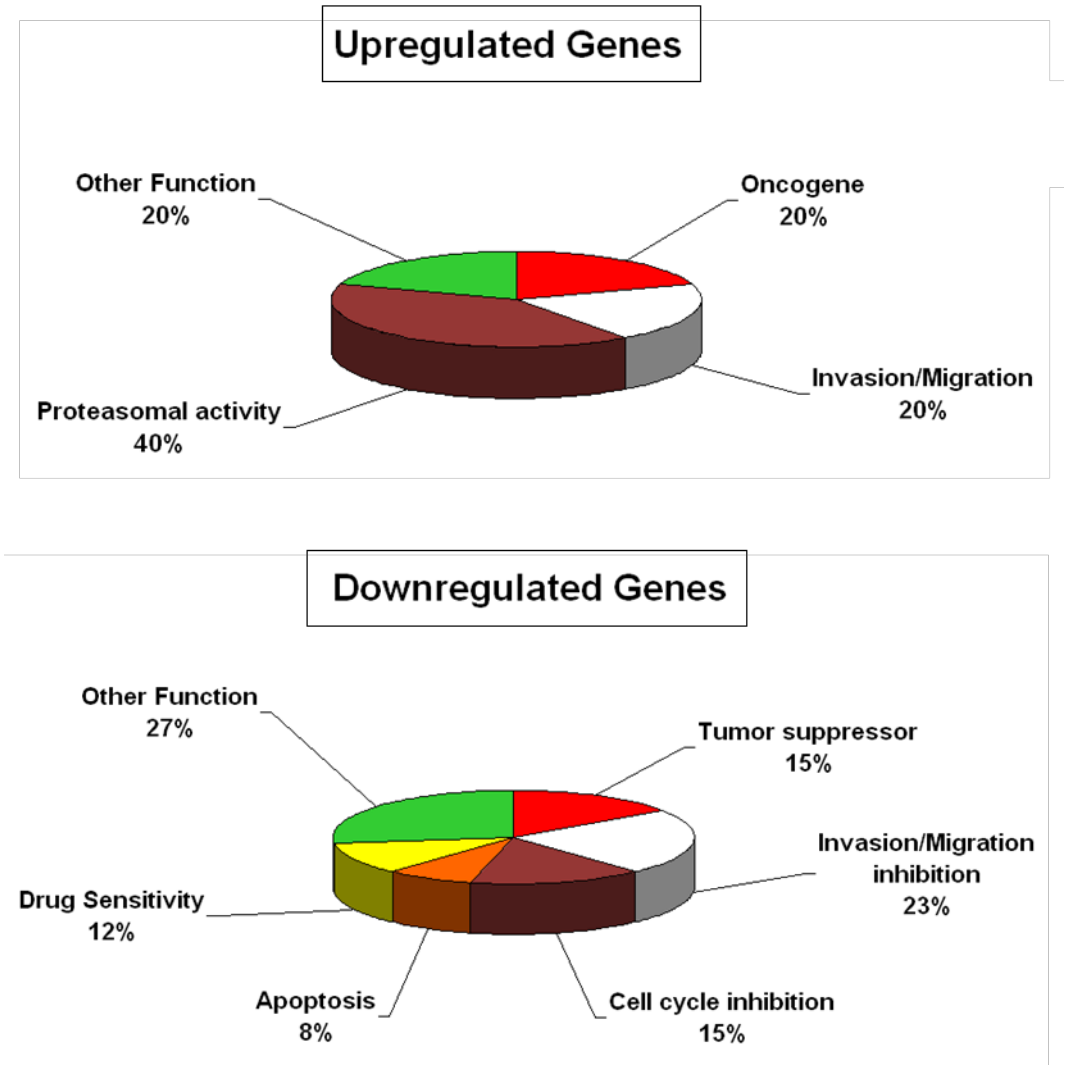

Figure R.34. Clustering by cellular function of those genes found upregulated (top) or downregulated (bottom) in both “NHC Lent-shRNA-SOX17 cells and CCA human cells (EGI1)” compared to “NHC and NHC Lent-shRNA-control” cells. Gene information collected from Pubmed, Uniprot or Genecards.

R.8.2.3. Comparison #3: “C_SOX17” vs “CCA and C_Ctrl”

A *volcanoplot* analysis was performed in order to compare the gene expression (mRNA) profile between “C_SOX17” and “CCA and C_Ctrl” groups (Figure R.35). Thus, the expression of those genes differentially expressed between “CCA Lent-SOX17” and its controls “CCA human cells (EGI1) and CCA Lent-control cells” were compared.

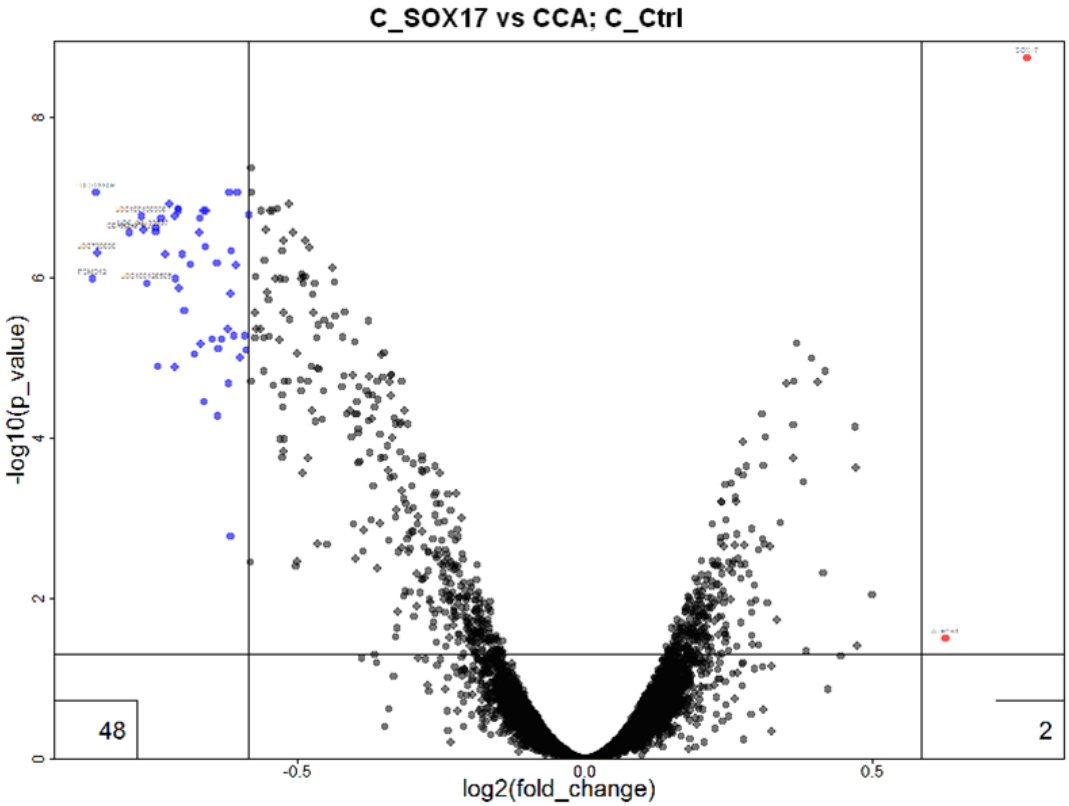

Figure R.35. *Volcanoplot* analysis comparing the mRNA levels betweem "CCA Lent-SOX17" and "CCA human cells (EGI1) and CCA Lent-control cells". Dots represent the expression of each particular gene. Blue dots represent genes downregulated (>-1.5-fold change; *p* value <0.05) and red dots represent genes overexpressed (>+1.5-fold change; *p* value <0.05). Statistical variables: Log2 (Fold change >+/- 1.5) and Log10 (*p* value <0.05).

Additionally, *heatmaps* showing the semi-quantitative expression of those genes differentially expressed (>+/-1.5-fold change and *p* value <0.05) were generated (Figure R.36).

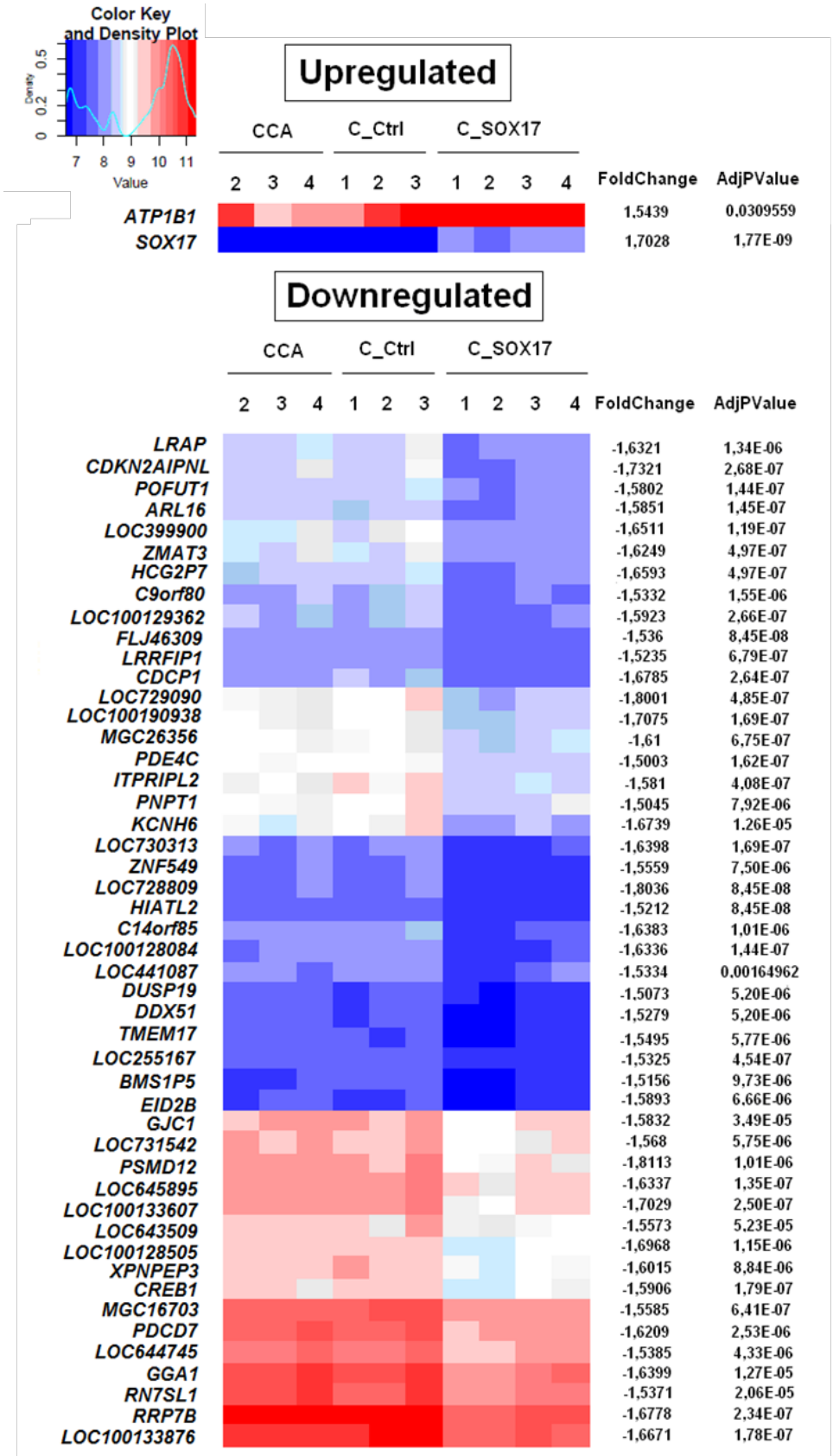

Figure R.36. *Heatmaps* showing those genes found upregulated (top) or downregulated (bottom) in "CCA Lent-SOX17" cells compared to "CCA human cells (EGI1) and CCA Lent-control cells".

Experimental overexpression of SOX17 in CCA human cells (EGI1) only induced the upregulation of *ATP1B1* (in addition to SOX17), which has been reported to promote FGF2 secretion [257] that participates in biliary cell differentiation [258]. On the other hand, experimental overexpression of SOX17 in CCA human cells (EGI1) resulted in decreased expression of multiple genes (Figure R.37). Some of these downregulated genes have pro-tumorigenic capacity; thus, they may promote cell proliferation (i.e. *CREB1* [259], *KCNH6* [260], *MGC16703*, *POFUT1* [261], *CDKN2AIPNL*, *PDE4C* [262], *ZMAT3* [263]), invasion/migration (i.e. *CDCP1* [264], *CREB1* [265], *KCNH6* [260], *LRRFIP1* [266], *POFUT1* [267]), neoangiogenesis (i.e. *KCNH6* [260]) and survival (i.e. *ZMAT3* [263], *XPNPEP3* [268], *DUSP19* [269]). In addition, other genes found downregulated under SOX17 overexpression in CCA human cells (EGI1) are involved in cell differentiation (*EID2B*, *POFUT1* [267]), development (*C14orf85*, also known as *ITPK1* antisense RNA 1 [270]), homeostasis of mitochondria (*PNPT1* [271], *XPNPEP3* [268]), endoplasmic reticulum (*RN7SL1* [272]), ribosome biogenesis (*BMS1P5*, *DDX51* [273], *RRP7B*), DNA damage response and/or genomic stability (*C9orf80*, also named *INTS3* [274], *CDKN2AIPNL*), calcium release (*ITPRIPL2*), transporter activity (*HIATL2*) and chemoresistance (*CDCP1* [275]).

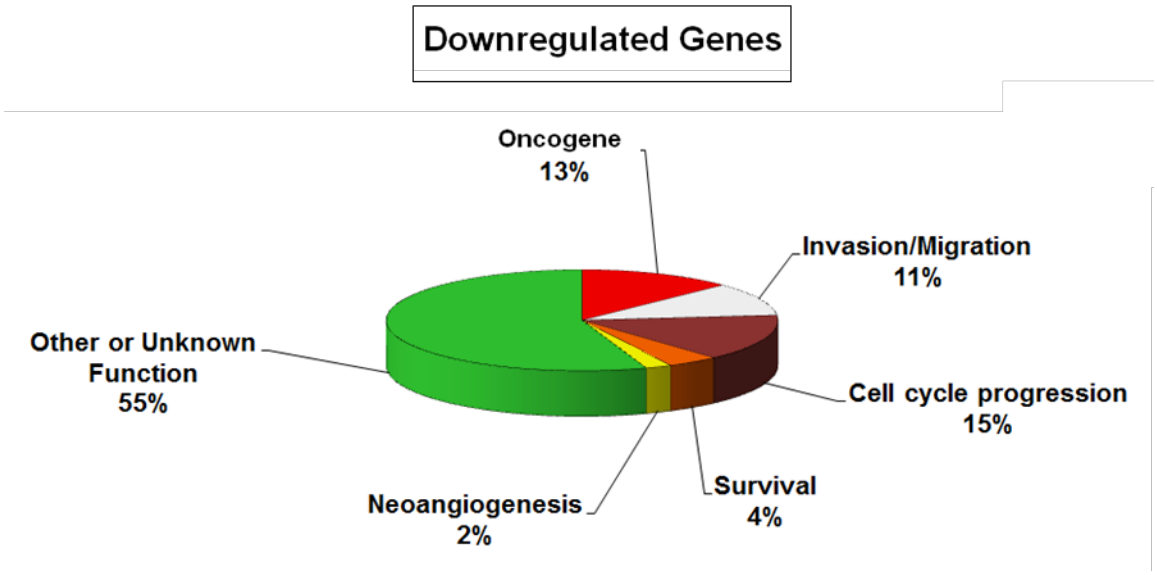

Figure R.37. Clustering by cellular function of those genes found downregulated in "CCA Lent-SOX17" compared to "CCA human cells (EGI1) and CCA Lent-control cells". Gene information collected from Pubmed, Uniprot or Genecards.

R.8.2.4. Comparison #4: "C_SOX17 and NHC" vs "CCA and C_Ctrl"

A *volcanoplot* analysis was performed to compare the gene expression (mRNA) profile between "C_SOX17 and NHC" and "CCA and C_Ctrl" groups (Figure R.38). Thus, the expression of those genes similarly expressed between "CCA Lent-SOX17 and NHC" cells were compared with " CCA human cells (EGI1) and CCA Lent-control cells".

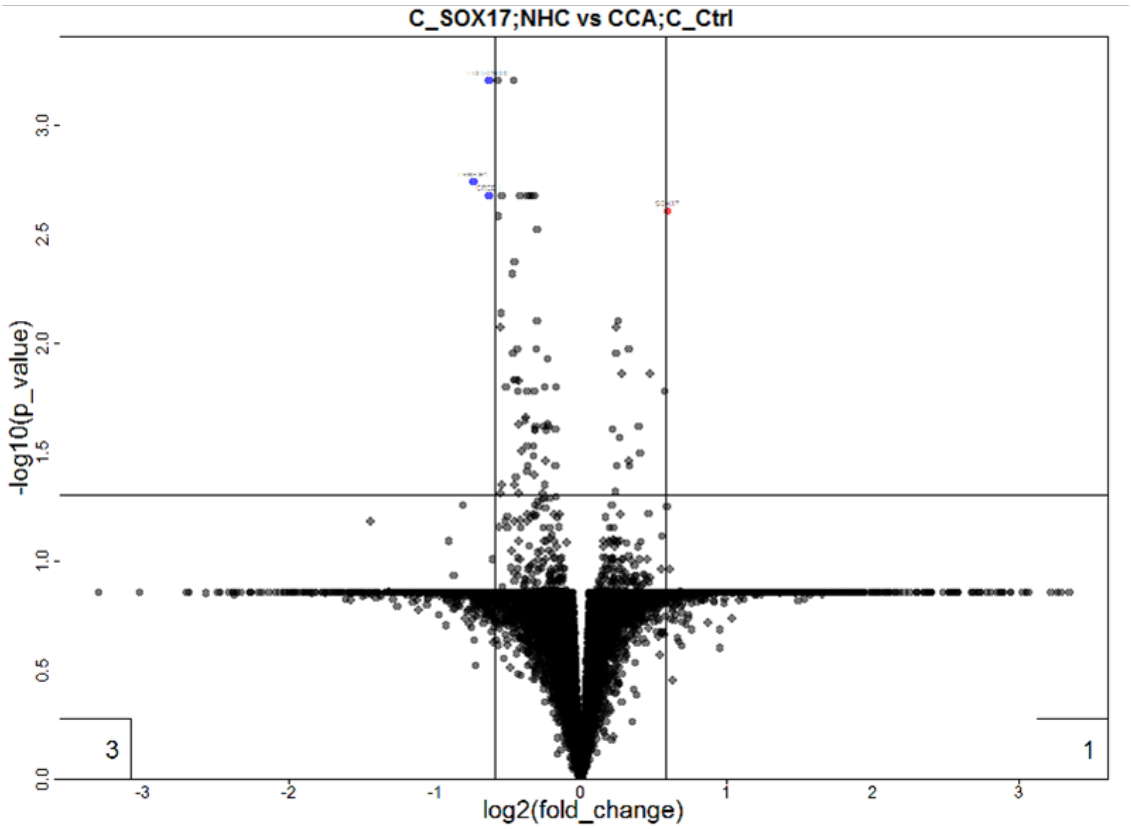

Figure R.38. *Volcanoplot* analysis comparing the mRNA levels between "CCA Lent-SOX17 and NHC" cells and its controls "CCA human cells (EGI1) and CCA Lent-control cells". Dots represent the expression of each particular gene. Blue dots represent genes downregulated (>-1.5-fold change; *p* value <0.05) and red dots represent genes overexpressed (>+1.5-fold change; *p* value <0.05). Statistical variables: Log2 (Fold change >+/- 1.5) and Log10 (*p* value <0.05).

This last comparison determined the similarities between NHC cells and CCA Lent-SOX17 compared to controls, CCA human cells (EGI1) and CCA Lent-control cells. Two genes appeared to be downregulated in "C_SOX17 and NHC" group, *CREB1* [276] and *LRRFIP1* [277], which are key players in tumor proliferation and invasion, respectively.

R.9. Mechanisms of regulation of SOX17 expression in normal human cholangiocytes and CCA human cells

R.9.1. DNMT1 and 3B are overexpressed in CCA human cells compared to normal human cholangiocytes in culture

Epigenetic alterations have been described in CCA, including hypermethylation of gene promoters [107, 278]. Methylation is carried out by DNMT enzymes (DNMT1, 3a and 3b), which have the function of transferring a methyl group onto DNA cytosines [279]. Some of those enzymes, DNMT1 and DNMT3b, have been identified to be overexpressed in CCA [280]. DNMT1 seems to be the key constitutive player in DNA methylation, whilst DNMT3b has been reported to support the function of DNMT1 [280]. However, no data has previously been published related to DNMT3a and CCA. We analyzed the expression of DNMT1, 3a and 3b in three diverse CCA human cell lines compared to NHC. Our data showed that both DNMT1 and DNMT3b are overexpressed in all three CCA human cell lines compared to NHC (Figure R.39).

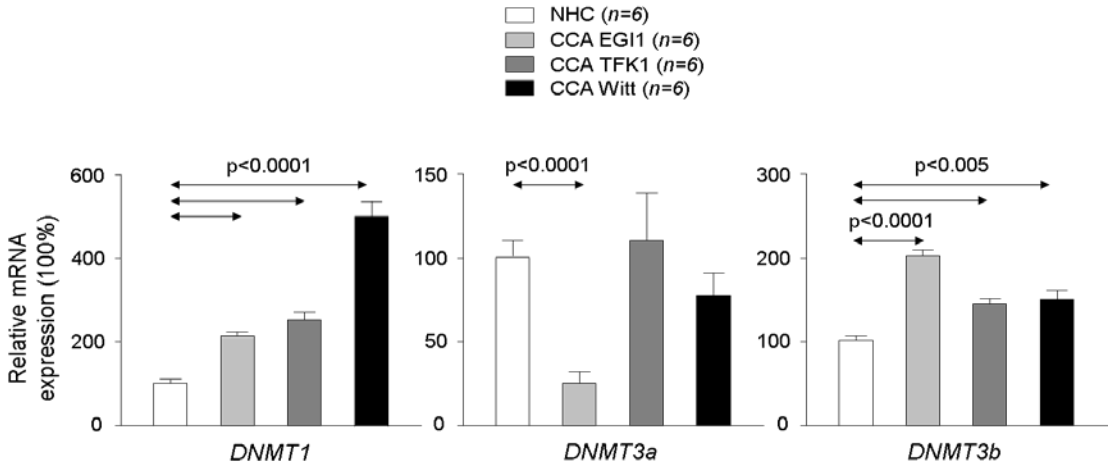

Figure R.39. Relative *DNMT1*, *DNMT3a* and *DNMT3b* mRNA levels in three CCA human cell lines (EGI1, TFK1, Witt) compared to NHC. *GADPH* was used as housekeeping normalizing gene. n=number of samples in each condition.

R.9.2. Both TGFβ1 and Wnt3a decrease *SOX17* mRNA expression in normal human cholangiocytes in culture

We studied the molecular mechanisms involved in the regulation of *SOX17* expression in NHC. In particular, we evaluated the role of two ligands found highly present in the inflammatory microenvironment of human CCAs such as TGFβ1 and Wnt3a. TGFβ1 promotes inflammation [281, 282] and/or fibrogenesis [283], whereas Wnt3a stimulates proliferation through the Wnt/β-catenin pathway [284, 285]. Our data showed that treatment of NHC with either TGFβ1 (5 ng/mL) or Wnt3a (100 ng/mL) for 48 h reduced *SOX17* mRNA expression compared to non-treated cells (Figure R.40).

The promoter of *SOX17* gene was reported hypermethylated in CCA human tissues [106]. Therefore, we evaluated if the downregulation of *SOX17* expression induced by either TGFβ1 and/or Wnt3a was dependent of DNMT activity. For this purpose, we used decitabine (5'-aza-2'-deoxycytidine), an inhibitor of DNMT activity that particularly inhibits DNMT1, main constitutive DNMT in most cells including cholangiocytes [286] and the DNMT observed to be most significantly overexpressed in CCA (Figure R.39). Thus, NHC in the presence or absence of TGFβ1 or Wnt3a were treated with decitabine for 48 h. Our data showed that the presence of decitabine in the culture medium prevented the downregulation of *SOX17* expression mediated by either TGFβ1 or Wnt3a in NHC (Figure R.40). These data indicate that TGFβ1 and Wnt3a inhibit SOX17 expression in NHC through a DNMT-dependent methylation mechanism.

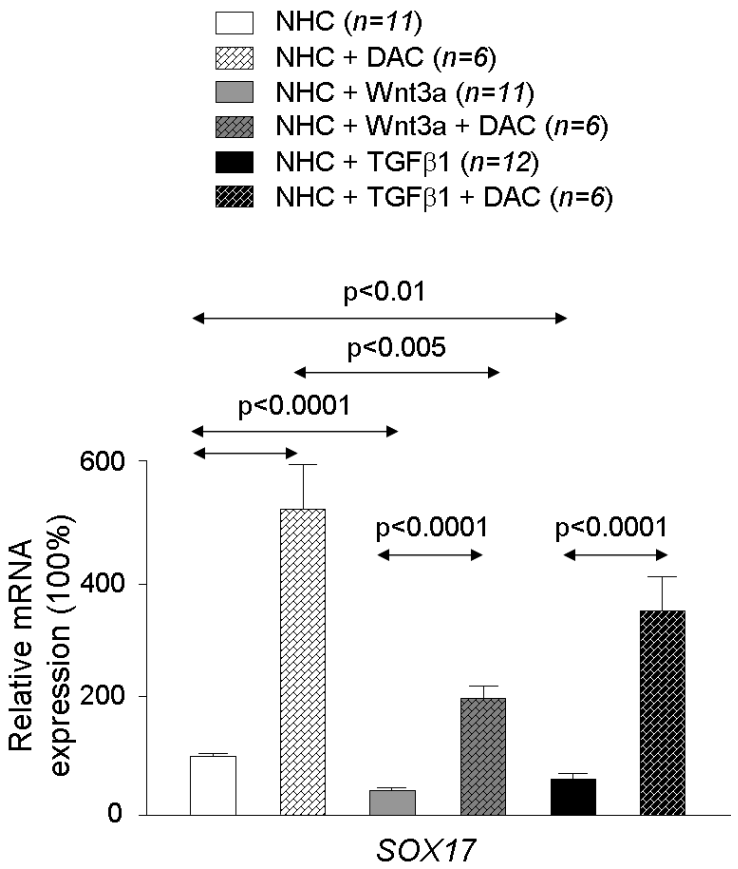

Figure R.40. Relative *SOX17* mRNA expression in NHC in the presence or absence of TGFβ1 (5 ng/mL) or Wnt3a (100 ng/mL) for 48 h. *GADPH* was used as housekeeping normalizing gene. n=number of samples in each condition.

R.9.3. Epigenetic regulation of SOX17 expression in CCA human cells

Our previous data showed that TGFβ1 and Wnt3a both inhibit *SOX17* expression in NHC by a DNMT-dependent mechanism. These data together with the hypermethylation of *SOX17* promoter reported in CCA human tissues [106] prompted us to study the role of both DNMT1 and inhibitors of DNMT activity on the regulation of *SOX17* expression in CCA human cells. Our data showed that the transfection of three different CCA human cell lines (i.e. EGI1, TFK1, and Witt) with siRNAs against DNMT1 decreased the mRNA expression of DNMT1 compared to control groups (i.e. non transfected cells or transfected with siRNAs control), and this event was associated with increased expression

of *SOX17* mRNA in all three CCA human cell lines (Figure R.41). Moreover, incubation of CCA human cells (i.e. EGI1, TFK1, and Witt) with decitabine increased the mRNA and protein expression levels of SOX17 in all three CCA human cell lines (Figure R.42).

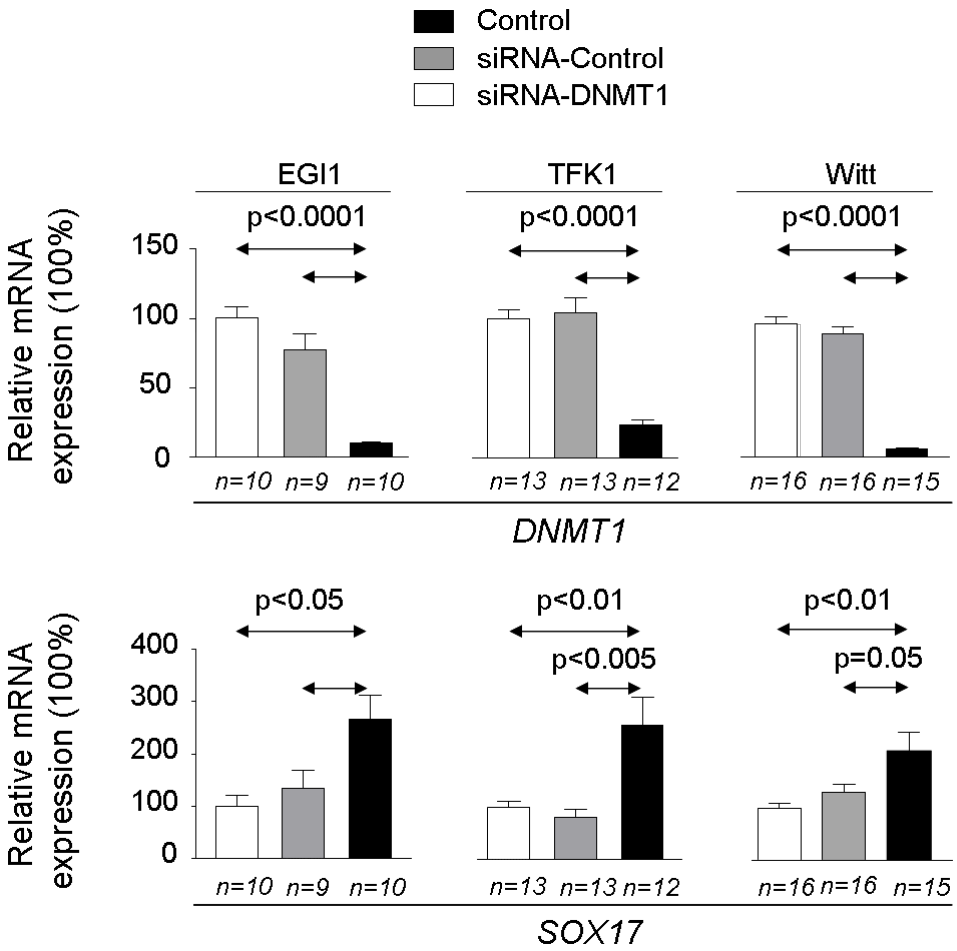

Figure R.41. Relative *DNMT1* and *SOX17* mRNA expression in three CCA human cell lines (EGI1, TFK1 and Witt) in the presence or absence of siRNA-control or siRNA-DNMT1 for 48 h. *GADPH* was used as housekeeping gene. n=number of samples in each condition.

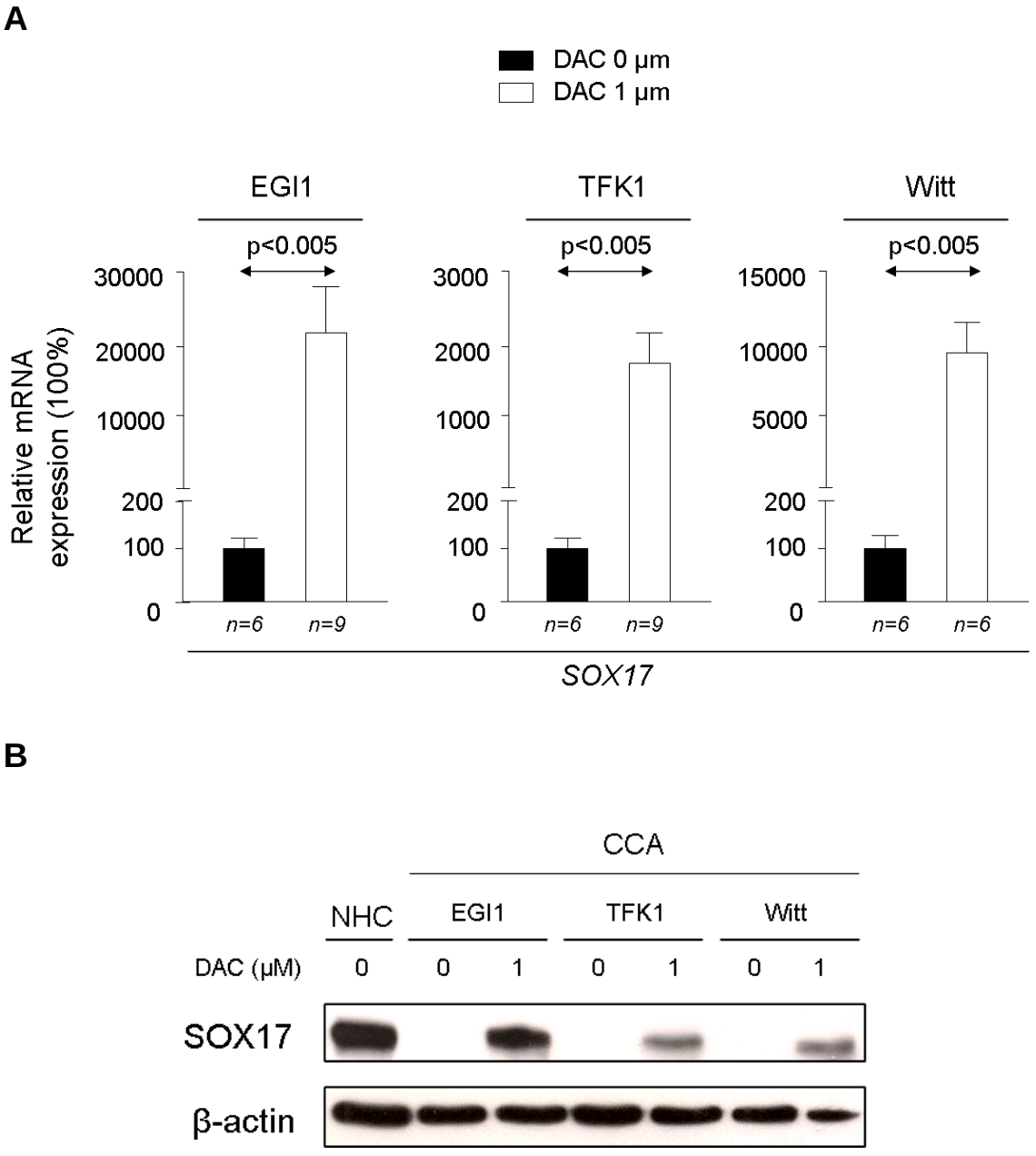

Figure R.42. Role of DNMT activity in the regulation of SOX17 expression in CCA human cells. A) Relative *SOX17* mRNA expression in three CCA human cell lines (EGI1, TFK1 and Witt) in the presence or absence of decitabine (1 µM) for 48 h. *GADPH* was used as housekeeping normalizing gene. B) Representative western blot of SOX17 protein expression in three CCA human cell lines (EGI1, TFK1 and witt) in the presence or absence of decitabine (1 µM). β-actin was used as normalizing loading control. n=number of samples in each condition.

R.10. Schematic summary of the results

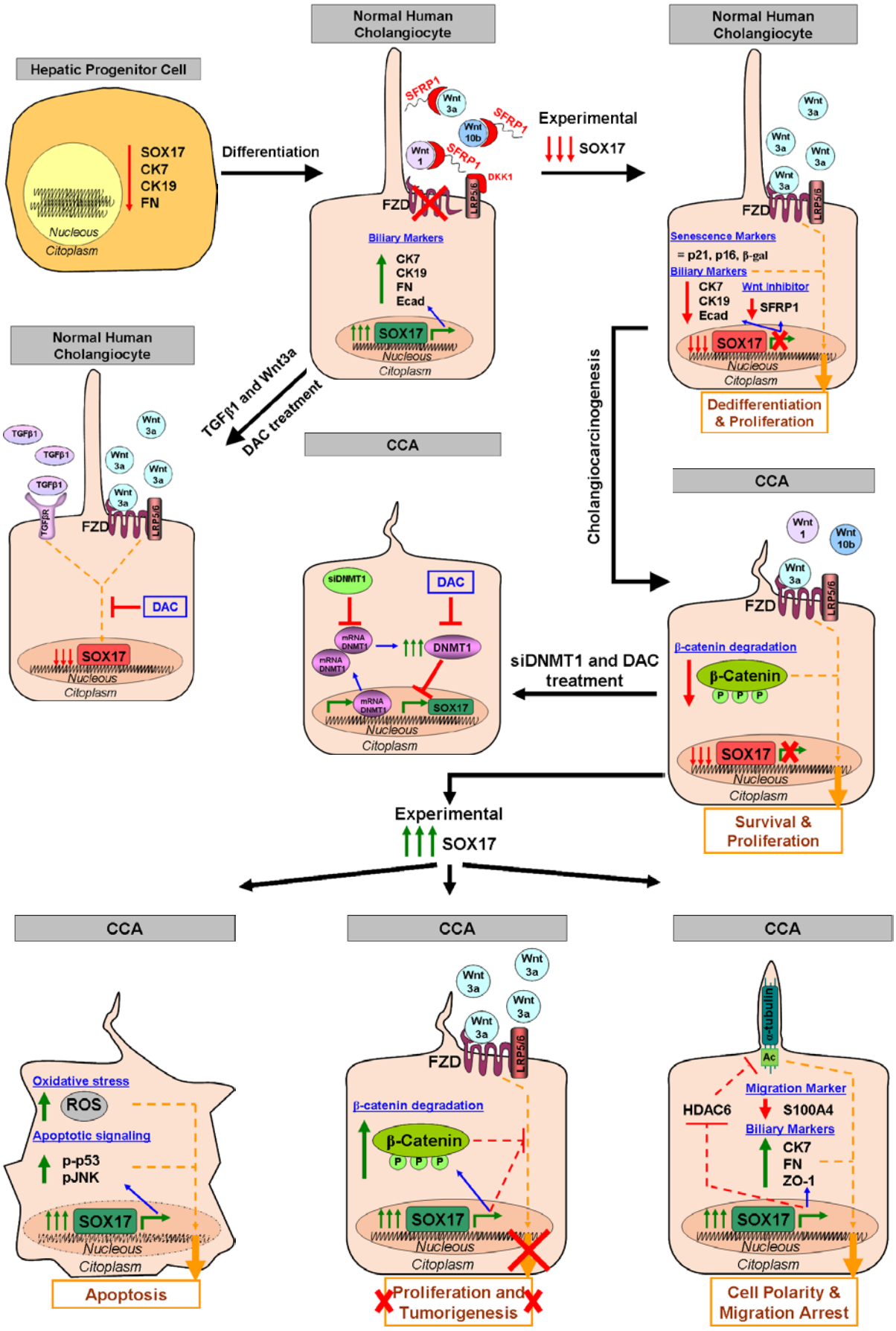

V. DISCUSSION

Cholangiocarcinoma (CCA) is a heterogeneous group of cancers with features of biliary tract differentiation. Incidence is increasing worldwide and already represents the second most common primary liver tumor and accounts for up to ~3% of all gastrointestinal cancers [41, 287]. CCAs are anatomically classified according to their localization in intrahepatic (iCCA), perihilar (pCCA) and distal (dCCA) [41, 287]. Their etiopathogenesis remains obscure; some risk factors such as viral hepatitis B and C, primary sclerosing cholangitis, liver fluke infection, hepatolithiasis, biliary malformations and congenital diseases have been described, but CCAs usually do not show any of them associated [41]. CCAs are very lethal because of their aggressiveness, late diagnosis and high chemoresistancence. They are generally diagnosed in advanced stages, when the disease is widespread. Thus, the 5-years survival rate after diagnosis is ~15% [288]. Currently, surgical approaches and liver transplantation are considered the only potential curative options, but are only indicated in a small proportion of patients who follow strict criteria and chances of recurrency are high. Other strategies like radiotherapy or chemotherapy are considered mainly palliative [8]. Therefore, there is an urgent need to look for new curative therapeutic options. In order to determine new potential targets for therapy it is mandatory to understand in detail the molecular mechanisms triggering the pathogenesis of this cancer.

Different genetic and epigenetic alterations have been described in CCA. Hypermethylation of the genome was recently reported in human CCA tissues compared to normal human livers [106]. Among other genes, the promoter of *SOX17* was found hypermethylated [106]. *SOX17* is a transcription factor member of the *SOX* family genes that is essential for the development of

definitive endoderm in mammals [187]. Thus, haploinsufficiency of *SOX17* in heterozygote mice embryos results in biliary atresia, acute embryonic hepatitis and perinatal death [189]. Therefore, SOX17 has been considered a key player in the embrionary development of the biliary tree [188]. However, the particular role of SOX17 in the differentiation of cholangiocytes remains unknown. Here, we evaluated the role of SOX17 in the regulation of the phenotype of normal human cholangiocytes (NHC) by using two different approaches; *i*) experimental differentiation of human iPSCs into NHC, and *ii*) dedifferentiation of NHC in culture.

It was recently reported that human iPSCs can be differentiated into NHC. Isolated human myofibroblasts transfected with vectors expressing *OCT4*, *SOX2*, *KLF4* and c*MYC* induced stem cell pluripotency, and a stepwise differentiation using Activin A, Wnt3a, FGF2, BMP4, SHH, JAG-1 and TGFβ, leads to iPSC-derived cholangiocytes (as previously described in Materials and Methods, section M.2.1) [207]. These cells show typical cholangiocyte features such as expression of CK7, CK19, PKD2, CFTR, and AE2, and also present the primary cilium [207]. Following this approach, we found that SOX17 protein expression is highly induced in the last step of the differentiation process of human iPSCs into NHC, i.e. in the differentiation of hepatic progenitor cells into mature cholangiocytes. This event was also associated with increased expression of CK7 and CK19. In order to determine the regulatory role of SOX17 in the differentiation of hepatic progenitor cells into mature NHC, we knocked-down SOX17 in different steps of the differentiation process of iPSCs into cholangiocytes by using Lent-shRNA-SOX17. Our data indicated that experimental downregulation of SOX17 protein during the differentiation of iPSC

into cholangiocytes decreases the protein levels of CK7 and CK9. Since the induction of SOX17 protein expression in the last step of the experimenral differentiation process is very high, the use of Lent-shRNA-SOX17 only partially (but significantly) decreases the expression of SOX17 and the resultant CK7 and CK19 proteins.

On the other hand, we evaluated the role of SOX17 in the regulation of the biliary phenotype of NHC in culture. Over cell passages *in vitro*, NHC progressively lose the expression of biliary and epithelial markers (such as CK7, CK19, and E-cadherin) and enter in senescence, which is characterized by: a) ovexpression of the senescent marker p21, b) β-galactosidase hyperactivity [220], c) downregulation of *CDK4* expression [289] and d) upregulation of $p16^{INK4A}$ expression (another senescence marker that inhibits CDK4 and thus induces cell cycle arrest [219, 289]. Notably, we found that SOX17 expression progressively decreases over culture-passages of NHC. In order to define the role of SOX17 in the dedifferentiation of NHC over culture-passages, we infected low passage cells with Lent-shRNA-SOX17 and then evaluated the expression of biliary epithelial markers. Our data revealed that experimental downregulation of SOX17 in low passage NHC resulted in downregulation of CK7 and CK19 expression; however, the expression of SOX17 did not affect senescence, since the expression of senescence markers, such as $p16^{INK4A}$ and p21, and the activity of β-galactosidase were unaffected by SOX17 downregulation.

Since SOX17 was suggested as a negative regulator of the Wnt/β-catenin pathway, we evaluated its role in the Wnt/β-catenin proliferation of NHC. Our data showed that the Wnt3a ligand does not modify the proliferation rate of

NHC. However, experimental downregulation of SOX17 expression in low passage NHC promotes a Wnt3a-dependent proliferation; this event was associated with decreased expression levels of *SFRP1*, a Wnt ligand inhibitor. This data indicated that downregulation of SOX17 expression in NHC promotes their transformation into a pro-mitotic state. This conclusion was supported by the data acquired from the mRNA array analysis, which showed a decreased mRNA expression of inhibitors of proliferation (*IGFBP3* [240], *DCBLD2* [251], *RARRES1* [247], *RYBP* [252]) after experimental SOX17 knocking-down in NHC. Moreover, the expression of genes that pomote tumorigenesis (*IFI27* [241], *IFI6* [242], *IFIT1* [243], *KIAA1199* [244, 245]) and are implicated in protein degradation (*DNAJA1* [255], *HSPA1B* [256]) appeared to be overexpressed, and inhibitors of cell migration/invasion downregulated (*CD24* [236, 237], *MPZL2* [238], *IFNGR1* [246], *SERPINA1* [249], *STX12* [250]) in NHC under SOX17 experimental downregulation.

The data resulting from these two experimental models (i.e. differentiation of iPSCs into mature cholangiocytes and NHC in culture) strongly indicate that SOX17 is a marker of biliary tract differentiation that also plays a key role in the regulation and maintenance of the cholangiocyte phenotype. These data are consistent with the aforementioned previous reports showing that *SOX17* heterozygote mice show biliary abnormalities and perinatal death [16, 187, 189].

Based on these results, and on the recently reported data showing that the *SOX17* promoter is found hypermethylated in CCA human tissues, we evaluated the expression of SOX17 in both CCA human tissue and cell lines (i.e. EGI1, TFK1 and Witt). Since normal human liver biopsies are mainly composed by hepatocytes, which show very low expression of SOX17 [221] the

SOX17 mRNA levels in CCA human tissue were compared to both low passages of NHC and normal gallbladder human tissue (which is highly composed by cholangiocytes) [222]. Our data revealed that *SOX17* mRNA expression is downregulated in CCA human tissue compared to both primary culture of NHC and normal human gallbladder tissue. In addition, *SOX17* mRNA expression was found strongly reduced in all three CCA human cell lines compared to NHC in culture. The immunofluorescence (IF) studies in human liver tissue showed that CK19-positive cells (i.e. cholangiocytes) possess high expression of SOX17, which is localized mainly perinuclearly in the bile duct epithelium cells; on the other hand, almost undetectable SOX17 expression was found by IF in CCA human tissue. All these data indicate that downregulation of SOX17 expression is a general and specific event occurring in CCAs and that could play a key role in the etiopathogenesis of this disease. These data are consistent with recent studies showing hypermethylation of SOX17 promoter in CCA human tissue [106].

In order to explore the potential role of SOX17 in the pathogenesis of CCA, we generated lentiviruses overexpressing SOX17 (Lent-SOX17). These viruses were used to infect the CCA human cells (i.e. EGI1), which show very low (mRNA and protein) SOX17 expression and high tumorigenic capacity. First, we infected these tumoral cells with different MOIs (i.e. 1, 3, 5, 10, 15). Western blot analysis showed a MOI-dependent overexpression of SOX17 in CCA human cells, reaching to a plateau at a MOI of 5. Then, we analyzed by IF the percentage of cells infected with different MOIs of Lent-SOX17, and found that the MOI of 3 is the minimum needed to have ~100% of cell infection. The SOX17 overexpression was mainly found in the nucleous of the cells.

Therefore, we decided to use a MOI of 3 for further experiments, since it is the minimum amount needed to induce SOX17 overexpression in all the CCA human cells. Then, the role of SOX17 was evaluated on the tumorigenic capacity of CCA human cells *in vivo*. For this purpose, CCA human cells infected with Lent-SOX17, Lent-control or non-infected were subcutaneously injected in immunodeficient nude mice and the tumor generation and growth was monitored over 57 days. Experimenntal overexpression of SOX17 markedly reduced the subcutaneous generation of tumors and their growth compared to the controls. These data indicated that SOX17 acts as a tumor suppressor in CCA human cells. The tumor suppressor capacity of SOX17 was previously indicated in gastrointestinal tumors such as HCC [198], colorectal cancer [202], gastric tumors [197] and esophageal cancer [290]. Whilst in HCC cells restoration of SOX17 inhibits colony formation and cell growth by blocking β-catenin/TCF-dependent transcription [198], in colorrectal cancer SOX17 inhibits tumorigenesis through upregulation of miR-371-5p, which ultimately downregulates *SOX2* and Wnt/β-catenin signalling [202]. Furthermore, re-expression of SOX17 in esophageal cancer cells causes reduced foci formation, xenograft growth and metastasis [290]. In a mouse model of gastric tumorigenesis, SOX17 also reduces colony formation and Wnt signaling activity [197].

Then, we studied *in vitro* the mechanisms by which SOX17 functions as a tumor suppressor in CCA. Different biological processes altered in cholangiocarcinogenesis such as survival, proliferation, migration and differentiation were evaluated. Our data showed that SOX17 overexpression in CCA cells induces apoptosis in a MOI-dependent manner. Since Lent-SOX17

upregulates SOX17 expression in CCA human cells beyond the normal basal level in NHC, we evaluated the potential toxicity of SOX17 overdose. Thus, we tested the effect of Lent-SOX17 in NHC. In contrast to CCA human cells, overexpression of SOX17 did not promote apoptosis in NHC in culture, even at high MOIs of Lent-SOX17. Notably, this differential effect of SOX17 overexpression on the survival of CCA human cells *vs* NHC points out the potential therapeutic value of SOX17 regulation for the treatment of CCA human tumors.

Next, we studied the molecular mechanisms by which SOX17 overexpression promotes apoptosis in CCA cells. Since oxidative stress is considered a potential inducer of apoptosis [291], we evaluated the levels of ROS in CCA human cells. Our data demonstrated that CCA human cells overexpressing SOX17 presented higher ROS levels than non-infected or Lent-control CCA cells, suggesting that increased oxidative stress may be a cause for the increased apoptosis observed in CCA human cells under SOX17 overexpression. Then, we evaluated the caspase-3 activity, which promotes apoptosis [292]. Overexpression of SOX17 in CCA human cells increases the caspase-3 activity compared to the control conditions; moreover, this event was also associated with increased phosphorylation of the pro-apoptotic signaling pathways JNK [293, 294] and p53 [293, 295]. In aggreement with these results, the analysis of expression of the mRNA microarrays indicated that experimental overexpression of SOX17 in CCA human cells dysregulated the expression of key genes involved in mitochondrial homeostasis and apoptosis. Thus, SOX17 decreased the expression of *PNPT1* [a mitochondrial homeostasis keeper relevant in the mitochondrial RNA (mtRNA) import] [296], *DUSP19* (an indirect

JNK inhibitor, also known as SKRP1) [269, 297, 298], *ZMAT3* (an anti-apoptotic gene and a p53 inhibitor) [299] and *XPNPEP3* (an anti-apoptotic gene, also known as *APP3* [300], related to mitochondrial oxygen consumption) [301] in CCA human cells compared to the controls.

SOX17 was previously reported as a potential inhibitor of the Wnt/β-catenin pathways in different cancers such as breast cancer, colorectal cancer, hepatocarcinoma or gastric cancer [198, 199, 202, 302]. Since this molecular pathway is very relevant in cholangiocarcinogenesis [130, 229, 303, 304] and Wnt ligands are highly present in the tumor microenvironment [129, 305, 306], we evaluated the activity of this pro-tumorigenic pathway in those CCA human cells that showed experimental overexpression of SOX17 but with levels not sufficient to induce apoptosis. First, we observed that the presence of the Wnt3a ligand promotes the proliferation of CCA human cells in a dose-dependent manner. Of note, the Wnt3a-dependent proliferation was inhibited in CCA human cells under experimental overexpression of SOX17. SOX17 is known to inhibit the Wnt signaling by promoting the expression of the Wnt ligand inhibitor *SFRP1* [203] and/or by inhibiting β-catenin expression and activity. The degradation of β-catenin is mediated by a protein complex that contains the Ser/Thr kinases glycogen synthase kinase 3 (GSK3), casein kinase 1 (CK1), the scaffolding protein Axin, the APC protein, the E3-ubiquitin ligase and the protein phosphatase 2A (PP2A). The specific phosphorylation of β-catenin determines its activation (ser37/thr41 or thr41/ser45) or inactivation/degradation (ser33/37/thr41) [122] by ubiquitination and head towards the proteasome [307]. Our data revealed that experimental overexpression of SOX17 in CCA human cells increased the levels of β-catenin

phosphorylated in residues ser33/37/thr41, indicating its inactivation/degradation. Furthermore, the analysis of expression of the mRNA microarrays indicated that experimental overexpression of SOX17 in CCA human cells also downregulated the expression of some genes implicated in cell cycle and proliferation, such as *CREB1* [259], *KCNH6* [260], *MGC16703*, *POFUT1* [261], *CDKN2AIPNL* and *PDE4C* [262].

Another important feature of CCA tumors is their ability to invade adjacent tissues and/or migrate to other regions of the human body. Thus, we evaluated the invasion/migration acivity of those CCA human cells that showed experimental overexpression of SOX17 but with levels not sufficient to induce apoptosis. Our "cell scratching" *in vitro* data showed that experimental overexpression of SOX17 inhibited the invasion/migration capacity of CCA human cells compared to control conditions. These data were associated with downregulation of the pro-invasion/migration genes *S100A4* [308-312] as well as *CDCP1* [264], *CREB1* [265], *KCNH6* [260], *LRRFIP1* [266], *POFUT1* [267] (data obtained from the mRNA microarray).

On the other hand, we evaluated the role of SOX17 regulating the biliary phenotype in those of CCA human cells that did not enter apoptosis. We found that experimental overexpression of SOX17 in CCA human cells stimulated the expression of the biliary marker *CK7*, and epithelial markers *FN* [231] and *ZO-1* [232], which loss or failure have been related to cancer progression [231, 232]. In this regard, functional differentiated cholangiocytes present a single primary cilium extending from the apical membrane [11, 235]. This antenna-like organelle functions as a mechano-, chemo- and osmo-sensor detecting extracellular changes in bile flow and composition and regulating the

cholangiocyte function [11, 14, 313]. The primary cilia itself functions as a structural checkpoint that blocks cell cycle [314], thus its loss or shortening induces proliferation in some cholangiopathies [315]. In particular, CCA human cells show loss or decreased primary cilium length compared to normal biliary epithelial cells; this event is dependent on HDAC6 [115] that deacetylates the scaffold α-tubulin protein of the cilium. Our data revealed that experimental overexpression of SOX17 in CCA human cells increased the length of the primary cilium compared to the control conditions, indicating improved cell polarity and differentiation, and this event was associated with downregulation of HDAC6 mRNA expression. In this regard, a recent report indicated that molecular or pharmacological downregulation of HDAC6 expression in CCA human cells induces the restoration of primary cilium length and reduces cell proliferation, anchorage independent growth and invasion in a ciliary dependent manner [115, 235]. Future studies should evaluate in detail the mechanisms by which SOX17 regulates the primary cilium length in CCA human cells, as well as determine if these longer cilia are functional and respond to mechano-, chemo- and osmo-stimuli; moreover, their role in the proliferation of CCA human cells should be investigated.

Finally, we studied the molecular mechanisms triggering the downregulation of SOX17 expression in CCAs. For this purpose, we evaluated the role of two key molecules in cholangiocarcinogenesis such as TGFβ1 [282], a pro-inflammatory and pro-fibrotic protein [316], and the pro-mitotic Wnt3a ligand [317, 318]. We focused our studies in these two ligands because previously published data indicated that the cancer-associated fibroblasts (CAFs) and the activated macrophages, which are part of the tumor microenvironment, release

TGFβ1 [319] and Wnt3a [129] ligands respectively, and activate diverse tumorigenic signaling pathways into the proximate cells transforming them into cancerous cells [129, 320] or inducing their proliferation [321, 322]. Interestingly, incubation of NHC in culture with either TGFβ1 or Wnt3a decreased the mRNA expression of *SOX17*, and this event was prevented by the presence of the demethylating agent decitabine (5-aza-2'-deoxycytidine), which inhibits DNMTs activity by a covalent binding to these enzymes [323]. These data indicate that molecules present in chronic inflammatory processes and in the tumor microenvironment are able to downregulate the expression of the biliary marker *SOX17* via a DNA methylation-dependent mechanism. As mentioned above, hypermethylation of *SOX17* promoter was reported in CCA human tissues compared to controls [106]. Here, we found that both CCA human cells and tissues are characterized by downregulation or absent expression of *SOX17*. In order to test if the downregulation of SOX17 expression in CCA human cells is caused by epigenetic regulation, particularly hypermethylation of the *SOX17* promoter, we evaluated the role of DNMTs in this process. First, we found that the expression of both DNMT1 (main constitutive DNA methyltransferase)[324] and DNMT3b is increased in CCA human cells compared to normal human cholangiocytes. Notably, experimental knock-down of *DNMT1* expression in CCA cells with specific siRNAs resulted in the upregulation of *SOX17* mRNA expression. In addition, the use of decitabine increased both SOX17 mRNA and protein levels in all three CCA human cell lines analyzed (i.e. EGI1, TFK1 and Witt).

In summary, all these data strongly indicate that SOX17 is a key transcription factor that regulates the differentiation and maintainance of the

biliary phenotype. Therefore, SOX17 may be considered and used as a biliary epithelial marker. Downregulation of *SOX17* expression in NHC may occur during chronic inflammatory processes by the action of molecules such as TGFβ1 and Wnt3a, among others, via methylation of *SOX17* gene promoter. Downregulation of SOX17 expression is a general and specific event necessary for cholangiocarcinogenesis because it functions as tumor suppressor promoting apoptosis, inhibiting both the Wnt/β-catenin-dependent proliferation and cell invasion/migration, and restoring the expression of key biliary epithelial markers as well as the length of the primary cilium. The characteristic downregulation of SOX17 expression in CCA human cells might be considered a marker of diagnosis and bad prognosis, although future studies in long cohorts of patients are still necessary.

Overall, therapeutic strategies aimed to normalize/increase the expression levels of SOX17 in CCA human tumors might be highly effective. In this regard, we are going to explore in future studies the use of gene therapy with adeno-associated viruses overexpressing SOX17. In the aforementioned studies, we used lentiviruses as vectors to overexpress SOX17 because of their high infection efficiency (independently of cell status) and genome integration capacity. However, we are going to generate adenoviruses overexpressing SOX17 for *in vivo* studies, which show high tropism to liver cells. The use of adenoviruses *in vivo* is more appropriate and safe than lentiviruses, because the latter may cause gene sequence dysruptions when it integrates aleatorily into the host genome. We are going to generate adenoviruses that encode *SOX17* ORF under the regulatory expression of a constitute promoter; our aim will be to evaluate the therapeutic value of the intravenous injection of these

viruses in an orthotopic mouse model of CCA recently settled up in our laboratory. The fact that experimental overexpression of SOX17 in NHC did not affect their survival and proliferation, minimizes the potential side effects in normal biliary cells. However, future studies must be carried out in order to determine the potential side effects associated to SOX17 overexpression in other cell types such as normal hepatocytes. In this regard, we are going to design adenoviruses in which *SOX17* expression will be regulated under CK19-promoter (pr-CK19) as a specific way to force selective *SOX17* expression in CCA human cells. Moreover, we are also considering the option of using promoters of relevant pro-oncogenes in CCA to specifically express *SOX17* in these malignant cholangiocytes. On the other hand, to increase the security and in agreement with the last gene-therapy advances, we will carry out similar *in vivo* assays using adeno-associated viruses (AAV) encoding *SOX17*. The increasing number of clinical trials using non-pathogenic parvovirus AAV for gene transfer makes these vectors the best candidates for next-generation gene-therapy [325, 326].

CCAs are very chemorresistant tumors. So, we are going to check if SOX17 modulates the chemosensibility or chemoresistance of CCA human cells to the antitumoral drugs commonly used in CCA, such as gemcitabine, 5-FU or cisplatin. We are going to evaluate the effect of SOX17 in the modulation of the expression of several genes involved in the chemoresistance status of CCAs [327].

Moreover, the epigenetic regulation of SOX17 expression in CCAs with demethylating agents may be considered for future therapeutic approaches. In this regard, demethylating agents have been shown to improve CCA prognosis,

as it has been reported that decitabine inhibits CCA cell growth *in vitro* and in a mouse xenograft model [328]. Decitabine is a drug approved by the food and drug administration (FDA) for the treatment of human diseases such as myelodysplastic syndromes [329]. So, taking into account this information and the relevance of decitabine as inhibitor of the *SOX17* promoter hypermethylation in CCA human cells, it is suggested as a good therapeutic drug to be considered in the clinic.

VI. CONCLUSIONS

The key findings reported here indicate that SOX17 is a key regulator of the differentiation and maintenance of the biliary phenotype and acts as a tumor suppressor in CCA, being considered a potential therapeutic target. Our data indicate that:

I. SOX17 regulates the differentiation of iPSC cells into cholangiocytes and is particularly expressed in last step of the differentiation process, i.e. from hepatic progenitor to induced differentiated cholangiocytes.

II. SOX17 is highly constitutive expressed in well differentiated human cholangiocytes and, similarly to CK7 and CK19, may be considered a biliary marker.

III. SOX17 regulates the expression of the biliary markers CK7 and CK19 in normal human cholangiocytes and does not affect cell senescence.

IV. Experimental downregulation of SOX17 expression in normal human cholangiocytes promotes their Wnt/β-catenin-dependent proliferation.

V. The expression of SOX17 is reduced in CCA human biopsies and cell lines compared to their controls.

VI. Experimental overexpression of SOX17 in CCA human cells inhibits their tumorigenic capacity by increasing apoptosis and downregulating the Wnt/β-catenin proliferation and cell migration.

VII. Experimental overexpression of SOX17 in CCA human cells increases the expression of biliary epithelial markers and restores the primary cilium length.

VIII. The expression of SOX17 in normal human cholangiocytes is inhibited by the presence of TGFβ1 or Wnt3a via a DNA methylation mechanism.

IX. The basal expression of SOX17 is downregulated in CCA human cells via a DNMT1-dependent mechanism; experimental knocking-down of DNMT1 expression or the inhibition of its activity both restore SOX17 expression in CCA human cells.

VII. SUMMARY IN SPANISH

(RESUMEN EN ESPAÑOL)

S.1. Antecedentes y objetivos

El colangiocarcinoma (CCA) es un grupo heterogéneo de tumores caracterizados por la expresión de marcadores de diferenciación bilar. Su incidencia está aumentando en todo el mundo y representa ya el segundo tipo de tumor hepático más común después del carcinoma hepatocelular (HCC). El CCA es muy letal debido a su agresividad, diagnóstico tardío y elevada quimiorresistencia. A nivel molecular, el CCA está caracterizado por alteraciones genéticas y epigenéticas que determinan su patogénesis. Recientemente se ha descubierto que el genoma de los tumores de CCA se encuentra globalmente hipermetilado. En este sentido, se ha indicado que el promotor de *SOX17* se encuentra entre dichos genes hipermetilados. SOX17 parece ser un factor de transcripción clave en la embriogénesis biliar ya que ratones deficientes de SOX17 ($SOX17^{-/-}$) presentan letalidad prematura debido a alteraciones biliares. Por ello, en este proyecto de investigación estudiamos el papel de SOX17 en la diferenciación y mantenimiento del fenotipo de los colangiocitos así como su relevancia en el proceso de colangiocarcinogénesis.

S.2. Métodos

Se evaluó la expresión y función de SOX17 durante la diferenciación de las células madre humanas pluripotentes inducidas (iPSCs) a colangiocitos, en la desdiferenciación de colangiocitos humanos normales (NHC) y en el CCA. Para ello se utilizaron lentivirus que sobreexpresan o inhiben SOX17 (Lent-SOX17 y Lent-shRNA-SOX17, respectivamente). Se realizaron ensayos de tumorigénesis en ratones inmunodeficientes y se analizó la apoptosis, proliferación, migración, estrés oxidativo, y fenotipo de las células tumorales en

ausencia o presencia de SOX17. Además, se realizaron estudios de expresión génica mediante *microarrays*.

S.3. Resultados

La expression de SOX17 está altamente inducida en la última etapa de la diferenciación iPSCs a colangiocitos, en particular en la fase de célula hepática progenitora a colangiocito diferenciado; además, SOX17 promueve en dicha fase la expresión de los marcadores biliares (CK) 7 y 19. Por otro lado, SOX17 también promueve el mantenimiento del fenotipo biliar en NHC a través de la expresión de CK7 y CK19, y sin afectar a la senescencia celular. La inhibición de la expresión de SOX17 mediante Lent-shRNA-SOX17 promueve la proliferación celular dependiente de la ruta Wnt/β-catenin. La expression de SOX17 se encuentra disminuida en células de CCA humano en cultivo (y biopsias tumorales humanas) en comparación con NHC o tejido de la vesícula biliar humana. En el modelo de tumorogénesis en ratones inmunodeficientes, en la inyección subcutánea de células de CCA humano (que sobreexpresaran o no SOX17) la sobreexpresión de SOX17 disminuye su capacidad tumorigénica en comparación con sus controles. Dicho fenómeno es mediado a nivel molecular por el efecto de SOX17 aumentando el estrés oxidativo y la apoptosis en las células de CCA, así como inhibiendo su proliferación dependiente de la ruta Wnt/β-catenin y la migración celular. Curiosamente, la sobreexpresión de SOX17 en NHC no afecta a su supervivencia. Por otra parte, la sobreexpresión de SOX17 provoca una sobreexpresión de marcadores biliares epiteliares en las células de CCA humano, así como la restauración de la longitud del cilio primario. Tanto Wnt3a como TGFβ1

disminuyen la expresión de SOX17 en NHC de manera dependiente de metilación del DNA. La inhibición de la DNMT1 en las células de CCA humano con siRNAs o fármacos induce el aumento de los niveles de expresión de SOX17.

S.4. Conclusión

SOX17 regula la diferenciación y el mantenimiento del fenotipo biliar y su expression se encuentra epigenéticamente inhibida en el CCA. SOX17 actúa como supresor tumoral en el CCA, y la restauración de sus níveles de expresión puede tener un importante valor terapéutico.

VIII. REFERENCES

1. Juza, R.M. and E.M. Pauli, *Clinical and surgical anatomy of the liver: a review for clinicians.* Clin Anat, 2014. 27(5): p. 764-9.
2. Liu, Y., et al., *Hepatocyte cocultures with endothelial cells and fibroblasts on micropatterned fibrous mats to promote liver-specific functions and capillary formation capabilities.* Biomacromolecules, 2014. 15(3): p. 1044-54.
3. Zakim and Boyer, *Hepatology, sixth edition*. 2012.
4. Abdel-Misih, S.R. and M. Bloomston, *Liver anatomy.* Surg Clin North Am, 2010. 90(4): p. 643-53.
5. Gordillo, M., T. Evans, and V. Gouon-Evans, *Orchestrating liver development.* Development, 2015. 142(12): p. 2094-108.
6. Carpino, G., et al., *Biliary tree stem/progenitor cells in glands of extrahepatic and intraheptic bile ducts: an anatomical in situ study yielding evidence of maturational lineages.* J Anat, 2012. 220(2): p. 186-99.
7. Roskams, T.A., et al., *Nomenclature of the finer branches of the biliary tree: canals, ductules, and ductular reactions in human livers.* Hepatology, 2004. 39(6): p. 1739-45.
8. Razumilava, N. and G.J. Gores, *Cholangiocarcinoma.* Lancet, 2014. 383(9935): p. 2168-79.
9. Banales, J.M., J. Prieto, and J.F. Medina, *Cholangiocyte anion exchange and biliary bicarbonate excretion.* World J Gastroenterol, 2006. 12(22): p. 3496-511.
10. Banales, J.M., et al., *Bicarbonate-rich choleresis induced by secretin in normal rat is taurocholate-dependent and involves AE2 anion exchanger.* Hepatology, 2006. 43(2): p. 266-75.
11. Masyuk, A.I., T.V. Masyuk, and N.F. LaRusso, *Cholangiocyte primary cilia in liver health and disease.* Dev Dyn, 2008. 237(8): p. 2007-12.
12. Masyuk, A.I., et al., *Cholangiocyte cilia detect changes in luminal fluid flow and transmit them into intracellular Ca2+ and cAMP signaling.* Gastroenterology, 2006. 131(3): p. 911-20.
13. Banales, J.M., et al., *Hepatic cystogenesis is associated with abnormal expression and location of ion transporters and water channels in an animal model of autosomal recessive polycystic kidney disease.* Am J Pathol, 2008. 173(6): p. 1637-46.
14. Gradilone, S.A., et al., *Cholangiocyte cilia express TRPV4 and detect changes in luminal tonicity inducing bicarbonate secretion.* Proc Natl Acad Sci U S A, 2007. 104(48): p. 19138-43.
15. Masyuk, T.V., et al., *Biliary dysgenesis in the PCK rat, an orthologous model of autosomal recessive polycystic kidney disease.* Am J Pathol, 2004. 165(5): p. 1719-30.
16. Spence, J.R., et al., *Sox17 regulates organ lineage segregation of ventral foregut progenitor cells.* Dev Cell, 2009. 17(1): p. 62-74.
17. Roskams, T. and V. Desmet, *Embryology of extra- and intrahepatic bile ducts, the ductal plate.* Anat Rec (Hoboken), 2008. 291(6): p. 628-35.
18. Vijayan, V. and C.E. Tan, *Development of the human intrahepatic biliary system.* Ann Acad Med Singapore, 1999. 28(1): p. 105-8.
19. Perugorria, M.J., et al., *Polycystic liver diseases: advanced insights into the molecular mechanisms.* Nat Rev Gastroenterol Hepatol, 2014. 11(12): p. 750-61.

20. Tan, C.E. and G.J. Moscoso, *The developing human biliary system at the porta hepatis level between 29 days and 8 weeks of gestation: a way to understanding biliary atresia. Part 1.* Pathol Int, 1994. 44(8): p. 587-99.
21. Tan, J., et al., *Immunohistochemical evidence for hepatic progenitor cells in liver diseases.* Liver, 2002. 22(5): p. 365-73.
22. Van Eyken, P., et al., *The development of the intrahepatic bile ducts in man: a keratin-immunohistochemical study.* Hepatology, 1988. 8(6): p. 1586-95.
23. Clotman, F., et al., *The onecut transcription factor HNF6 is required for normal development of the biliary tract.* Development, 2002. 129(8): p. 1819-28.
24. Coffinier, C., et al., *Bile system morphogenesis defects and liver dysfunction upon targeted deletion of HNF1beta.* Development, 2002. 129(8): p. 1829-38.
25. Hunter, M.P., et al., *The homeobox gene Hhex is essential for proper hepatoblast differentiation and bile duct morphogenesis.* Dev Biol, 2007. 308(2): p. 355-67.
26. Clotman, F., et al., *Control of liver cell fate decision by a gradient of TGF beta signaling modulated by Onecut transcription factors.* Genes Dev, 2005. 19(16): p. 1849-54.
27. Cardinale, V., et al., *Multipotent stem/progenitor cells in human biliary tree give rise to hepatocytes, cholangiocytes, and pancreatic islets.* Hepatology, 2011. 54(6): p. 2159-72.
28. Cardinale, V., et al., *The biliary tree--a reservoir of multipotent stem cells.* Nat Rev Gastroenterol Hepatol, 2012. 9(4): p. 231-40.
29. Carpino, G., et al., *Evidence for multipotent endodermal stem/progenitor cell populations in human gallbladder.* J Hepatol, 2014. 60(6): p. 1194-202.
30. Lazaridis, K.N. and N.F. LaRusso, *The Cholangiopathies.* Mayo Clin Proc, 2015. 90(6): p. 791-800.
31. Eaton, J.E., et al., *Pathogenesis of primary sclerosing cholangitis and advances in diagnosis and management.* Gastroenterology, 2013. 145(3): p. 521-36.
32. O'Hara, S.P., et al., *HIV-1 Tat protein suppresses cholangiocyte toll-like receptor 4 expression and defense against Cryptosporidium parvum.* J Infect Dis, 2009. 199(8): p. 1195-204.
33. Leung, N., et al., *Early hepatitis B virus DNA reduction in hepatitis B e antigen-positive patients with chronic hepatitis B: A randomized international study of entecavir versus adefovir.* Hepatology, 2009. 49(1): p. 72-9.
34. Sampaziotis, F., et al., *Cholangiocytes derived from human induced pluripotent stem cells for disease modeling and drug validation.* Nat Biotechnol, 2015. 33(8): p. 845-52.
35. Vlachou, P.A., et al., *Improvement of ischemic cholangiopathy in three patients with hereditary hemorrhagic telangiectasia following treatment with bevacizumab.* J Hepatol, 2013. 59(1): p. 186-9.
36. Deltenre, P. and D.C. Valla, *Ischemic cholangiopathy.* Semin Liver Dis, 2008. 28(3): p. 235-46.
37. Mack, C.L., A.G. Feldman, and R.J. Sokol, *Clues to the etiology of bile duct injury in biliary atresia.* Semin Liver Dis, 2012. 32(4): p. 307-16.

38. Li, Y., et al., *Cholangitis: a histologic classification based on patterns of injury in liver biopsies.* Pathol Res Pract, 2005. 201(8-9): p. 565-72.
39. Zimmermann, M., et al., *New lanthanide-containing polytungstates derived from the cyclic P8W48 Anion: {Ln4(H2O)28[K subset P8W48O184(H4W4O12)2Ln2(H2O)10]13-}x, Ln = La, Ce, Pr, Nd.* Inorg Chem, 2007. 46(5): p. 1737-40.
40. Munoz-Garrido, P., et al., *MicroRNAs in biliary diseases.* World J Gastroenterol, 2012. 18(43): p. 6189-96.
41. Erice, O., et al., *Molecular Mechanisms of Cholangiocarcinogenesis: New Potential Targets For Therapy.* Curr Drug Targets, 2015.
42. Mosconi, S., et al., *Cholangiocarcinoma.* Crit Rev Oncol Hematol, 2009. 69(3): p. 259-70.
43. Malhi, H. and G.J. Gores, *Cholangiocarcinoma: modern advances in understanding a deadly old disease.* J Hepatol, 2006. 45(6): p. 856-67.
44. Bridgewater, J., et al., *Guidelines for the diagnosis and management of intrahepatic cholangiocarcinoma.* J Hepatol, 2014. 60(6): p. 1268-89.
45. Nakanuma, Y. and Y. Kakuda, *Pathologic classification of cholangiocarcinoma: New concepts.* Best Pract Res Clin Gastroenterol, 2015. 29(2): p. 277-93.
46. Han, J.K., et al., *Cholangiocarcinoma: pictorial essay of CT and cholangiographic findings.* Radiographics, 2002. 22(1): p. 173-87.
47. Nguyen, K. and J.T. Sing, Jr., *Review of endoscopic techniques in the diagnosis and management of cholangiocarcinoma.* World J Gastroenterol, 2008. 14(19): p. 2995-9.
48. Sripa, B., et al., *Liver fluke induces cholangiocarcinoma.* PLoS Med, 2007. 4(7): p. e201.
49. Blechacz, B., et al., *Clinical diagnosis and staging of cholangiocarcinoma.* Nat Rev Gastroenterol Hepatol, 2011. 8(9): p. 512-22.
50. Alvaro, D., et al., *Cholangiocarcinoma in Italy: A national survey on clinical characteristics, diagnostic modalities and treatment. Results from the "Cholangiocarcinoma" committee of the Italian Association for the Study of Liver disease.* Dig Liver Dis, 2011. 43(1): p. 60-5.
51. De Rose, A.M., et al., *Prognostic significance of tumor doubling time in mass-forming type cholangiocarcinoma.* J Gastrointest Surg, 2013. 17(4): p. 739-47.
52. Nakanuma, Y., et al., *Pathological classification of intrahepatic cholangiocarcinoma based on a new concept.* World J Hepatol, 2010. 2(12): p. 419-27.
53. Aishima, S. and Y. Oda, *Pathogenesis and classification of intrahepatic cholangiocarcinoma: different characters of perihilar large duct type versus peripheral small duct type.* J Hepatobiliary Pancreat Sci, 2015. 22(2): p. 94-100.
54. Komuta, M., et al., *Histological diversity in cholangiocellular carcinoma reflects the different cholangiocyte phenotypes.* Hepatology, 2012. 55(6): p. 1876-88.
55. Liau, J.Y., et al., *Morphological subclassification of intrahepatic cholangiocarcinoma: etiological, clinicopathological, and molecular features.* Mod Pathol, 2014. 27(8): p. 1163-73.

56. Nakanuma, Y., et al., *Pathological spectrum of intrahepatic cholangiocarcinoma arising in non-biliary chronic advanced liver diseases.* Pathol Int, 2011. 61(5): p. 298-305.
57. Komuta, M., et al., *Clinicopathological study on cholangiolocellular carcinoma suggesting hepatic progenitor cell origin.* Hepatology, 2008. 47(5): p. 1544-56.
58. Rycaj, K. and D.G. Tang, *Cell-of-Origin of Cancer versus Cancer Stem Cells: Assays and Interpretations.* Cancer Res, 2015. 75(19): p. 4003-11.
59. Cardinale, V., et al., *Multiple cells of origin in cholangiocarcinoma underlie biological, epidemiological and clinical heterogeneity.* World J Gastrointest Oncol, 2012. 4(5): p. 94-102.
60. Roskams, T., *Liver stem cells and their implication in hepatocellular and cholangiocarcinoma.* Oncogene, 2006. 25(27): p. 3818-22.
61. Blechacz, B. and G.J. Gores, *Cholangiocarcinoma: advances in pathogenesis, diagnosis, and treatment.* Hepatology, 2008. 48(1): p. 308-21.
62. Aljiffry, M., et al., *Evidence-based approach to cholangiocarcinoma: a systematic review of the current literature.* J Am Coll Surg, 2009. 208(1): p. 134-47.
63. Munoz, E.B., et al., *The effect of an educational intervention to improve patient antibiotic adherence during dispensing in a community pharmacy.* Aten Primaria, 2014. 46(7): p. 367-75.
64. Maroni, L., et al., *The significance of genetics for cholangiocarcinoma development.* Ann Transl Med, 2013. 1(3): p. 28.
65. Shin, H.R., et al., *Hepatitis B and C virus, Clonorchis sinensis for the risk of liver cancer: a case-control study in Pusan, Korea.* Int J Epidemiol, 1996. 25(5): p. 933-40.
66. Kaewpitoon, N., et al., *Opisthorchis viverrini: the carcinogenic human liver fluke.* World J Gastroenterol, 2008. 14(5): p. 666-74.
67. Sahani, D., et al., *Thorotrast-induced cholangiocarcinoma: case report.* Abdom Imaging, 2003. 28(1): p. 72-4.
68. Karnabatidis, D., et al., *Percutaneous trans-hepatic bilateral biliary stenting in Bismuth IV malignant obstruction.* World J Hepatol, 2013. 5(3): p. 114-9.
69. DeOliveira, M.L., P. Kambakamba, and P.A. Clavien, *Advances in liver surgery for cholangiocarcinoma.* Curr Opin Gastroenterol, 2013. 29(3): p. 293-8.
70. Rizvi, S. and G.J. Gores, *Current diagnostic and management options in perihilar cholangiocarcinoma.* Digestion, 2014. 89(3): p. 216-24.
71. Adam, A. and I.S. Benjamin, *The staging of cholangiocarcinoma.* Clin Radiol, 1992. 46(5): p. 299-303.
72. Hatzidakis, A. and A. Adam, *The interventional radiological management of cholangiocarcinoma.* Clin Radiol, 2003. 58(2): p. 91-6.
73. Marin, J.J., et al., *Mechanisms of Resistance to Chemotherapy in Gastric Cancer.* Anticancer Agents Med Chem, 2015.
74. Herraez, E., et al., *Expression of SLC22A1 variants may affect the response of hepatocellular carcinoma and cholangiocarcinoma to sorafenib.* Hepatology, 2013. 58(3): p. 1065-73.

75. Wlcek, K., et al., *The analysis of organic anion transporting polypeptide (OATP) mRNA and protein patterns in primary and metastatic liver cancer.* Cancer Biol Ther, 2011. 11(9): p. 801-11.
76. Sasaki, H., et al., *Concurrent analysis of human equilibrative nucleoside transporter 1 and ribonucleotide reductase subunit 1 expression increases predictive value for prognosis in cholangiocarcinoma patients treated with adjuvant gemcitabine-based chemotherapy.* Br J Cancer, 2014. 111(7): p. 1275-84.
77. Namwat, N., et al., *Characterization of 5-fluorouracil-resistant cholangiocarcinoma cell lines.* Chemotherapy, 2008. 54(5): p. 343-51.
78. Hahnvajanawong, C., et al., *Orotate phosphoribosyl transferase mRNA expression and the response of cholangiocarcinoma to 5-fluorouracil.* World J Gastroenterol, 2012. 18(30): p. 3955-61.
79. Martinez-Becerra, P., et al., *No correlation between the expression of FXR and genes involved in multidrug resistance phenotype of primary liver tumors.* Mol Pharm, 2012. 9(6): p. 1693-704.
80. Harnois, D.M., et al., *Bcl-2 is overexpressed and alters the threshold for apoptosis in a cholangiocarcinoma cell line.* Hepatology, 1997. 26(4): p. 884-90.
81. Liu, D., et al., *Microsatellite instability in thorotrast-induced human intrahepatic cholangiocarcinoma.* Int J Cancer, 2002. 102(4): p. 366-71.
82. Limpaiboon, T., et al., *Promoter hypermethylation is a major event of hMLH1 gene inactivation in liver fluke related cholangiocarcinoma.* Cancer Lett, 2005. 217(2): p. 213-9.
83. Sasaki, T., et al., *A randomized phase II study of gemcitabine and S-1 combination therapy versus gemcitabine monotherapy for advanced biliary tract cancer.* Cancer Chemother Pharmacol, 2013. 71(4): p. 973-9.
84. Smith, A.C., et al., *Randomised trial of endoscopic stenting versus surgical bypass in malignant low bileduct obstruction.* Lancet, 1994. 344(8938): p. 1655-60.
85. Berr, F., et al., *Photodynamic therapy for advanced bile duct cancer: evidence for improved palliation and extended survival.* Hepatology, 2000. 31(2): p. 291-8.
86. Ortner, M.E., et al., *Successful photodynamic therapy for nonresectable cholangiocarcinoma: a randomized prospective study.* Gastroenterology, 2003. 125(5): p. 1355-63.
87. Czito, B.G., M.S. Anscher, and C.G. Willett, *Radiation therapy in the treatment of cholangiocarcinoma.* Oncology (Williston Park), 2006. 20(8): p. 873-84; discussion 886-8, 893-5.
88. Andersen, J.B. and S.S. Thorgeirsson, *Genetic profiling of intrahepatic cholangiocarcinoma.* Curr Opin Gastroenterol, 2012. 28(3): p. 266-72.
89. Gwak, G.Y., et al., *Detection of response-predicting mutations in the kinase domain of the epidermal growth factor receptor gene in cholangiocarcinomas.* J Cancer Res Clin Oncol, 2005. 131(10): p. 649-52.
90. Leone, F., et al., *Somatic mutations of epidermal growth factor receptor in bile duct and gallbladder carcinoma.* Clin Cancer Res, 2006. 12(6): p. 1680-5.
91. Riener, M.O., et al., *Rare PIK3CA hotspot mutations in carcinomas of the biliary tract.* Genes Chromosomes Cancer, 2008. 47(5): p. 363-7.

92. Xu, R.F., et al., *KRAS and PIK3CA but not BRAF genes are frequently mutated in Chinese cholangiocarcinoma patients.* Biomed Pharmacother, 2011. 65(1): p. 22-6.
93. Isa, T., et al., *Analysis of microsatellite instability, K-ras gene mutation and p53 protein overexpression in intrahepatic cholangiocarcinoma.* Hepatogastroenterology, 2002. 49(45): p. 604-8.
94. Tada, M., M. Omata, and M. Ohto, *High incidence of ras gene mutation in intrahepatic cholangiocarcinoma.* Cancer, 1992. 69(5): p. 1115-8.
95. Churi, C.R., et al., *Mutation profiling in cholangiocarcinoma: prognostic and therapeutic implications.* PLoS One, 2014. 9(12): p. e115383.
96. Wu, W.R., et al., *Clinicopathological significance of aberrant Notch receptors in intrahepatic cholangiocarcinoma.* Int J Clin Exp Pathol, 2014. 7(6): p. 3272-9.
97. El Khatib, M., et al., *Activation of Notch signaling is required for cholangiocarcinoma progression and is enhanced by inactivation of p53 in vivo.* PLoS One, 2013. 8(10): p. e77433.
98. Zender, S., et al., *A critical role for notch signaling in the formation of cholangiocellular carcinomas.* Cancer Cell, 2013. 23(6): p. 784-95.
99. Akhoondi, S., et al., *FBXW7/hCDC4 is a general tumor suppressor in human cancer.* Cancer Res, 2007. 67(19): p. 9006-12.
100. Fujimoto, A., et al., *Whole-genome mutational landscape of liver cancers displaying biliary phenotype reveals hepatitis impact and molecular diversity.* Nat Commun, 2015. 6: p. 6120.
101. Wu, Y.M., et al., *Identification of targetable FGFR gene fusions in diverse cancers.* Cancer Discov, 2013. 3(6): p. 636-47.
102. Arai, Y., et al., *Fibroblast growth factor receptor 2 tyrosine kinase fusions define a unique molecular subtype of cholangiocarcinoma.* Hepatology, 2014. 59(4): p. 1427-34.
103. Ross, J.S., et al., *New routes to targeted therapy of intrahepatic cholangiocarcinomas revealed by next-generation sequencing.* Oncologist, 2014. 19(3): p. 235-42.
104. Borad, M.J., et al., *Integrated genomic characterization reveals novel, therapeutically relevant drug targets in FGFR and EGFR pathways in sporadic intrahepatic cholangiocarcinoma.* PLoS Genet, 2014. 10(2): p. e1004135.
105. Nakamura, H., et al., *Genomic spectra of biliary tract cancer.* Nat Genet, 2015. 47(9): p. 1003-10.
106. Goeppert, B., et al., *Global alterations of DNA methylation in cholangiocarcinoma target the Wnt signaling pathway.* Hepatology, 2014. 59(2): p. 544-54.
107. Isomoto, H., *Epigenetic alterations associated with cholangiocarcinoma (review).* Oncol Rep, 2009. 22(2): p. 227-32.
108. Tischoff, I., C. Wittekind, and A. Tannapfel, *Role of epigenetic alterations in cholangiocarcinoma.* J Hepatobiliary Pancreat Surg, 2006. 13(4): p. 274-9.
109. Stutes, M., S. Tran, and S. DeMorrow, *Genetic and epigenetic changes associated with cholangiocarcinoma: from DNA methylation to microRNAs.* World J Gastroenterol, 2007. 13(48): p. 6465-9.
110. Sandhu, D.S., A.M. Shire, and L.R. Roberts, *Epigenetic DNA hypermethylation in cholangiocarcinoma: potential roles in pathogenesis,*

diagnosis and identification of treatment targets. Liver Int, 2008. 28(1): p. 12-27.
111. Isomoto, H., et al., *Sustained IL-6/STAT-3 signaling in cholangiocarcinoma cells due to SOCS-3 epigenetic silencing.* Gastroenterology, 2007. 132(1): p. 384-96.
112. Esteller, M., *Aberrant DNA methylation as a cancer-inducing mechanism.* Annu Rev Pharmacol Toxicol, 2005. 45: p. 629-56.
113. Egger, G., et al., *Epigenetics in human disease and prospects for epigenetic therapy.* Nature, 2004. 429(6990): p. 457-63.
114. Sriraksa, R. and T. Limpaiboon, *Histone deacetylases and their inhibitors as potential therapeutic drugs for cholangiocarcinoma - cell line findings.* Asian Pac J Cancer Prev, 2013. 14(4): p. 2503-8.
115. Gradilone, S.A., et al., *HDAC6 inhibition restores ciliary expression and decreases tumor growth.* Cancer Res, 2013. 73(7): p. 2259-70.
116. Pisarello, M.J., et al., *MicroRNAs in the Cholangiopathies: Pathogenesis, Diagnosis, and Treatment.* J Clin Med, 2015. 4(9): p. 1688-712.
117. Haga, H., et al., *Emerging insights into the role of microRNAs in the pathogenesis of cholangiocarcinoma.* Gene Expr, 2014. 16(2): p. 93-9.
118. Chen, L., et al., *The role of microRNA expression pattern in human intrahepatic cholangiocarcinoma.* J Hepatol, 2009. 50(2): p. 358-69.
119. Yang, R., et al., *MicroRNA-144 suppresses cholangiocarcinoma cell proliferation and invasion through targeting platelet activating factor acetylhydrolase isoform 1b.* BMC Cancer, 2014. 14: p. 917.
120. Braconi, C., N. Huang, and T. Patel, *MicroRNA-dependent regulation of DNA methyltransferase-1 and tumor suppressor gene expression by interleukin-6 in human malignant cholangiocytes.* Hepatology, 2010. 51(3): p. 881-90.
121. Baarsma, H.A., M. Konigshoff, and R. Gosens, *The WNT signaling pathway from ligand secretion to gene transcription: molecular mechanisms and pharmacological targets.* Pharmacol Ther, 2013. 138(1): p. 66-83.
122. Maher, M.T., et al., *Beta-catenin phosphorylated at serine 45 is spatially uncoupled from beta-catenin phosphorylated in the GSK3 domain: implications for signaling.* PLoS One, 2010. 5(4): p. e10184.
123. Cruciat, C.M. and C. Niehrs, *Secreted and transmembrane wnt inhibitors and activators.* Cold Spring Harb Perspect Biol, 2013. 5(3): p. a015081.
124. Lim, K., et al., *Cyclooxygenase-2-derived prostaglandin E2 activates beta-catenin in human cholangiocarcinoma cells: evidence for inhibition of these signaling pathways by omega 3 polyunsaturated fatty acids.* Cancer Res, 2008. 68(2): p. 553-60.
125. Han, C., et al., *Regulation of Wnt/beta-catenin pathway by cPLA2alpha and PPARdelta.* J Cell Biochem, 2008. 105(2): p. 534-45.
126. Oishi, N. and X.W. Wang, *Novel therapeutic strategies for targeting liver cancer stem cells.* Int J Biol Sci, 2011. 7(5): p. 517-35.
127. Sugimachi, K., et al., *Altered expression of beta-catenin without genetic mutation in intrahepatic cholangiocarcinoma.* Mod Pathol, 2001. 14(9): p. 900-5.
128. Tokumoto, N., et al., *Immunohistochemical and mutational analyses of Wnt signaling components and target genes in intrahepatic cholangiocarcinomas.* Int J Oncol, 2005. 27(4): p. 973-80.

129. Loilome, W., et al., *Activated macrophages promote Wnt/beta-catenin signaling in cholangiocarcinoma cells.* Tumour Biol, 2014. 35(6): p. 5357-67.
130. Boulter, L., et al., *WNT signaling drives cholangiocarcinoma growth and can be pharmacologically inhibited.* J Clin Invest, 2015. 125(3): p. 1269-85.
131. He, X., et al., *LDL receptor-related proteins 5 and 6 in Wnt/beta-catenin signaling: arrows point the way.* Development, 2004. 131(8): p. 1663-77.
132. Wells, R.G., *Fibrogenesis. V. TGF-beta signaling pathways.* Am J Physiol Gastrointest Liver Physiol, 2000. 279(5): p. G845-50.
133. El-Bassiouni, N.E., et al., *Role of fibrogenic markers in chronic hepatitis C and associated hepatocellular carcinoma.* Mol Biol Rep, 2012. 39(6): p. 6843-50.
134. Clarke, C., et al., *Selenium supplementation attenuates procollagen-1 and interleukin-8 production in fat-loaded human C3A hepatoblastoma cells treated with TGFbeta1.* Biochim Biophys Acta, 2010. 1800(6): p. 611-8.
135. Wang, H., et al., *TGF-beta1 Reduces miR-29a Expression to Promote Tumorigenicity and Metastasis of Cholangiocarcinoma by Targeting HDAC4.* PLoS One, 2015. 10(10): p. e0136703.
136. Araki, K., et al., *E/N-cadherin switch mediates cancer progression via TGF-beta-induced epithelial-to-mesenchymal transition in extrahepatic cholangiocarcinoma.* Br J Cancer, 2011. 105(12): p. 1885-93.
137. Ling, H., et al., *Transforming growth factor beta neutralization ameliorates pre-existing hepatic fibrosis and reduces cholangiocarcinoma in thioacetamide-treated rats.* PLoS One, 2013. 8(1): p. e54499.
138. Gubbay, J., et al., *A gene mapping to the sex-determining region of the mouse Y chromosome is a member of a novel family of embryonically expressed genes.* Nature, 1990. 346(6281): p. 245-50.
139. Sinclair, A.H., et al., *A gene from the human sex-determining region encodes a protein with homology to a conserved DNA-binding motif.* Nature, 1990. 346(6281): p. 240-4.
140. Stros, M., D. Launholt, and K.D. Grasser, *The HMG-box: a versatile protein domain occurring in a wide variety of DNA-binding proteins.* Cell Mol Life Sci, 2007. 64(19-20): p. 2590-606.
141. Wegner, M., *All purpose Sox: The many roles of Sox proteins in gene expression.* Int J Biochem Cell Biol, 2010. 42(3): p. 381-90.
142. Sudbeck, P. and G. Scherer, *Two independent nuclear localization signals are present in the DNA-binding high-mobility group domains of SRY and SOX9.* J Biol Chem, 1997. 272(44): p. 27848-52.
143. Gasca, S., et al., *A nuclear export signal within the high mobility group domain regulates the nucleocytoplasmic translocation of SOX9 during sexual determination.* Proc Natl Acad Sci U S A, 2002. 99(17): p. 11199-204.
144. Malki, S., B. Boizet-Bonhoure, and F. Poulat, *Shuttling of SOX proteins.* Int J Biochem Cell Biol, 2010. 42(3): p. 411-6.
145. Koopman, P., et al., *Male development of chromosomally female mice transgenic for Sry.* Nature, 1991. 351(6322): p. 117-21.

146. Bowles, J., G. Schepers, and P. Koopman, *Phylogeny of the SOX family of developmental transcription factors based on sequence and structural indicators.* Dev Biol, 2000. 227(2): p. 239-55.
147. She, Z.Y. and W.X. Yang, *SOX family transcription factors involved in diverse cellular events during development.* Eur J Cell Biol, 2015. 94(12): p. 547-63.
148. Kamachi, Y., M. Uchikawa, and H. Kondoh, *Pairing SOX off: with partners in the regulation of embryonic development.* Trends Genet, 2000. 16(4): p. 182-7.
149. Kamachi, Y. and H. Kondoh, *Sox proteins: regulators of cell fate specification and differentiation.* Development, 2013. 140(20): p. 4129-44.
150. Sarkar, A. and K. Hochedlinger, *The sox family of transcription factors: versatile regulators of stem and progenitor cell fate.* Cell Stem Cell, 2013. 12(1): p. 15-30.
151. Bernard, P. and V.R. Harley, *Acquisition of SOX transcription factor specificity through protein-protein interaction, modulation of Wnt signalling and post-translational modification.* Int J Biochem Cell Biol, 2010. 42(3): p. 400-10.
152. Wilson, M. and P. Koopman, *Matching SOX: partner proteins and co-factors of the SOX family of transcriptional regulators.* Curr Opin Genet Dev, 2002. 12(4): p. 441-6.
153. Castillo, S.D. and M. Sanchez-Cespedes, *The SOX family of genes in cancer development: biological relevance and opportunities for therapy.* Expert Opin Ther Targets, 2012. 16(9): p. 903-19.
154. Garraway, L.A. and W.R. Sellers, *Lineage dependency and lineage-survival oncogenes in human cancer.* Nat Rev Cancer, 2006. 6(8): p. 593-602.
155. Dong, C., D. Wilhelm, and P. Koopman, *Sox genes and cancer.* Cytogenet Genome Res, 2004. 105(2-4): p. 442-7.
156. Visvader, J.E., *Cells of origin in cancer.* Nature, 2011. 469(7330): p. 314-22.
157. Ben-Porath, I., et al., *An embryonic stem cell-like gene expression signature in poorly differentiated aggressive human tumors.* Nat Genet, 2008. 40(5): p. 499-507.
158. Lengerke, C., et al., *Expression of the embryonic stem cell marker SOX2 in early-stage breast carcinoma.* BMC Cancer, 2011. 11: p. 42.
159. Saigusa, S., et al., *Correlation of CD133, OCT4, and SOX2 in rectal cancer and their association with distant recurrence after chemoradiotherapy.* Ann Surg Oncol, 2009. 16(12): p. 3488-98.
160. Azzam, N.A., et al., *Nerve cables formed in silicone chambers reconstitute a perineurial but not a vascular endoneurial permeability barrier.* J Comp Neurol, 1991. 314(4): p. 807-19.
161. Rhodes, D.R., et al., *Large-scale meta-analysis of cancer microarray data identifies common transcriptional profiles of neoplastic transformation and progression.* Proc Natl Acad Sci U S A, 2004. 101(25): p. 9309-14.
162. Aue, G., et al., *Sox4 cooperates with PU.1 haploinsufficiency in murine myeloid leukemia.* Blood, 2011. 118(17): p. 4674-81.

163. Aaboe, M., et al., *SOX4 expression in bladder carcinoma: clinical aspects and in vitro functional characterization.* Cancer Res, 2006. 66(7): p. 3434-42.
164. Medina, P.P., et al., *The SRY-HMG box gene, SOX4, is a target of gene amplification at chromosome 6p in lung cancer.* Hum Mol Genet, 2009. 18(7): p. 1343-52.
165. Andersen, C.L., et al., *Dysregulation of the transcription factors SOX4, CBFB and SMARCC1 correlates with outcome of colorectal cancer.* Br J Cancer, 2009. 100(3): p. 511-23.
166. Sinner, D., et al., *Sox17 and Sox4 differentially regulate beta-catenin/T-cell factor activity and proliferation of colon carcinoma cells.* Mol Cell Biol, 2007. 27(22): p. 7802-15.
167. Liu, P., et al., *Sex-determining region Y box 4 is a transforming oncogene in human prostate cancer cells.* Cancer Res, 2006. 66(8): p. 4011-9.
168. Pramoonjago, P., A.S. Baras, and C.A. Moskaluk, *Knockdown of Sox4 expression by RNAi induces apoptosis in ACC3 cells.* Oncogene, 2006. 25(41): p. 5626-39.
169. Matheu, A., et al., *Oncogenicity of the developmental transcription factor Sox9.* Cancer Res, 2012. 72(5): p. 1301-15.
170. Guo, W., et al., *Slug and Sox9 cooperatively determine the mammary stem cell state.* Cell, 2012. 148(5): p. 1015-28.
171. Swartling, F.J., et al., *Distinct neural stem cell populations give rise to disparate brain tumors in response to N-MYC.* Cancer Cell, 2012. 21(5): p. 601-13.
172. Muller, P., et al., *SOX9 mediates the retinoic acid-induced HES-1 gene expression in human breast cancer cells.* Breast Cancer Res Treat, 2010. 120(2): p. 317-26.
173. Passeron, T., et al., *Upregulation of SOX9 inhibits the growth of human and mouse melanomas and restores their sensitivity to retinoic acid.* J Clin Invest, 2009. 119(4): p. 954-63.
174. Bakos, R.M., et al., *Nestin and SOX9 and SOX10 transcription factors are coexpressed in melanoma.* Exp Dermatol, 2010. 19(8): p. e89-94.
175. Thomsen, M.K., et al., *SOX9 elevation in the prostate promotes proliferation and cooperates with PTEN loss to drive tumor formation.* Cancer Res, 2010. 70(3): p. 979-87.
176. Drivdahl, R., et al., *Suppression of growth and tumorigenicity in the prostate tumor cell line M12 by overexpression of the transcription factor SOX9.* Oncogene, 2004. 23(26): p. 4584-93.
177. Aleman, A., et al., *Identification of DNA hypermethylation of SOX9 in association with bladder cancer progression using CpG microarrays.* Br J Cancer, 2008. 98(2): p. 466-73.
178. Ling, S., et al., *An EGFR-ERK-SOX9 signaling cascade links urothelial development and regeneration to cancer.* Cancer Res, 2011. 71(11): p. 3812-21.
179. Carvajal-Cuenca, A., et al., *In situ mantle cell lymphoma: clinical implications of an incidental finding with indolent clinical behavior.* Haematologica, 2012. 97(2): p. 270-8.

180. Ek, S., et al., *Nuclear expression of the non B-cell lineage Sox11 transcription factor identifies mantle cell lymphoma.* Blood, 2008. 111(2): p. 800-5.
181. Castillo, S.D., et al., *Novel transcriptional targets of the SRY-HMG box transcription factor SOX4 link its expression to the development of small cell lung cancer.* Cancer Res, 2012. 72(1): p. 176-86.
182. Weigle, B., et al., *Highly specific overexpression of the transcription factor SOX11 in human malignant gliomas.* Oncol Rep, 2005. 13(1): p. 139-44.
183. Hide, T., et al., *Sox11 prevents tumorigenesis of glioma-initiating cells by inducing neuronal differentiation.* Cancer Res, 2009. 69(20): p. 7953-9.
184. Thu, K.L., et al., *SOX15 and other SOX family members are important mediators of tumorigenesis in multiple cancer types.* Oncoscience, 2014. 1(5): p. 326-35.
185. Acloque, H., et al., *Reciprocal repression between Sox3 and snail transcription factors defines embryonic territories at gastrulation.* Dev Cell, 2011. 21(3): p. 546-58.
186. Katoh, M., *Molecular cloning and characterization of human SOX17.* Int J Mol Med, 2002. 9(2): p. 153-7.
187. Kanai-Azuma, M., et al., *Depletion of definitive gut endoderm in Sox17-null mutant mice.* Development, 2002. 129(10): p. 2367-79.
188. Uemura, M., et al., *Expression and function of mouse Sox17 gene in the specification of gallbladder/bile-duct progenitors during early foregut morphogenesis.* Biochem Biophys Res Commun, 2010. 391(1): p. 357-63.
189. Uemura, M., et al., *Sox17 haploinsufficiency results in perinatal biliary atresia and hepatitis in C57BL/6 background mice.* Development, 2013. 140(3): p. 639-48.
190. Stefanovic, S., et al., *Interplay of Oct4 with Sox2 and Sox17: a molecular switch from stem cell pluripotency to specifying a cardiac fate.* J Cell Biol, 2009. 186(5): p. 665-73.
191. Corada, M., et al., *Sox17 is indispensable for acquisition and maintenance of arterial identity.* Nat Commun, 2013. 4: p. 2609.
192. Gimelli, S., et al., *Mutations in SOX17 are associated with congenital anomalies of the kidney and the urinary tract.* Hum Mutat, 2010. 31(12): p. 1352-9.
193. Suraweera, N., et al., *Mutations within Wnt pathway genes in sporadic colorectal cancers and cell lines.* Int J Cancer, 2006. 119(8): p. 1837-42.
194. Fu, D.Y., et al., *Sox17, the canonical Wnt antagonist, is epigenetically inactivated by promoter methylation in human breast cancer.* Breast Cancer Res Treat, 2010. 119(3): p. 601-12.
195. Zhang, W., et al., *Epigenetic inactivation of the canonical Wnt antagonist SRY-box containing gene 17 in colorectal cancer.* Cancer Res, 2008. 68(8): p. 2764-72.
196. Silva, A.L., et al., *Boosting Wnt activity during colorectal cancer progression through selective hypermethylation of Wnt signaling antagonists.* BMC Cancer, 2014. 14: p. 891.
197. Du, Y.C., et al., *Induction and down-regulation of Sox17 and its possible roles during the course of gastrointestinal tumorigenesis.* Gastroenterology, 2009. 137(4): p. 1346-57.

198. Jia, Y., et al., *SOX17 antagonizes WNT/beta-catenin signaling pathway in hepatocellular carcinoma.* Epigenetics, 2010. 5(8): p. 743-9.
199. Yang, T., et al., *Sox17 inhibits hepatocellular carcinoma progression by downregulation of KIF14 expression.* Tumour Biol, 2014. 35(11): p. 11199-207.
200. Jia, Y., et al., *Inhibition of SOX17 by microRNA 141 and methylation activates the WNT signaling pathway in esophageal cancer.* J Mol Diagn, 2012. 14(6): p. 577-85.
201. Chiyomaru, T., et al., *Genistein suppresses prostate cancer growth through inhibition of oncogenic microRNA-151.* PLoS One, 2012. 7(8): p. e43812.
202. Li, Y., et al., *The SOX17/miR-371-5p/SOX2 axis inhibits EMT, stem cell properties and metastasis in colorectal cancer.* Oncotarget, 2015. 6(11): p. 9099-112.
203. Chen, H.L., et al., *Modulation of the Wnt/beta-catenin pathway in human oligodendroglioma cells by Sox17 regulates proliferation and differentiation.* Cancer Lett, 2013. 335(2): p. 361-71.
204. Chew, L.J., et al., *SRY-box containing gene 17 regulates the Wnt/beta-catenin signaling pathway in oligodendrocyte progenitor cells.* J Neurosci, 2011. 31(39): p. 13921-35.
205. Francois, M., P. Koopman, and M. Beltrame, *SoxF genes: Key players in the development of the cardio-vascular system.* Int J Biochem Cell Biol, 2010. 42(3): p. 445-8.
206. McCubrey, J.A., et al., *GSK-3 as potential target for therapeutic intervention in cancer.* Oncotarget, 2014. 5(10): p. 2881-911.
207. De Assuncao, T.M., et al., *Development and characterization of human-induced pluripotent stem cell-derived cholangiocytes.* Lab Invest, 2015. 95(6): p. 684-96.
208. Kudva, Y.C., et al., *Transgene-free disease-specific induced pluripotent stem cells from patients with type 1 and type 2 diabetes.* Stem Cells Transl Med, 2012. 1(6): p. 451-61.
209. Grubman, S.A., et al., *Regulation of intracellular pH by immortalized human intrahepatic biliary epithelial cell lines.* Am J Physiol, 1994. 266(6 Pt 1): p. G1060-70.
210. Banales, J.M., et al., *Up-regulation of microRNA 506 leads to decreased Cl-/HCO3- anion exchanger 2 expression in biliary epithelium of patients with primary biliary cirrhosis.* Hepatology, 2012. 56(2): p. 687-97.
211. Knuth, A., et al., *Biliary adenocarcinoma. Characterisation of three new human tumor cell lines.* J Hepatol, 1985. 1(6): p. 579-96.
212. Zach, S., E. Birgin, and F. Rückert, *Primary Cholangiocellular Carcinoma Cell Lines.* J Stem Cell Res Transplant, 2015. 2(1): p. 1013.
213. Chen, Q., et al., *Monocyte chemotactic protein-1 promotes the proliferation and invasion of osteosarcoma cells and upregulates the expression of AKT.* Mol Med Rep, 2015. 12(1): p. 219-25.
214. Li, W., *Volcano plots in analyzing differential expressions with mRNA microarrays.* J Bioinform Comput Biol, 2012. 10(6): p. 1231003.
215. Li, W., et al., *Using volcano plots and regularized-chi statistics in genetic association studies.* Comput Biol Chem, 2014. 48: p. 77-83.

216. Tong, Z., et al., *Application of biomaterials to advance induced pluripotent stem cell research and therapy.* Embo J, 2015. 34(8): p. 987-1008.
217. Singh, V.K., et al., *Induced pluripotent stem cells: applications in regenerative medicine, disease modeling, and drug discovery.* Front Cell Dev Biol, 2015. 3: p. 2.
218. Lee, A.Y., et al., *Comparative studies on proliferation, molecular markers and differentiation potential of mesenchymal stem cells from various tissues (adipose, bone marrow, ear skin, abdominal skin, and lung) and maintenance of multipotency during serial passages in miniature pig.* Res Vet Sci, 2015. 100: p. 115-24.
219. Krishnamurthy, J., et al., *Ink4a/Arf expression is a biomarker of aging.* J Clin Invest, 2004. 114(9): p. 1299-307.
220. Lee, B.Y., et al., *Senescence-associated beta-galactosidase is lysosomal beta-galactosidase.* Aging Cell, 2006. 5(2): p. 187-95.
221. Tuleuova, N., et al., *Using growth factor arrays and micropatterned co-cultures to induce hepatic differentiation of embryonic stem cells.* Biomaterials, 2010. 31(35): p. 9221-31.
222. Chignard, N., et al., *Bile acid transport and regulating functions in the human biliary epithelium.* Hepatology, 2001. 33(3): p. 496-503.
223. Li, W., et al., *Melatonin Induces Cell Apoptosis in AGS Cells Through the Activation of JNK and P38 MAPK and the Suppression of Nuclear Factor-Kappa B: a Novel Therapeutic Implication for Gastric Cancer.* Cell Physiol Biochem, 2015. 37(6): p. 2323-38.
224. Bao, M.H., et al., *Effects of miR590 on oxLDLinduced endothelial cell apoptosis: Roles of p53 and NFkappaB.* Mol Med Rep, 2016. 13(1): p. 867-73.
225. Green, D.R. and F. Llambi, *Cell Death Signaling.* Cold Spring Harb Perspect Biol, 2015. 7(12).
226. Vaeteewoottacharn, K., et al., *Perturbation of proteasome function by bortezomib leading to ER stress-induced apoptotic cell death in cholangiocarcinoma.* J Cancer Res Clin Oncol, 2013. 139(9): p. 1551-62.
227. Tusskorn, O., et al., *Phenethyl isothiocyanate induces apoptosis of cholangiocarcinoma cells through interruption of glutathione and mitochondrial pathway.* Naunyn Schmiedebergs Arch Pharmacol, 2013. 386(11): p. 1009-16.
228. Matchimakul, P., et al., *Apoptosis of cholangiocytes modulated by thioredoxin of carcinogenic liver fluke.* Int J Biochem Cell Biol, 2015. 65: p. 72-80.
229. Wang, W., et al., *Involvement of Wnt/beta-catenin signaling in the mesenchymal stem cells promote metastatic growth and chemoresistance of cholangiocarcinoma.* Oncotarget, 2015. 6(39): p. 42276-89.
230. Mbom, B.C., et al., *Nek2 phosphorylates and stabilizes beta-catenin at mitotic centrosomes downstream of Plk1.* Mol Biol Cell, 2014. 25(7): p. 977-91.
231. Ruoslahti, E., *Fibronectin in cell adhesion and invasion.* Cancer Metastasis Rev, 1984. 3(1): p. 43-51.
232. Rao, R.K. and G. Samak, *Bile duct epithelial tight junctions and barrier function.* Tissue Barriers, 2013. 1(4): p. e25718.

233. Techasen, A., et al., *Cytokines released from activated human macrophages induce epithelial mesenchymal transition markers of cholangiocarcinoma cells.* Asian Pac J Cancer Prev, 2012. 13 Suppl: p. 115-8.
234. Franzen, C.A., et al., *Urothelial cells undergo epithelial-to-mesenchymal transition after exposure to muscle invasive bladder cancer exosomes.* Oncogenesis, 2015. 4: p. e163.
235. Gradilone, S.A., M.J. Lorenzo Pisarellob, and N.F. LaRussob, *Primary Cilia in Tumor Biology: The Primary Cilium as a Therapeutic Target in Cholangiocarcinoma.* Curr Drug Targets, 2015.
236. Keeratichamroen, S., et al., *Expression of CD24 in cholangiocarcinoma cells is associated with disease progression and reduced patient survival.* Int J Oncol, 2011. 39(4): p. 873-81.
237. Su, M.C., et al., *CD24 expression is a prognostic factor in intrahepatic cholangiocarcinoma.* Cancer Lett, 2006. 235(1): p. 34-9.
238. Arumugam, T., et al., *Epithelial to mesenchymal transition contributes to drug resistance in pancreatic cancer.* Cancer Res, 2009. 69(14): p. 5820-8.
239. Anderson, K.R., et al., *The L6 domain tetraspanin Tm4sf4 regulates endocrine pancreas differentiation and directed cell migration.* Development, 2011. 138(15): p. 3213-24.
240. Ma, X., et al., *Impact of the IGFBP3 A-202C polymorphism on susceptibility and clinicopathologic features of breast cancer.* Biomed Pharmacother, 2015. 71: p. 108-11.
241. Li, S., et al., *Interferon alpha-inducible protein 27 promotes epithelial-mesenchymal transition and induces ovarian tumorigenicity and stemness.* J Surg Res, 2015. 193(1): p. 255-64.
242. Cheriyath, V., et al., *G1P3, an IFN-induced survival factor, antagonizes TRAIL-induced apoptosis in human myeloma cells.* J Clin Invest, 2007. 117(10): p. 3107-17.
243. Danish, H.H., et al., *Interferon-induced protein with tetratricopeptide repeats 1 (IFIT1) as a prognostic marker for local control in T1-2 N0 breast cancer treated with breast-conserving surgery and radiation therapy (BCS + RT).* Breast J, 2013. 19(3): p. 231-9.
244. Shostak, K., et al., *NF-kappaB-induced KIAA1199 promotes survival through EGFR signalling.* Nat Commun, 2014. 5: p. 5232.
245. Jami, M.S., et al., *Functional proteomic analysis reveals the involvement of KIAA1199 in breast cancer growth, motility and invasiveness.* BMC Cancer, 2014. 14: p. 194.
246. Wee, Z.N., et al., *EZH2-mediated inactivation of IFN-gamma-JAK-STAT1 signaling is an effective therapeutic target in MYC-driven prostate cancer.* Cell Rep, 2014. 8(1): p. 204-16.
247. Oldridge, E.E., et al., *Retinoic acid represses invasion and stem cell phenotype by induction of the metastasis suppressors RARRES1 and LXN.* Oncogenesis, 2013. 2: p. e45.
248. Wang, W., et al., *RYBP expression is associated with better survival of patients with hepatocellular carcinoma (HCC) and responsiveness to chemotherapy of HCC cells in vitro and in vivo.* Oncotarget, 2014. 5(22): p. 11604-19.

249. Normandin, K., et al., *Protease inhibitor SERPINA1 expression in epithelial ovarian cancer.* Clin Exp Metastasis, 2010. 27(1): p. 55-69.
250. Williams, K.C. and M.G. Coppolino, *SNARE-dependent interaction of Src, EGFR and beta1 integrin regulates invadopodia formation and tumor cell invasion.* J Cell Sci, 2014. 127(Pt 8): p. 1712-25.
251. Feng, H., et al., *EGFR phosphorylation of DCBLD2 recruits TRAF6 and stimulates AKT-promoted tumorigenesis.* J Clin Invest, 2014. 124(9): p. 3741-56.
252. Krohn, A., et al., *Recurrent deletion of 3p13 targets multiple tumour suppressor genes and defines a distinct subgroup of aggressive ERG fusion-positive prostate cancers.* J Pathol, 2013. 231(1): p. 130-41.
253. Sadeghi, M.M., et al., *ESDN is a marker of vascular remodeling and regulator of cell proliferation in graft arteriosclerosis.* Am J Transplant, 2007. 7(9): p. 2098-105.
254. Rong, G., et al., *Candidate markers that associate with chemotherapy resistance in breast cancer through the study on Taxotere-induced damage to tumor microenvironment and gene expression profiling of carcinoma-associated fibroblasts (CAFs).* PLoS One, 2013. 8(8): p. e70960.
255. Qiao, S., et al., *Thiostrepton is an inducer of oxidative and proteotoxic stress that impairs viability of human melanoma cells but not primary melanocytes.* Biochem Pharmacol, 2012. 83(9): p. 1229-40.
256. Negroni, L., et al., *Integrative quantitative proteomics unveils proteostasis imbalance in human hepatocellular carcinoma developed on nonfibrotic livers.* Mol Cell Proteomics, 2014. 13(12): p. 3473-83.
257. Zacherl, S., et al., *A direct role for ATP1A1 in unconventional secretion of fibroblast growth factor 2.* J Biol Chem, 2015. 290(6): p. 3654-65.
258. Yanai, M., et al., *FGF signaling segregates biliary cell-lineage from chick hepatoblasts cooperatively with BMP4 and ECM components in vitro.* Dev Dyn, 2008. 237(5): p. 1268-83.
259. Yao, W.J., et al., *MicroRNA-506 inhibits esophageal cancer cell proliferation via targeting CREB1.* Int J Clin Exp Pathol, 2015. 8(9): p. 10868-74.
260. Arcangeli, A., *Expression and role of hERG channels in cancer cells.* Novartis Found Symp, 2005. 266: p. 225-32; discussion 232-4.
261. Annani-Akollor, M.E., et al., *Downregulated protein O-fucosyl transferase 1 (Pofut1) expression exerts antiproliferative and antiadhesive effects on hepatocytes by inhibiting Notch signalling.* Biomed Pharmacother, 2014. 68(6): p. 785-90.
262. Selige, J., A. Hatzelmann, and T. Dunkern, *The differential impact of PDE4 subtypes in human lung fibroblasts on cytokine-induced proliferation and myofibroblast conversion.* J Cell Physiol, 2011. 226(8): p. 1970-80.
263. Chen, D.B. and H.J. Yang, *Comparison of gene regulatory networks of benign and malignant breast cancer samples with normal samples.* Genet Mol Res, 2014. 13(4): p. 9453-62.
264. Chou, C.T., et al., *Prognostic Significance of CDCP1 Expression in Colorectal Cancer and Effect of Its Inhibition on Invasion and Migration.* Ann Surg Oncol, 2015. 22(13): p. 4335-43.

265. Ryu, B.J., et al., *PF-3758309, p21-activated kinase 4 inhibitor, suppresses migration and invasion of A549 human lung cancer cells via regulation of CREB, NF-kappaB, and beta-catenin signalings.* Mol Cell Biochem, 2014. 389(1-2): p. 69-77.
266. Ariake, K., et al., *GCF2/LRRFIP1 promotes colorectal cancer metastasis and liver invasion through integrin-dependent RhoA activation.* Cancer Lett, 2012. 325(1): p. 99-107.
267. Liu, S., et al., *LIF upregulates poFUT1 expression and promotes trophoblast cell migration and invasion at the fetal-maternal interface.* Cell Death Dis, 2014. 5: p. e1396.
268. O'Toole, J.F., et al., *Individuals with mutations in XPNPEP3, which encodes a mitochondrial protein, develop a nephronophthisis-like nephropathy.* J Clin Invest, 2010. 120(3): p. 791-802.
269. Patterson, K.I., et al., *Dual-specificity phosphatases: critical regulators with diverse cellular targets.* Biochem J, 2009. 418(3): p. 475-89.
270. Wilson, M.P., et al., *Neural tube defects in mice with reduced levels of inositol 1,3,4-trisphosphate 5/6-kinase.* Proc Natl Acad Sci U S A, 2009. 106(24): p. 9831-5.
271. von Ameln, S., et al., *A mutation in PNPT1, encoding mitochondrial-RNA-import protein PNPase, causes hereditary hearing loss.* Am J Hum Genet, 2012. 91(5): p. 919-27.
272. Ullu, E. and A.M. Weiner, *Human genes and pseudogenes for the 7SL RNA component of signal recognition particle.* Embo J, 1984. 3(13): p. 3303-10.
273. Srivastava, L., et al., *Mammalian DEAD box protein Ddx51 acts in 3' end maturation of 28S rRNA by promoting the release of U8 snoRNA.* Mol Cell Biol, 2010. 30(12): p. 2947-56.
274. Kar, A., et al., *RPA70 depletion induces hSSB1/2-INTS3 complex to initiate ATR signaling.* Nucleic Acids Res, 2015. 43(10): p. 4962-74.
275. He, Y., et al., *Elevated CDCP1 predicts poor patient outcome and mediates ovarian clear cell carcinoma by promoting tumor spheroid formation, cell migration and chemoresistance.* Oncogene, 2015.
276. Wang, Y.W., et al., *High expression of cAMP-responsive element-binding protein 1 (CREB1) is associated with metastasis, tumor stage and poor outcome in gastric cancer.* Oncotarget, 2015. 6(12): p. 10646-57.
277. Douchi, D., et al., *Silencing of LRRFIP1 reverses the epithelial-mesenchymal transition via inhibition of the Wnt/beta-catenin signaling pathway.* Cancer Lett, 2015. 365(1): p. 132-40.
278. Limpaiboon, T., *Epigenetic aberrations in cholangiocarcinoma: potential biomarkers and promising target for novel therapeutic strategies.* Asian Pac J Cancer Prev, 2012. 13 Suppl: p. 41-5.
279. Qu, Y., S. Dang, and P. Hou, *Gene methylation in gastric cancer.* Clin Chim Acta, 2013. 424: p. 53-65.
280. Zuo, S., et al., *Suppressing effects of down-regulating DNMT1 and DNMT3b expression on the growth of human cholangiocarcinoma cell line.* J Huazhong Univ Sci Technolog Med Sci, 2008. 28(3): p. 276-80.
281. Soumyakrishnan, S., et al., *Daidzein exhibits anti-fibrotic effect by reducing the expressions of Proteinase activated receptor 2 and TGFbeta1/smad mediated inflammation and apoptosis in Bleomycin-induced experimental pulmonary fibrosis.* Biochimie, 2014. 103: p. 23-36.

282. Chen, Y., et al., *TGF-beta1 expression is associated with invasion and metastasis of intrahepatic cholangiocarcinoma.* Biol Res, 2015. 48: p. 26.
283. Monceau, V., et al., *Enhanced sensitivity to low dose irradiation of ApoE-/- mice mediated by early pro-inflammatory profile and delayed activation of the TGFbeta1 cascade involved in fibrogenesis.* PLoS One, 2013. 8(2): p. e57052.
284. Sobel, K., et al., *Wnt-3a-activated human fibroblasts promote human keratinocyte proliferation and matrix destruction.* Int J Cancer, 2015. 136(12): p. 2786-98.
285. Golestaneh, N., et al., *Wnt signaling promotes proliferation and stemness regulation of spermatogonial stem/progenitor cells.* Reproduction, 2009. 138(1): p. 151-62.
286. Kar, S., et al., *An insight into the various regulatory mechanisms modulating human DNA methyltransferase 1 stability and function.* Epigenetics, 2012. 7(9): p. 994-1007.
287. Rizvi, S. and G.J. Gores, *Pathogenesis, diagnosis, and management of cholangiocarcinoma.* Gastroenterology, 2013. 145(6): p. 1215-29.
288. Cheng, C.T., et al., *Peritumoral SPARC expression and patient outcome with resectable intrahepatic cholangiocarcinoma.* Onco Targets Ther, 2015. 8: p. 1899-907.
289. Sheppard, K.E. and G.A. McArthur, *The cell-cycle regulator CDK4: an emerging therapeutic target in melanoma.* Clin Cancer Res, 2013. 19(19): p. 5320-8.
290. Kuo, I.Y., et al., *Low SOX17 expression is a prognostic factor and drives transcriptional dysregulation and esophageal cancer progression.* Int J Cancer, 2014. 135(3): p. 563-73.
291. Circu, M.L. and T.Y. Aw, *Reactive oxygen species, cellular redox systems, and apoptosis.* Free Radic Biol Med, 2010. 48(6): p. 749-62.
292. Kaleem, S., et al., *Eupalitin induces apoptosis in prostate carcinoma cells through ROS generation and increase of caspase-3 activity.* Cell Biol Int, 2015.
293. Dhanasekaran, D.N. and E.P. Reddy, *JNK signaling in apoptosis.* Oncogene, 2008. 27(48): p. 6245-51.
294. Liu, J.J., et al., *15,16-Dihydrotanshinone I from the Functional Food Salvia miltiorrhiza Exhibits Anticancer Activity in Human HL-60 Leukemia Cells: in Vitro and in Vivo Studies.* Int J Mol Sci, 2015. 16(8): p. 19387-400.
295. Halaby, M.J., et al., *Translational Control Protein 80 Stimulates IRES-Mediated Translation of p53 mRNA in Response to DNA Damage.* Biomed Res Int, 2015. 2015: p. 708158.
296. Vedrenne, V., et al., *Mutation in PNPT1, which encodes a polyribonucleotide nucleotidyltransferase, impairs RNA import into mitochondria and causes respiratory-chain deficiency.* Am J Hum Genet, 2012. 91(5): p. 912-8.
297. Wei, C.H., et al., *Crystal structure of a novel mitogen-activated protein kinase phosphatase, SKRP1.* Proteins, 2011. 79(11): p. 3242-6.
298. Zama, T., et al., *Scaffold role of a mitogen-activated protein kinase phosphatase, SKRP1, for the JNK signaling pathway.* J Biol Chem, 2002. 277(26): p. 23919-26.

299. Bersani, C., et al., *Wig-1 regulates cell cycle arrest and cell death through the p53 targets FAS and 14-3-3sigma.* Oncogene, 2014. 33(35): p. 4407-17.
300. Inoue, M., et al., *Aminopeptidase P3, a new member of the TNF-TNFR2 signaling complex, induces phosphorylation of JNK1 and JNK2.* J Cell Sci, 2015. 128(4): p. 656-69.
301. Stames, E.M. and J.F. O'Toole, *Mitochondrial aminopeptidase deletion increases chronological lifespan and oxidative stress resistance while decreasing respiratory metabolism in S. cerevisiae.* PLoS One, 2013. 8(10): p. e77234.
302. Fu, D.Y., et al., *Decreased expression of SOX17 is associated with tumor progression and poor prognosis in breast cancer.* Tumour Biol, 2015. 36(10): p. 8025-34.
303. Huang, G.L., et al., *Retinoid X receptor alpha enhances human cholangiocarcinoma growth through simultaneous activation of Wnt/beta-catenin and nuclear factor-kappaB pathways.* Cancer Sci, 2015.
304. Wang, J., et al., *Underexpression of LKB1 tumor suppressor is associated with enhanced Wnt signaling and malignant characteristics of human intrahepatic cholangiocarcinoma.* Oncotarget, 2015. 6(22): p. 18905-20.
305. Zhang, K.S., et al., *Inhibition of Wnt signaling induces cell apoptosis and suppresses cell proliferation in cholangiocarcinoma cells.* Oncol Rep, 2013. 30(3): p. 1430-8.
306. DeMorrow, S., et al., *The endocannabinoid anandamide inhibits cholangiocarcinoma growth via activation of the noncanonical Wnt signaling pathway.* Am J Physiol Gastrointest Liver Physiol, 2008. 295(6): p. G1150-8.
307. Stamos, J.L. and W.I. Weis, *The beta-catenin destruction complex.* Cold Spring Harb Perspect Biol, 2013. 5(1): p. a007898.
308. Jin, T., et al., *S100A4 expression is closely linked to genesis and progression of glioma by regulating proliferation, apoptosis, migration and invasion.* Asian Pac J Cancer Prev, 2015. 16(7): p. 2883-7.
309. Yuan, T.M., et al., *The S100A4 D10V polymorphism is related to cell migration ability but not drug resistance in gastric cancer cells.* Oncol Rep, 2014. 32(6): p. 2307-18.
310. Kuper, C., F.X. Beck, and W. Neuhofer, *NFAT5-mediated expression of S100A4 contributes to proliferation and migration of renal carcinoma cells.* Front Physiol, 2014. 5: p. 293.
311. Wang, H., et al., *Activation of the PI3K/Akt/mTOR/p70S6K pathway is involved in S100A4-induced viability and migration in colorectal cancer cells.* Int J Med Sci, 2014. 11(8): p. 841-9.
312. Zhang, J., et al., *S100A4 regulates migration and invasion in hepatocellular carcinoma HepG2 cells via NF-kappaB-dependent MMP-9 signal.* Eur Rev Med Pharmacol Sci, 2013. 17(17): p. 2372-82.
313. Masyuk, A.I., et al., *Biliary exosomes influence cholangiocyte regulatory mechanisms and proliferation through interaction with primary cilia.* Am J Physiol Gastrointest Liver Physiol, 2010. 299(4): p. G990-9.
314. Izawa, I., et al., *Current topics of functional links between primary cilia and cell cycle.* Cilia, 2015. 4: p. 12.

315. Masyuk, T.V., A.I. Masyuk, and N.F. LaRusso, *TGR5 in the Cholangiociliopathies.* Dig Dis, 2015. 33(3): p. 420-5.
316. Zhou, H.B., J.Y. Hu, and H.P. Hu, *Hepatitis B virus infection and intrahepatic cholangiocarcinoma.* World J Gastroenterol, 2014. 20(19): p. 5721-9.
317. Shen, D.Y., et al., *Inhibition of Wnt/beta-catenin signaling downregulates P-glycoprotein and reverses multi-drug resistance of cholangiocarcinoma.* Cancer Sci, 2013. 104(10): p. 1303-8.
318. Huang, G.L., et al., *beta-escin reverses multidrug resistance through inhibition of the GSK3beta/beta-catenin pathway in cholangiocarcinoma.* World J Gastroenterol, 2015. 21(4): p. 1148-57.
319. McDonald, L.T., et al., *Hematopoietic stem cell-derived cancer-associated fibroblasts are novel contributors to the pro-tumorigenic microenvironment.* Neoplasia, 2015. 17(5): p. 434-48.
320. Sukowati, C.H., et al., *The role of multipotent cancer associated fibroblasts in hepatocarcinogenesis.* BMC Cancer, 2015. 15: p. 188.
321. Verras, M., et al., *Wnt3a growth factor induces androgen receptor-mediated transcription and enhances cell growth in human prostate cancer cells.* Cancer Res, 2004. 64(24): p. 8860-6.
322. Qi, L., et al., *Wnt3a expression is associated with epithelial-mesenchymal transition and promotes colon cancer progression.* J Exp Clin Cancer Res, 2014. 33: p. 107.
323. Oka, M., et al., *De novo DNA methyltransferases Dnmt3a and Dnmt3b primarily mediate the cytotoxic effect of 5-aza-2'-deoxycytidine.* Oncogene, 2005. 24(19): p. 3091-9.
324. Subramaniam, D., et al., *DNA methyltransferases: a novel target for prevention and therapy.* Front Oncol, 2014. 4: p. 80.
325. Gaj, T., B.E. Epstein, and D.V. Schaffer, *Genome Engineering Using Adeno-associated Virus: Basic and Clinical Research Applications.* Mol Ther, 2015.
326. Kotterman, M.A. and D.V. Schaffer, *Engineering adeno-associated viruses for clinical gene therapy.* Nat Rev Genet, 2014. 15(7): p. 445-51.
327. Marin, J.J., et al., *Molecular Bases Of Chemoresistance In Cholangiocarcinoma.* Curr Drug Targets, 2015.
328. Wang, B., et al., *Decitabine inhibits the cell growth of cholangiocarcinoma in cultured cell lines and mouse xenografts.* Oncol Lett, 2014. 8(5): p. 1919-1924.
329. Malik, P. and A.F. Cashen, *Decitabine in the treatment of acute myeloid leukemia in elderly patients.* Cancer Manag Res, 2014. 6: p. 53-61.